

PROPERTY OF  
DIVISION  
OF  
METEOROLOGY

EPA-600/4-81-070  
August 1981

LONG-RANGE TRANSPORT AND TRANSFORMATION OF SO<sub>2</sub> AND SULFATE  
Refinement, Application, and Verification of Models

Grant No. R 805271

ENVIRONMENTAL SCIENCES RESEARCH LABORATORY  
OFFICE OF RESEARCH AND DEVELOPMENT  
U.S. ENVIRONMENTAL PROTECTION AGENCY  
RESEARCH TRIANGLE PARK, NC 27711

LONG-RANGE TRANSPORT AND TRANSFORMATION OF SO<sub>2</sub> AND SULFATE  
Refinement, Application, and Verification of Models

by

Teizi Henmi and Elmar R. Reiter

Department of Atmospheric Science  
Colorado State University  
Fort Collins, Colorado 80523

Grant No. R 805271

Project Officer

George C. Holzworth  
Meteorology and Assessment Division  
Environmental Sciences Research Laboratory  
Research Triangle Park, NC 27711

ENVIRONMENTAL SCIENCES RESEARCH LABORATORY  
OFFICE OF RESEARCH AND DEVELOPMENT  
U.S. ENVIRONMENTAL PROTECTION AGENCY  
RESEARCH TRIANGLE PARK, NC 27711

## DISCLAIMER

This report has been reviewed by the Environmental Science Research Laboratory, U.S. Environmental Protection Agency, and approved for publication. Approval does not signify that the contents necessarily reflect the views and policies of the U.S. Environmental Protection Agency, nor does mention of trade names or commercial products constitute endorsement or recommendation for use.

## ABSTRACT

Improvements have been made in the long-range transport model of  $\text{SO}_2$  and sulfate. Trajectories of the mean wind of the mixing layer are calculated using wind and temperature sounding data. Heights of the daytime and nighttime mixing layers are determined by temperature sounding data. Trajectories of the mean winds of the nighttime ground-based stable layer and of the daytime mixing layer, and trajectories of the mean wind of the layer between daytime mixing height and nighttime stable layer height are taken into consideration. Interpolation schemes of concentrations along the trajectories into grid points, as well as the interpolation scheme of precipitation rate at meteorological stations into the midpoint of trajectory segments, have been modified in order to save computing time. This model is developed to calculate particularly the 24-hour concentration distributions of  $\text{SO}_2$  and sulfate.

The model has been applied to calculate the distribution patterns of concentrations and deposition amounts of  $\text{SO}_2$  and sulfate over the area between  $35^\circ\text{N}$  and  $45^\circ\text{N}$  and between  $75^\circ\text{W}$  and  $95^\circ\text{W}$  for the dates of January 25 and July 11, 1976.

Although statistically significant correlations between the observed concentrations and calculated concentrations are obtained both for  $\text{SO}_2$  and for sulfate, the results also show the limitation of applicability of the model to the calculation of 24-hour average concentrations.

A climatological model of long-range transport of  $\text{SO}_2$  and sulfate has been also developed in this research project in order to calculate long-term distributions of  $\text{SO}_2$  and sulfate concentrations as well as the acidity of precipitation. The budget of sulfur over eastern North America can also be studied.

The model has been applied to calculate the distribution patterns of monthly-averaged concentrations of  $\text{SO}_2$  and sulfate for the months of January 1977 and March 1979 over the area between  $35^\circ\text{N}$  and  $55^\circ\text{N}$  and between  $62^\circ\text{W}$  and  $95^\circ\text{W}$ . The calculated concentrations for the month of January 1977 were compared with the observed concentrations, resulting in statistically significant correlations between the observed concentrations and the calculated concentrations. For the month of March 1979, calculated pH values were compared with those observed at 17 stations located over the eastern United States. Highly statistically significant correlation coefficients between these variables were obtained.

According to the calculation of sulfur budgets, major portions of sulfur emitted over eastern North America were removed by wet and dry deposition over the region. The contribution of transported sulfur from the United States to Canada is substantial for the sulfur over Canada. On the contrary, transported amounts of sulfur from Canada to the United States were small. The fraction of outflow amount of sulfur to the Atlantic Ocean was substantially smaller than the previously estimated amount by Galloway and Whelpdale (1980).

From empirical studies of precipitation chemistry data, statistically significant correlations between observed pH and the contents of  $\text{SO}_4^{=}$  and  $\text{NO}_3^-$  ions were found. Inclusions of  $\text{NO}_x/\text{NO}_3^-$  transport and removal processes in the long-range transport model would have improved the predictability of precipitation acidity.

## CONTENTS

|  |     |
|--|-----|
| ABSTRACT . . . . .   | iii |
| FIGURES . . . . .  | vii |
| TABLES . . . . .   | x   |
| ACKNOWLEDGMENT . . . . .   | xi  |
| 1. Introduction . . . . .  | 1   |
| 2. Summary and Conclusion . . . . .  | 3   |
| 3. Improvement of the Model for 24-Hour Average Concentrations . . .   | 5   |
| 3.1 Mixing Layer Height . . . . .  | 5   |
| 3.2 Interpolation Schemes of Concentrations for Grid Points . .  | 5   |
| 3.3 Increase of the Number of Trajectories Per Day . . . . .   | 7   |
| 3.4 Removal and Transformation Terms . . . . .   | 7   |
| 4. Results of Model Applications for 24-Hour Average Concentrations<br>of SO <sub>2</sub> and of Sulfate . . . . . | 10  |
| 4.1 Results and Discussion . . . . .   | 10  |
| 5. Development of a Climatological Model of SO <sub>2</sub> and Sulfate<br>Transport . . . . .                     | 23  |
| 5.1 Introduction . . . . .   | 23  |
| 5.2 Model . . . . .  | 23  |
| 6. Results of Climatological Model Applications to Eastern North<br>America . . . . .                              | 34  |
| 6.1 Introduction . . . . .   | 34  |
| 6.2 Results . . . . .  | 38  |
| 6.3 Comparison of Calculated Results with Observations . . . . .   | 38  |

|     |   |    |
|-----|---|----|
| 6.4 | Mass Budget of Sulfur Over the Northeastern United States .                       | 57 |
| 7.  | Investigation of a Prediction Method of the Acidity of<br>Precipitation . . . . . | 62 |
| 7.1 | Introduction . . . . .  | 62 |
|     | References . . . . .  | 74 |

## FIGURES

| <u>Number</u> |  | <u>Page</u> |
|---------------|--|-------------|
| 1             | Scheme of calculating 24-hour average concentrations. Here M is the number of days and K is the number of trajectories in a day . . . . .                                    | 8           |
| 2             | Locations and intensities of SO <sub>2</sub> emission sources (x 10 <sup>3</sup> ton/year) . . . . .   | 11          |
| 3             | Distribution of SO <sub>2</sub> concentrations (µg/m <sup>3</sup> ) at the surface level on (a) January 25, 1976 and (b) July 11, 1976 . . . . .                             | 12          |
| 4             | Distribution of sulfate concentrations (µg/m <sup>3</sup> ) at the surface level on (a) January 25, 1976 and (b) July 11, 1976 . . . . .                                     | 13          |
| 5             | Distribution of SO <sub>2</sub> deposition amounts due to dry and wet deposition on (a) January 25, 1976 and (b) July 25, 1976 . . . . .                                     | 15          |
| 6             | Distribution of sulfate deposition amounts (kg/km <sup>2</sup> ) due to dry and wet deposition on (a) January 25, 1976 and (b) July 11, 1976 . . . . .                       | 16          |
| 7             | Distribution of SO <sub>2</sub> deposition amounts (kg/km <sup>2</sup> ) due to precipitation on (a) January 25, 1976 and (b) July 11, 1976 . . . . .                        | 17          |
| 8             | Distribution of sulfate deposition amounts (kg/km <sup>2</sup> ) due to precipitation on (a) January 25, 1976 and (b) July 11, 1976 . . . . .                                | 18          |
| 9             | Relationship between calculated and observed SO <sub>2</sub> concentrations on (a) January 25, 1976 and (b) July 11, 1976 . . . . .  | 19          |
| 10            | Relationship between calculated and observed sulfate concentrations on (a) January 25, 1976 and (b) July 11, 1976 . . . . .  | 20          |
| 11a           | Average values of the dispersion parameter of $\Sigma_x$ and its standard deviation in the x direction due to the meandering of trajectories as a function of time . . . . . | 27          |



| <u>Number</u> |   | <u>Page</u> |
|---------------|---|-------------|
| 11b           | Same as Fig. 11a, except for y direction. . . . .   | 28          |
| 12a           | Average values of the dispersion parameter of $\sigma_x$ and its<br>standard deviation due to vertical wind shear . . . . .   | 29          |
| 12b           | Same as Fig. 12a, except for $\sigma_y$ . . . . .   | 30          |
| 13            | Division of the region into four major areas. For the<br>U.S. the grid points are indexed by 1, Canada by 2, the<br>Great Lakes by 3, and the Atlantic Ocean by 4 . . . . . | 32          |
| 14            | Locations and intensity of SO <sub>2</sub> emission sources<br>(x 10 <sup>3</sup> ton/year). . . . .  | 35          |
| 15a           | Monthly precipitation amounts (mm) for January, 1977 . . . .  | 36          |
| 15b           | Distribution of monthly precipitation amounts (mm) for<br>March 1979 . . . . .  | 37          |
| 16a           | Distribution of SO <sub>2</sub> concentrations ( $\mu\text{g}/\text{m}^3$ ) for January 1977 .  | 39          |
| 16b           | Distribution of SO <sub>2</sub> concentrations ( $\mu\text{g}/\text{m}^3$ ) for March 1979 . .  | 40          |
| 17a           | Distribution of sulfate concentrations ( $\mu\text{g}/\text{m}^3$ ) for January<br>1977. . . . .  | 41          |
| 17b           | Distribution of sulfate concentrations ( $\mu\text{g}/\text{m}^3$ ) for March<br>1979. . . . .  | 42          |
| 18a           | Dry deposition amounts ( $\text{kg}/\text{km}^2$ ) of SO <sub>2</sub> for January 1977 . . .  | 43          |
| 18b           | Dry deposition amounts ( $\text{kg}/\text{km}^2$ ) of SO <sub>2</sub> for March 1979 . . . .  | 44          |
| 19a           | Dry deposition amounts ( $\text{kg}/\text{km}^2$ ) of sulfate for January 1977 .  | 45          |
| 19b           | Dry deposition amounts ( $\text{kg}/\text{km}^2$ ) of sulfate for March 1979 . .  | 46          |
| 20a           | Wet deposition amounts ( $\text{kg}/\text{km}^2$ ) of SO <sub>2</sub> for January 1977 . . .  | 47          |
| 20b           | Wet deposition amounts ( $\text{kg}/\text{km}^2$ ) of SO <sub>2</sub> for March 1979 . . . .  | 48          |
| 21a           | Wet deposition amounts ( $\text{kg}/\text{km}^2$ ) of sulfate for January 1977 .  | 49          |
| 21b           | Wet deposition amounts ( $\text{kg}/\text{km}^2$ ) of sulfate for March 1979 . .  | 50          |
| 22a           | pH distribution for January 1977. . . . .   | 51          |
| 22b           | pH distribution for March 1979. . . . .   | 52          |

| <u>Number</u> |  | <u>Page</u> |
|---------------|--|-------------|
| 23            | Observed concentration distribution of $\text{SO}_2$ for January, 1977. [From Bhumralkar et al. (1980).]   | 53          |
| 24            | Observed concentration distribution of sulfate for January, 1977. [From Bhumralkar et al. (1980).]   | 54          |
| 25            | Calculated $\text{SO}_2$ concentration versus observed $\text{SO}_2$ concentration for January 1977  | 55          |
| 26            | Calculated sulfate concentration versus observed sulfate concentration for January 1977.   | 56          |
| 27            | Diagram showing the relationship between observed pH and calculated pH   | 59          |
| 28            | Concentrations of $\text{SO}_4^{=}$ ions and $\text{NO}_3^-$ ions in precipitation water, (A) data from "Atmospheric Turbidity" and "Precipitation Chemistry Data for the World" and (B) data from Hales and Dana (1979) | 63          |
| 29            | Same as Fig. 28, except $\text{SO}_4^{=}$ ions and $\text{NH}_4^+$ ions  | 64          |
| 30            | Same as Fig. 28, except $\text{NO}_3^-$ ions and $\text{NH}_4^+$ ions  | 65          |
| 31            | Emission rates of $\text{SO}_2$ and that of $\text{NO}_x$ . Data obtained from EPA   | 67          |
| 32            | Observed pH and pH calculated using Granat's (1972) theory. "Atmospheric Turbidity" and "Precipitation Data for the World", 1974, were used  | 69          |
| 33            | Observed pH and pH calculated from $-\log_{10}[2\text{SO}_4^{=}]$ . (A) "Atmospheric Turbidity" and "Precipitation Chemistry Data for the World". (B) Data from Hales and Dana (1979)                                    | 70          |
| 34            | Observed pH and pH calculated from $\log_{10} \{2[\text{SO}_4^{=}] + [\text{NO}_3^-]\}$ . (A) "Atmospheric Turbidity" and Precipitation Chemistry Data for the World", (B) data from Hales and Dana (1979).              | 71          |

## TABLES

| <u>Number</u> |   | <u>Page</u> |
|---------------|---|-------------|
| 1             | Correlation coefficient between the observed concentrations and the calculated concentrations . . . . .   | 21          |
| 2             | Sulfur budget of region . . . . .   | 21          |
| 3             | Site name, geographical location and monthly average pH for March 1979 . . . . .  | 58          |
| 4             | Sulfur mass budget for January 1977 . . . . .   | 60          |
| 5             | Sulfur mass budget for March 1979 . . . . .   | 61          |
| 6             | Correlation coefficients . . . . .  | 62          |
| 7             | Correlation coefficients . . . . .  | 68          |
| 8             | Correlation coefficient and regression parameters of the relationship between pH, $-\log_{10}\{[\text{NO}_3^-] + 2[\text{SO}_4^{=}] \}$ and $-\log_{10}\{2[\text{SO}_4^{=}] \}$ . . . . . | 73          |

## ACKNOWLEDGMENTS

Part of the calculations reported in this document was conducted on the EPA computer. Mr. Adrian Busse of the Environmental Sciences Research Laboratory was very helpful in running our program on the computer. Thanks are also due to the project officer, Mr. G.C. Holzworth, for giving us constructive suggestions.

The trajectory calculation portion of our models in this report is an expansion and modification of an original scheme developed by Mr. J.L. Heffter, Air Resources Laboratories, NOAA at Silver Springs, Maryland.

## SECTION 1

### INTRODUCTION

There is growing public, scientific, and governmental concern over the long-range transport and transformation of sulfur oxides and nitric oxides and other industrial pollutants, and their subsequent consequences for human welfare and for the environment, notably the increase of acidity of precipitation. Over the northeastern United States and Scandinavia, precipitation with high acidity, which is caused by the scavenging removal of such pollutants as  $\text{SO}_2$ , sulfate and nitrate, has been observed. The average pH of the Adirondack lakes has already dropped from 6.5 in the 1930's to 4.8 now; more than 90 of those lakes are completely fishless (Science News, 1979).

In the last several years, our major research efforts have been to develop a long-range transport model of  $\text{SO}_2$  and sulfate which, as input, uses the data observed routinely at weather stations, and to apply the model for studying the air quality of the eastern United States. Our model can be classified as a Lagrangian, forward-trajectory model. The most prominent feature of the model is that trajectories of mean winds of the nighttime stable layer and daytime mixing layer, and trajectories of the mean winds of the layer between daytime mixing height and nighttime stable layer height are taken into consideration. The model has been applied to calculate the geographical distributions of 24-hour average concentrations of  $\text{SO}_2$  and sulfate over the region between  $35^\circ\text{N}$  and  $45^\circ\text{N}$  and between  $75^\circ\text{W}$  and  $95^\circ\text{W}$ , which encompasses the Ohio River basin.

Although statistically significant correlations between observed concentrations and calculated concentrations are obtained both for  $\text{SO}_2$  and for sulfate, the results also showed the limitation of applicability of the model to the calculation of 24-hour average concentrations. The model can be used to calculate overall patterns of distribution, but it is improper to simulate minor details of such patterns. The details of our model and the results of its application were reported by Henmi and Reiter (1979) and Henmi (1979 and 1980).

Further improvements of the model have been made for the calculation of 24-hour average concentrations. Details of improvements are described in Section 3. The results of application of the improved model are given in Section 4.

It is possible to calculate long-term (monthly, seasonal or annual) average concentrations by repeatedly using the model developed for the

24-hour average concentrations. However, due to the large amount of computing time required for this process it is not practical to do so.

Realizing this disadvantage, we have developed a model which is suitable for calculating long-term average concentrations. This model has been applied to compute the distribution of average acidity of monthly precipitation over the region of eastern North America and to estimate the budget of sulfur over the region. This climatological model and the results of its applications are described in Sections 5 and 6, respectively.

In order to find empirical relationships between the acidity of precipitation and the concentrations of ions, we have analyzed available data of precipitation chemistry. The results of the analysis are described in Section 7.

## SECTION 2

### SUMMARY AND CONCLUSION

In this report we have described the improvements made in our long-range transport model of  $\text{SO}_2$  and sulfate (Henmi and Reiter, 1979).

Trajectories of the mean wind of the mixing layer are calculated using the wind and temperature sounding data. The heights of the daytime and nighttime mixing layer are determined by temperature sounding data. In order to save computing time, interpolation schemes of concentrations along the trajectories into grid points, as well as the interpolation scheme of precipitation rate at meteorological stations into the midpoint of trajectory segments have been modified, resulting in substantial savings of computing time. Additional improvements include the change of the magnitude of removal and transformation terms and the increase in the number of trajectories per day.

The model has been applied to calculate the distribution patterns of concentrations and deposition amounts of  $\text{SO}_2$  and sulfate for the dates of January 25 and July 11, 1976. Correlations between the calculated concentrations of  $\text{SO}_2$  and sulfate and the observed concentrations of these compounds are examined. Although statistically significant correlations between the observed concentrations and the calculated concentrations are obtained both for  $\text{SO}_2$  and for sulfate, the results also show the limitation of applicability of the model to the calculation of 24-hour average concentrations. The model can be used to calculate the overall patterns of distribution, but it is improper to simulate the minor details of such patterns. This limitation may be mainly due to the following facts:

- (1) Annual emission data of  $\text{SO}_2$ , instead of the daily emission data, were used as input data.
- (2) Small emission sources were neglected. Thus, the local effects due to these sources were not included in the distribution patterns.
- (3) Measurements of  $\text{SO}_2$  and sulfate may be subject to errors. Furthermore, measurements may reflect local rather than regional effects.

- (4) Model parameters, such as dry and wet deposition velocities and the transformation rate of  $\text{SO}_2$  to sulfate, may need further improvement.
- (5) There may be inaccuracies in trajectory calculations. During the periods of calculations for January 25 and July 11, 1976, the region was under the influence of frontal systems. Trajectories leaving the area near the fronts may have been inappropriately calculated.
- (6) The model does not consider the effect of relatively short-range dispersion, which in some cases may have significantly affected the observed concentrations.

In order to calculate long-term distribution of  $\text{SO}_2$  and sulfate concentrations, as well as the acidity of precipitation, a climatological model of long-range transport of  $\text{SO}_2$  and sulfate has been developed. The model can be applied to study the budget of sulfur over eastern North America.

The model has been applied to calculate monthly-average concentrations of  $\text{SO}_2$  and sulfate for the months of January 1977 and March 1979. The calculated concentrations of  $\text{SO}_2$  and sulfate for the month of January 1977 were compared with the observed concentrations over the eastern United States, resulting in statistically significant correlations between the observed concentrations and the calculated concentrations. For the month of March 1979, calculated pH values were compared with those observed at 17 stations located over the eastern United States. Highly statistically significant correlation coefficients between these variables were obtained.

The calculation of sulfur budgets showed that major portions of sulfur emitted over eastern North America were removed by wet and dry deposition over the region. The contribution of transported sulfur from the United States to Canada is substantial for the sulfur over Canada. On the contrary, transported amounts of sulfur from Canada to the United States are small. The fraction of outflow amount of sulfur to the Atlantic Ocean was substantially smaller than the previously estimated amount by Galloway and Whelpdale (1980).

From empirical studies of precipitation chemistry data, it was concluded that there were statistically significant correlations between observed pH and the contents of  $\text{SO}_4^{2-}$  and  $\text{NO}_3^-$  ions. Therefore, it was possible to predict the acidity of precipitation from our model. Inclusions of  $\text{NO}_x/\text{NO}_3^-$  transport and removal processes in our long-range transport model would have improved the predictability of precipitation acidity.



### SECTION 3

#### IMPROVEMENT OF THE MODEL FOR 24-HOUR AVERAGE CONCENTRATIONS

##### MIXING LAYER HEIGHT

The model developed previously used the wind data for 1974 provided by the Air Resources Laboratories, NOAA at Silver Springs, Maryland. In order to run the model using wind and temperature sounding data for the years 1975, 1976 and 1977, which were obtained from the Air Resources Laboratories, the computer programs of the model had to be modified substantially. In the previous model, the daytime mixing layer height and the nighttime stable layer height were defined from climatological data, and trajectories of the mean wind of the layers were calculated. In contrast, the present version of the model incorporates vertical temperature profiles along a trajectory to determine mixing layer depths over which average transport winds are calculated. The top of the daytime mixing layer is defined as the base of any nonsurface-based temperature inversion. A maximum inversion height is chosen as 3000 m. If no inversion occurs below 3000 m, this height is used for the top of the afternoon mixing layer and winds are averaged over that layer. The top of the nighttime stable layer is defined as the top of the surface-based temperature inversion. If no surface based inversion occurs, 500 m is substituted as the top of the nighttime stable layer.

##### INTERPOLATION SCHEMES OF CONCENTRATIONS FOR GRID POINTS

In the model previously developed (Henmi and Reiter, 1979), more than 90 percent of computing time was spent on interpolation schemes of concentrations along the trajectories into grid points. In order to save computing time, the computer program has been modified so that when the concentrations of  $\text{SO}_2$  and sulfate along the trajectory become lower than certain values (i.e.,  $0.5 \mu\text{g}/\text{m}^3$ ), the loop containing the interpolation schemes of concentrations along trajectories into grid points was bypassed. The result of a test run of the model showed that the distribution patterns of  $\text{SO}_2$  and sulfate were not different from those obtained without bypassing the loop.

An additional modification of the model has been made in the interpolation scheme of precipitation rates observed at meteorological stations into the midpoint of each trajectory segment. In the previous version of the model (Henmi and Reiter, 1979), an interpolation routine (i.e., triangle method) had been used. In the present model, the interpolation scheme used is a combination of inverse distance-squared weighting and the fitting of a linear surface so that the main advantage of each is retained - namely the

dominance of observations which are spatially close to the interpolation point, as well as the general distribution obtained from a number of observations. This scheme was originally used by English (1973).

The interpolation scheme consists of fitting a linear surface to the midpoint of a trajectory segment, with inverse distance-squared weighting applied to the observations. The surface chosen is the one for which the expression

$$\frac{r}{d} = \frac{ax}{d} + \frac{by}{d} + \frac{c}{d}, \quad (1)$$

applied to a number of precipitation rates observed at meteorological stations, has a least-square solution such that

$$\sum_{i=1}^N \frac{1}{d_i^2} r_i - (ax_i + by_i + c)^2 = \text{minimum} \quad (2)$$

In these equations

$d$  is the distance of a meteorological station from the midpoint of a trajectory segment,  
 $x$  and  $y$  are the longitudinal and latitudinal distances of a meteorological station from the midpoint of a trajectory segment,  
 $r$  is the precipitation rate at a meteorological station, and  $a$ ,  $b$ ,  $c$  are coefficients.

For each of the  $N$  chosen observations one can write

$$\frac{r_i}{d_i} = \frac{ax_i}{d_i} + \frac{by_i}{d_i} + \frac{c}{d_i} \quad (3)$$

where  $i = 1$  to  $N$ .

To interpolate the precipitation rates for the midpoint of trajectory segments, the present scheme chooses such rates observed at six meteorological stations which are located close to the midpoint of a trajectory segment. Interpolation into areas of no rainfall often leads to negative values, which are then set to zero. According to the precipitation field analysis by English (1973), six values give the most acceptable results, a pattern similar to what an analyst might produce by hand. A number less than six often leads to discontinuities and irregularities in the fields, whilst a number more than six tends to produce too much smoothing and also consumes more computer time.

The application of the above scheme has reduced the computing time of concentration calculations to 30 percent of that of the previous version of the model.

## INCREASE OF THE NUMBER OF TRAJECTORIES PER DAY

In the previous model, trajectories from each source area were calculated every 12 hours, starting at 6 and 18 CST, and each trajectory was pursued for 48 hours. In the present model, in order to increase the accuracy of calculations, four trajectories per day starting at 6, 12, 18 and 24 CST from each source area are calculated, and each trajectory is pursued for 48 hours. A trajectory is composed of a series of three-hour segments.

In order to calculate 24-hour average concentrations, we must take into consideration the contributions of trajectories which started up to 2 days earlier. In Fig. 1, the scheme for calculating 24-hour concentrations is shown. Trajectory segments drawn in thick solid lines were used to calculate the 24-hour average concentrations.

## REMOVAL AND TRANSFORMATION TERMS

### Dry Deposition

Recent results of dry deposition velocity estimates for  $\text{SO}_2$  and sulfate were reviewed by Garland (1978 and 1979). He concluded that the dry deposition velocity of  $\text{SO}_2$  was about 0.8 cm/sec and that of sulfate was 0.1 cm/sec. In accordance with these recent results, we use in the present model 1 cm/sec for the dry deposition velocity of  $\text{SO}_2$  and 0.1 cm/sec for that of sulfate.

### Wet Deposition

In the previous application, it was assumed that  $(\kappa/\chi)_v$  was  $5 \times 10^5$  for both  $\text{SO}_2$  and sulfate. Here,  $\kappa$  is the concentration of pollutants in rain-water and  $\chi$  the concentration of pollutants in air. The subscript  $v$  means that the ratio  $(\kappa/\chi)$  is formed on a volume basis. Recent observational results (Garland, 1978 and Hales and Dana, 1979) show that  $\text{SO}_2$  removal by rain is about an order of magnitude less efficient than sulfate removal. Therefore, we use the following scavenging velocities:

$$v_s = \left(\frac{\kappa}{\chi}\right)_v \cdot P = 1 \times 10^4 \times P \quad \text{for } \text{SO}_2 \quad (4)$$

$$v_s = \left(\frac{\kappa}{\chi}\right)_v \cdot P = 1 \times 10^5 \times P \quad \text{for sulfate.} \quad (5)$$

Here  $P$  is the precipitation rate (cm/hr). It has been reported that the sulfate content in precipitation varies depending on the season with a summertime peak (Pack, 1978 and Hales and Dana, 1979). The mechanism of precipitation formation and the condition of the environment may change with season. Rain can bring down dissolved gases. In the ice phase processes of precipitation formation, the growth of ice is a purification process and dissolved gases will be released back into cloud water. This feature can not be included in the present model and field studies on the role of ice in the

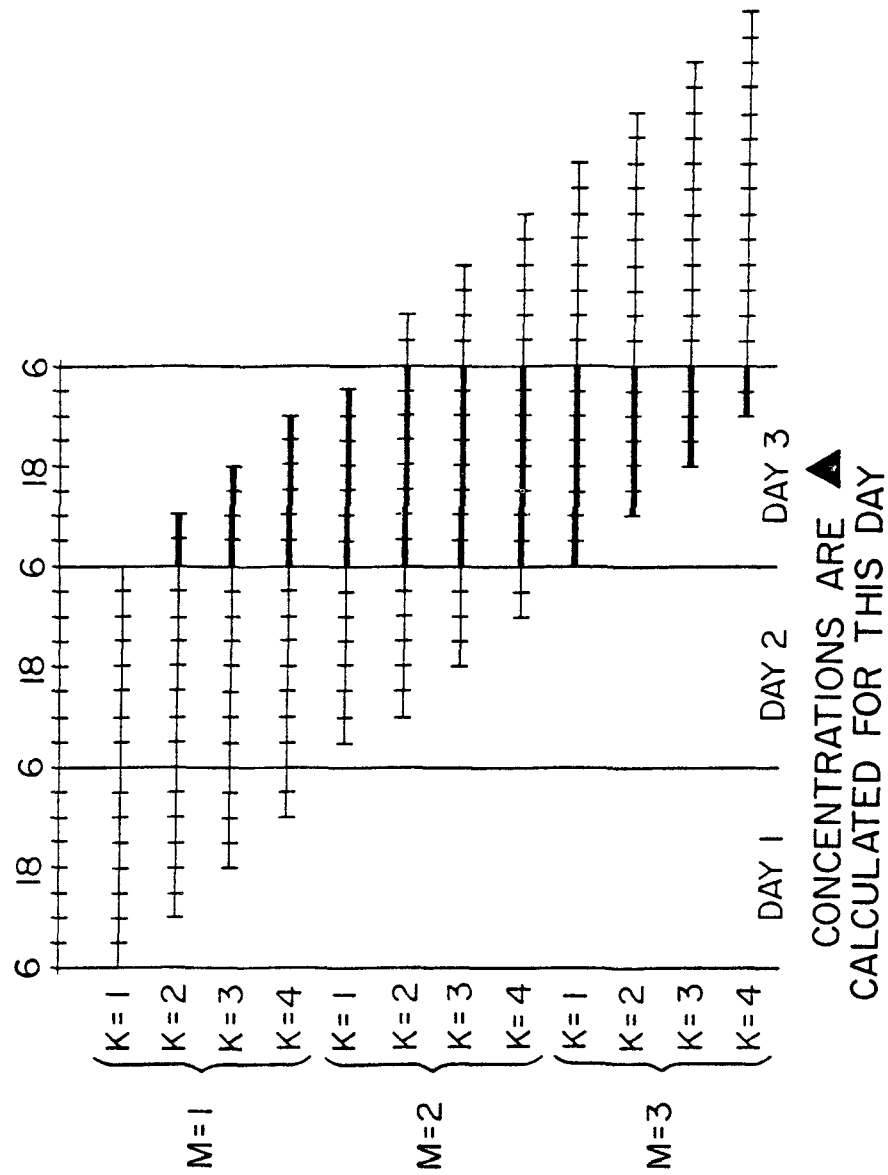


Fig. 1. Scheme of calculating 24-hour average concentrations. Here M is the number of days and K is the number of trajectories in a day.

scavenging processes will be needed for clues to an understanding of the seasonal variation of the amount of sulfate in precipitation.

### Transformation

The transformation rates of  $\text{SO}_2$  to sulfate depends on sunlight intensity and also appears to depend on water vapor concentration, back-ground ozone levels and the extent to which the plume has mixed with background air (Husar et al., 1978 and Wilson, 1978). Husar et al. reported that during the noon hours of summer the transformation rate is  $0.01 \sim 0.04 \text{ hr}^{-1}$  and below  $0.005 \text{ hr}^{-1}$  during the night. In accordance with these values and based on the results of preliminary calculation we select  $0.05 \text{ hr}^{-1}$  during the daytime and  $0.001 \text{ hr}^{-1}$  during the night in the present model.

## SECTION 4

### RESULTS OF MODEL APPLICATIONS FOR 24-HOUR AVERAGE CONCENTRATIONS OF $\text{SO}_2$ AND OF SULFATE

In this section we describe the results of model applications. We calculated the geographical distributions of the 24-hour average concentrations of  $\text{SO}_2$  and of sulfate over the region between  $35^\circ\text{N}$  and  $45^\circ\text{N}$  and between  $75^\circ\text{W}$  and  $95^\circ\text{W}$ , which encompasses the Ohio River basin. Part of the computations was conducted on the EPA computer. The dates chosen for computations were January 25, and July 11, 1976 on which the observed concentrations of  $\text{SO}_2$  and sulfate at stations located in the region were abundant.

#### INPUT DATA

Sixty point sources of  $\text{SO}_2$  whose emission rate is more than  $10^5$  ton/year were taken into consideration. The geographical locations and the emission rates are shown in Fig. 2 (Clark, 1979). The emission of  $\text{SO}_2$  from these sources contains about 90% of the total emissions over the area.

Upper-air data, which were prepared by ARL, NOAA and purchased from the NMC, contain upper air winds, temperature, and heights from rawinsonde stations for North America from the surface to 500 mb. Station identification information, including average terrain height at each station, and observed meteorological data were recorded for four observation times per day (00, 06, 12, and 18Z).

The precipitation rate data for 81 stations located in the region were used to calculate the wet deposition amounts.

#### RESULTS AND DISCUSSION

The distributions of 24-hour average concentrations of  $\text{SO}_2$  are shown in Figs. 3a and b. Figure 3a is for the date of January 25, 1976 and 3b for the date of July 11, 1976. On January 25 high concentrations are found in the northeastern part of the region. On the other hand, the southeastern part of the region was covered by high concentrations of  $\text{SO}_2$  on July 11. Predominant winds over the region on these dates were respectively from the southwest and from the northwest.

Figures 4a and b contain the distributions of sulfate concentration at the surface level. Again, high concentrations of sulfate can be found in the

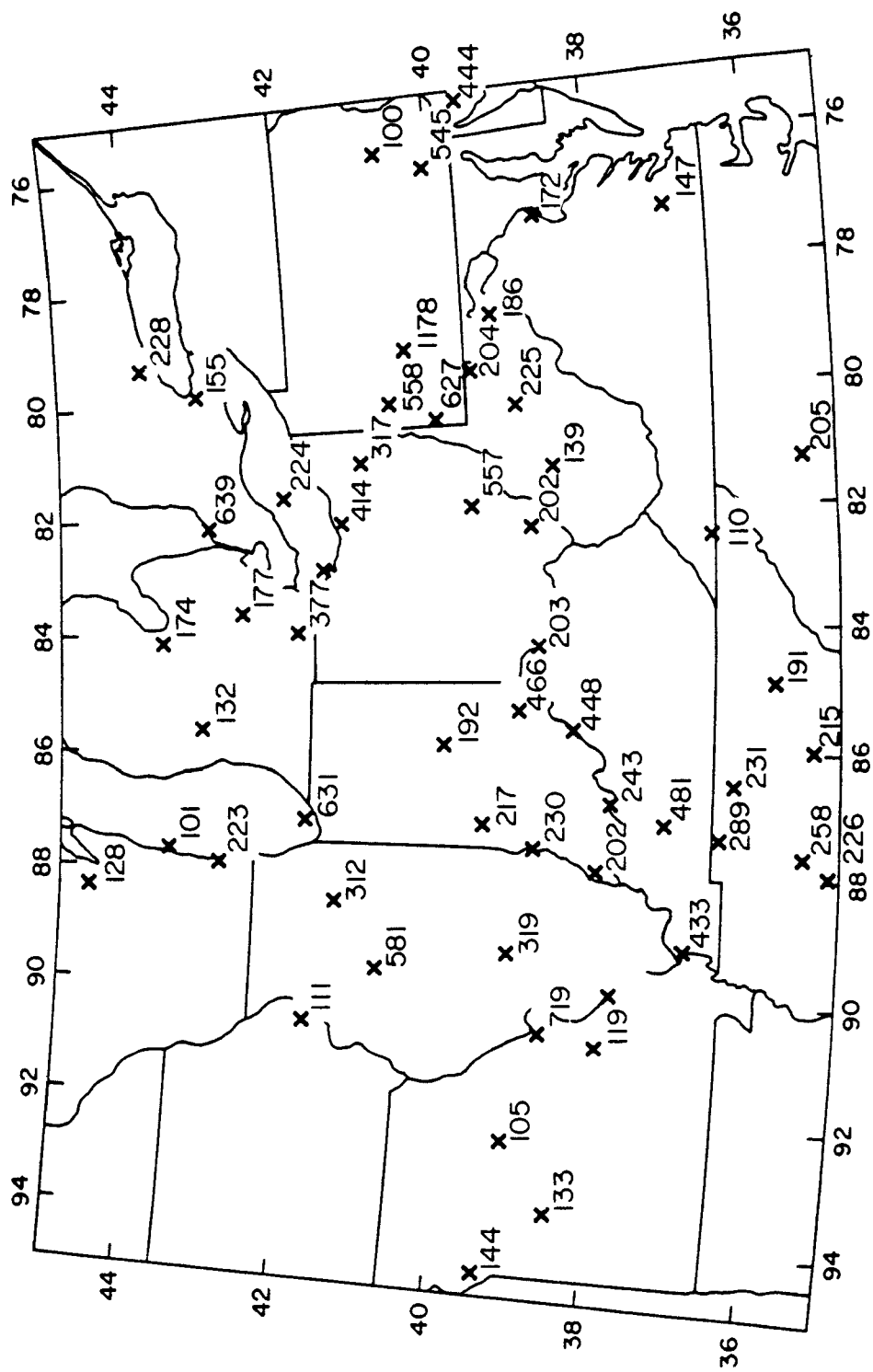


Fig. 2. Locations and intensities of SO<sub>2</sub> emission sources (x 10<sup>3</sup> ton/year).

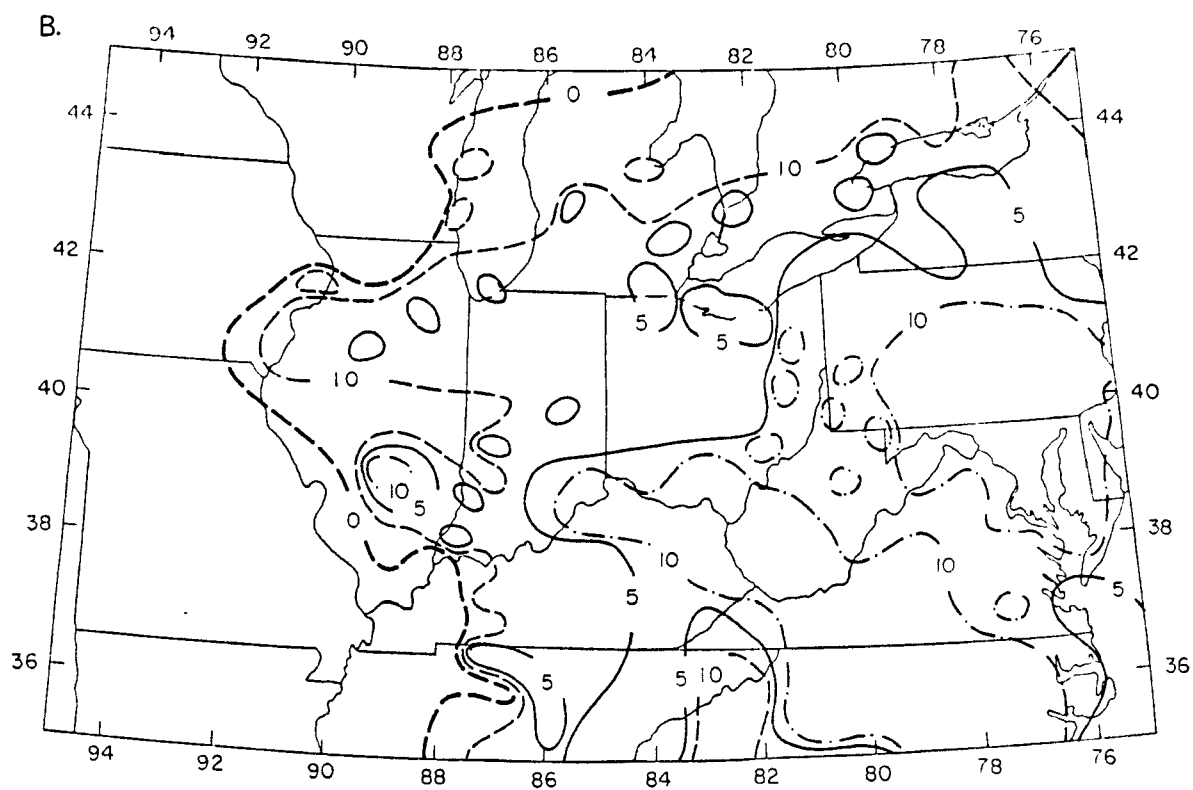
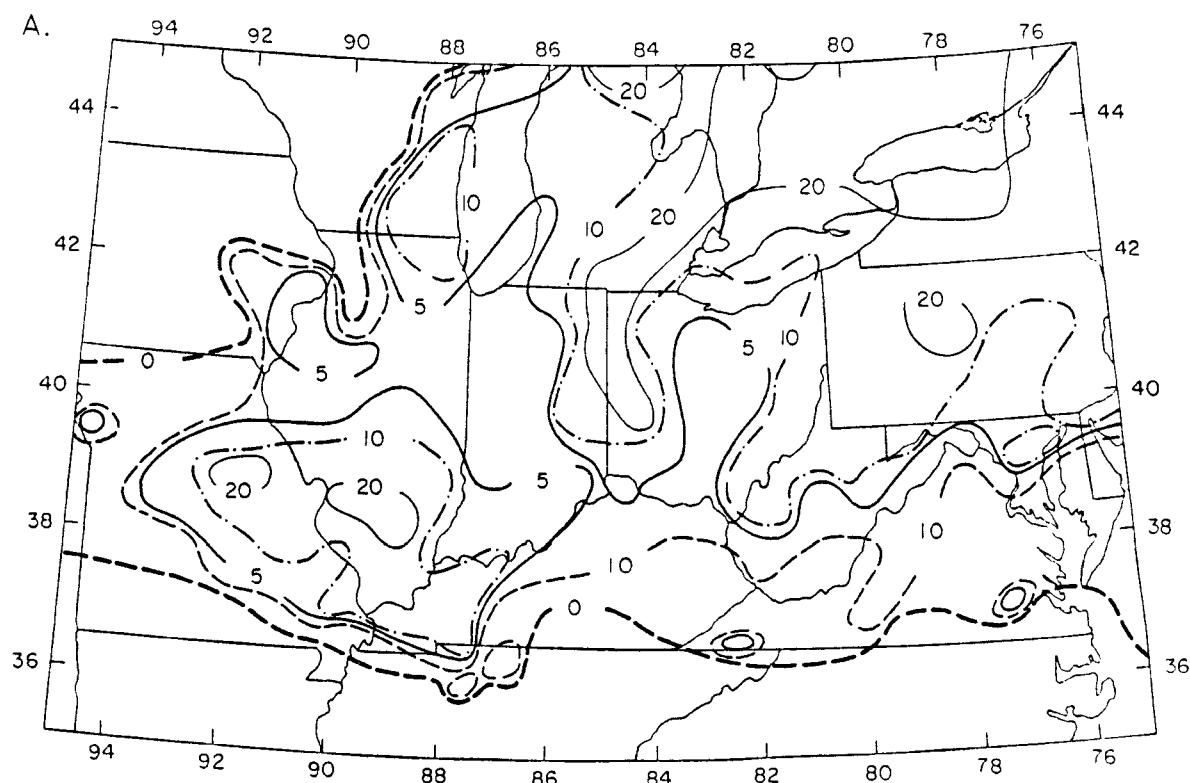


Fig. 3. Distribution of  $\text{SO}_2$  concentrations ( $\mu\text{g}/\text{m}^3$ ) at the surface level on (a) January 25, 1976 and (b) July 11, 1976.



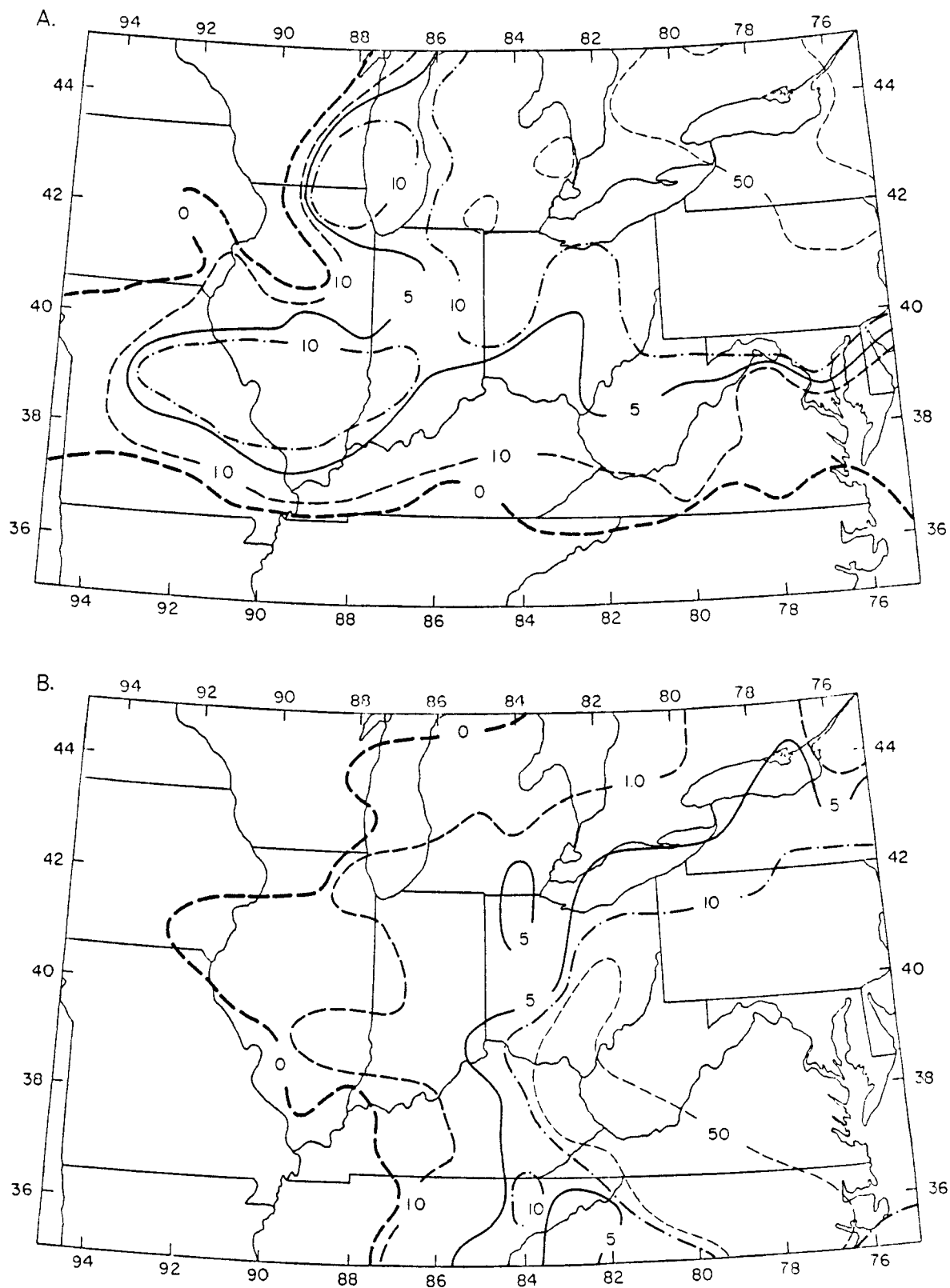


Fig. 4. Distribution of sulfate concentrations ( $\mu\text{g}/\text{m}^3$ ) at the surface level on (a) January 25, 1976 and (b) July 11, 1976.

northeastern part and in the southeastern part of the region on January 25 and July 11, respectively.

In both Fig. 3 and Fig. 4, it can be seen that the western part of the region was covered by clear air.

The distributions of deposition amounts of  $\text{SO}_2$  due to dry and wet depositions are shown in Figs. 5a and b. Figures 6a and b contain the distributions of deposition amounts of sulfate due to dry and wet depositions.

It can be seen from Figs. 7a and b that the removal of  $\text{SO}_2$  due to precipitation is inefficient. At the present time we are not certain how appropriate these results are due to the nonexistence of observed data of  $\text{SO}_2$  content in precipitation water. In the present model, the precipitation scavenging velocity is given by

$$v_s = 1 \times 10^4 \times P \text{ cm/sec} \quad (6)$$

where  $P$  is the precipitation rate (cm/hr). The validity of this assumption will be examined in the future.

Figures 8a and b show the distribution of wet deposition amounts ( $\text{kg/km}^2$ ) of sulfate. These amounts are substantial compared with those of  $\text{SO}_2$ .

In order to verify the performance of the model, concentrations of  $\text{SO}_2$  and sulfate calculated for the surface level were compared with concentrations observed at stations located in the region. The 24-hour average concentrations of  $\text{SO}_2$  and sulfate from observed data were supplied by EPA. The observed concentrations of  $\text{SO}_2$  are plotted against the calculated ones in Figs. 9a and b. Similar figures for sulfate are given in Figs. 10a and b.

From these figures it can be seen that the calculated  $\text{SO}_2$  concentrations are generally too low compared to the observed concentrations, and that the calculated sulfate concentrations are generally too high. These facts clearly indicate that the transformation rate from  $\text{SO}_2$  to sulfate used in the present calculations is too large.

Correlation coefficients between the observed concentrations and the calculated concentrations are given in Table 1.

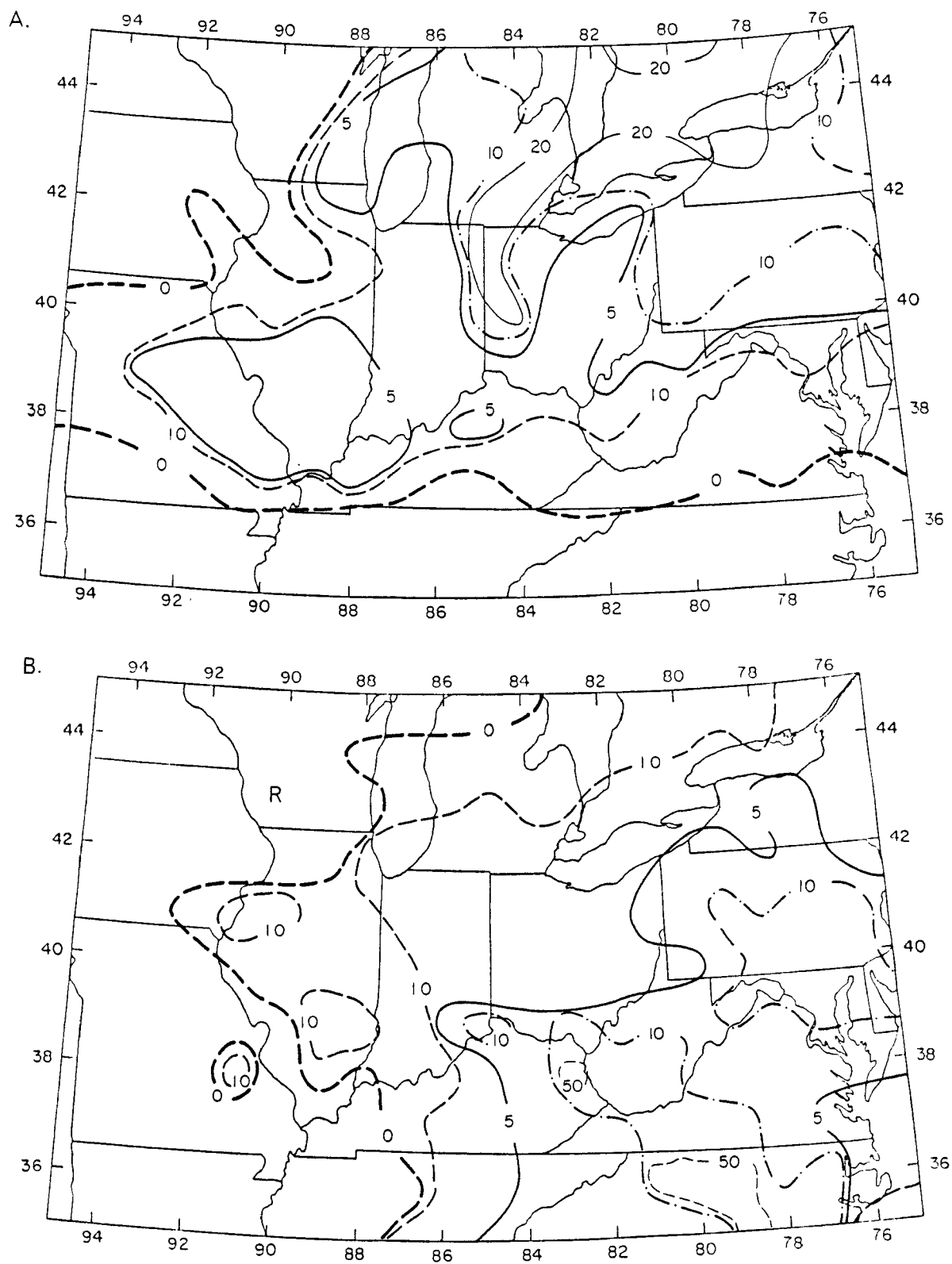


Fig. 5. Distribution of  $\text{SO}_2$  deposition amounts due to dry and wet deposition on (a) January 25, 1976 and (b) July 25, 1976.

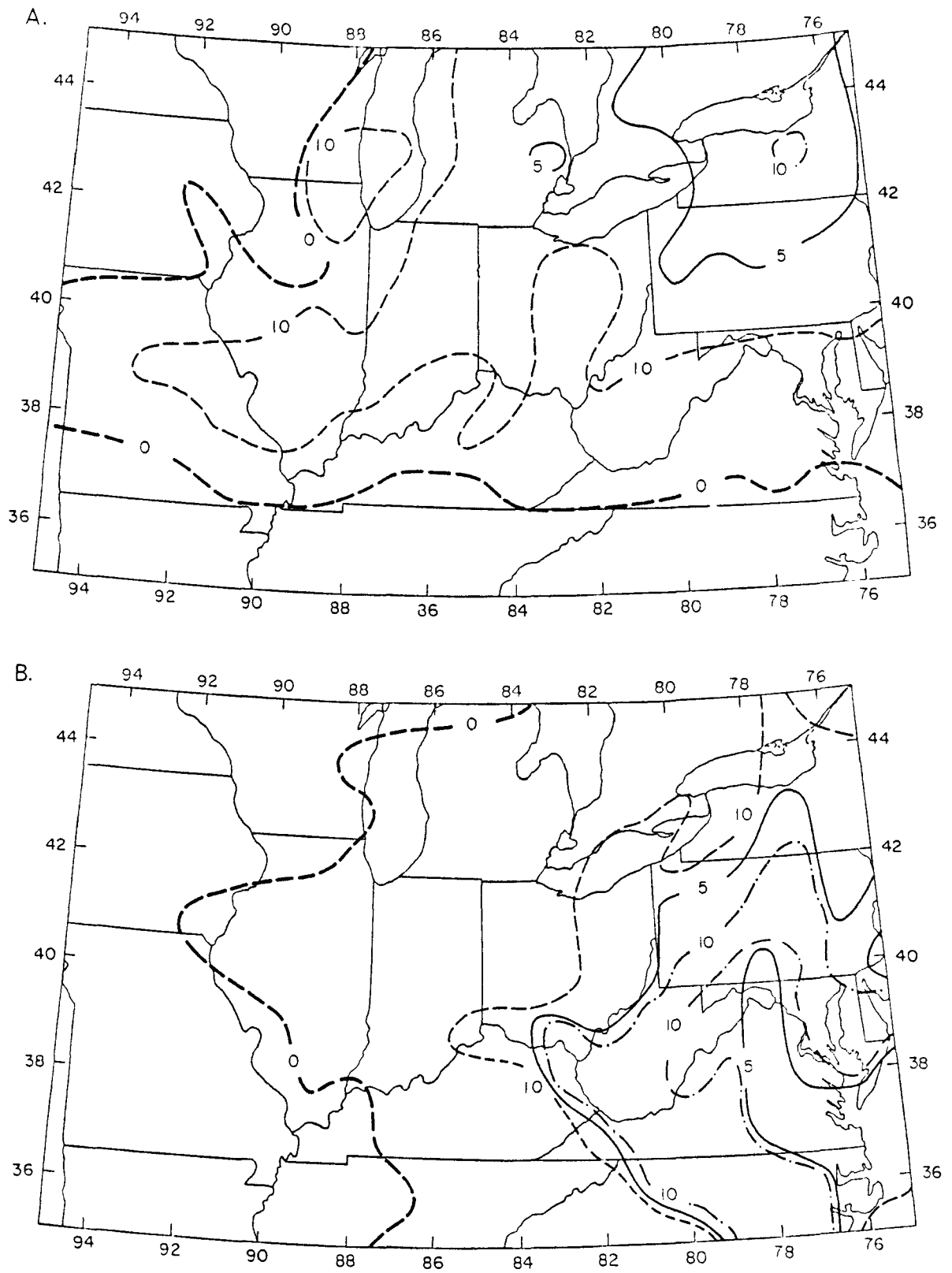


Fig. 6. Distribution of sulfate deposition amounts ( $\text{kg/km}^2$ ) due to dry and wet deposition on (a) January 25, 1976 and (b) July 11, 1976.

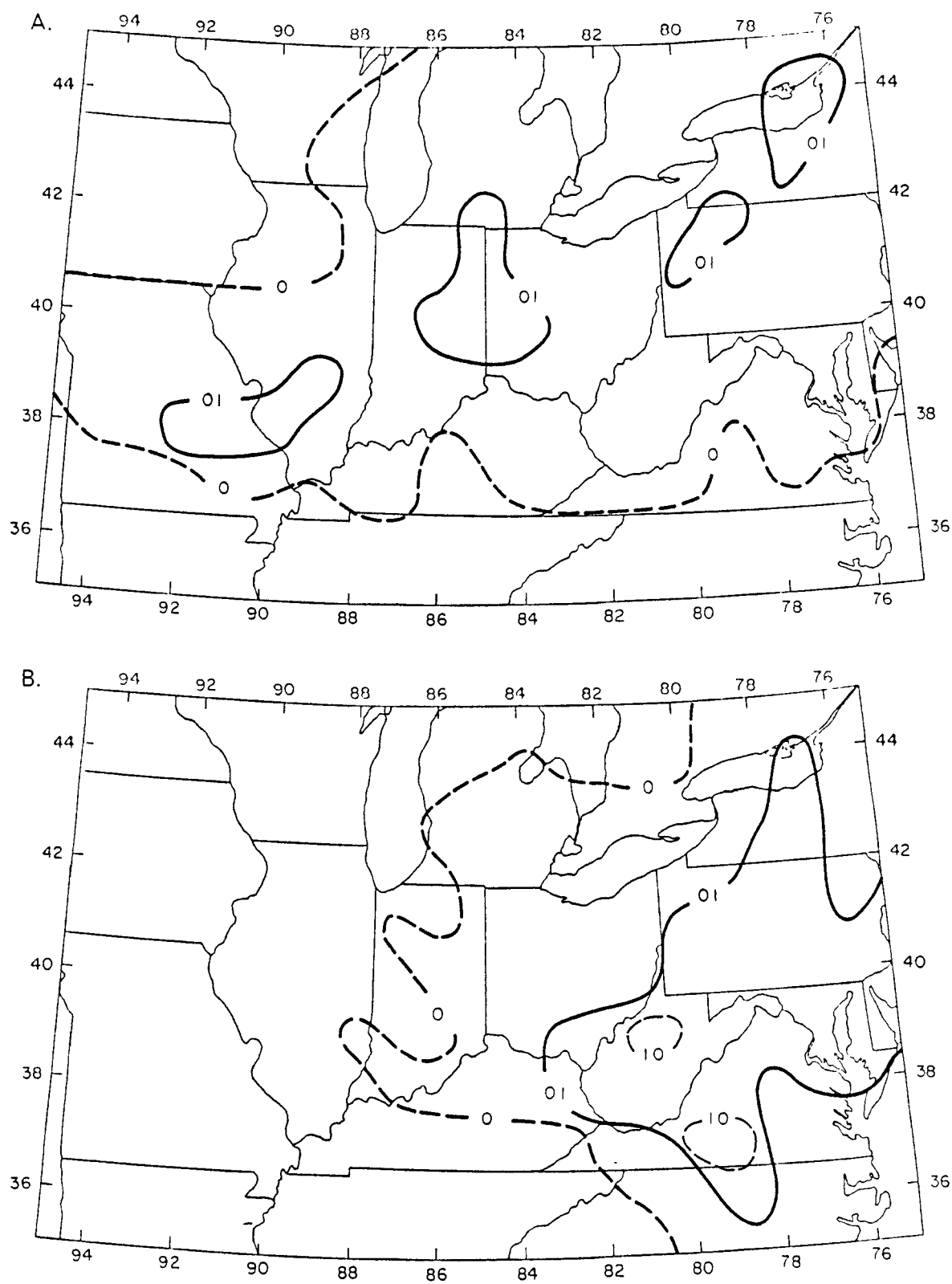


Fig. 7. Distribution of  $\text{SO}_2$  deposition amounts (kg/km<sup>2</sup>) due to precipitation on (a) January 25, 1976 and (b) July 11, 1976.

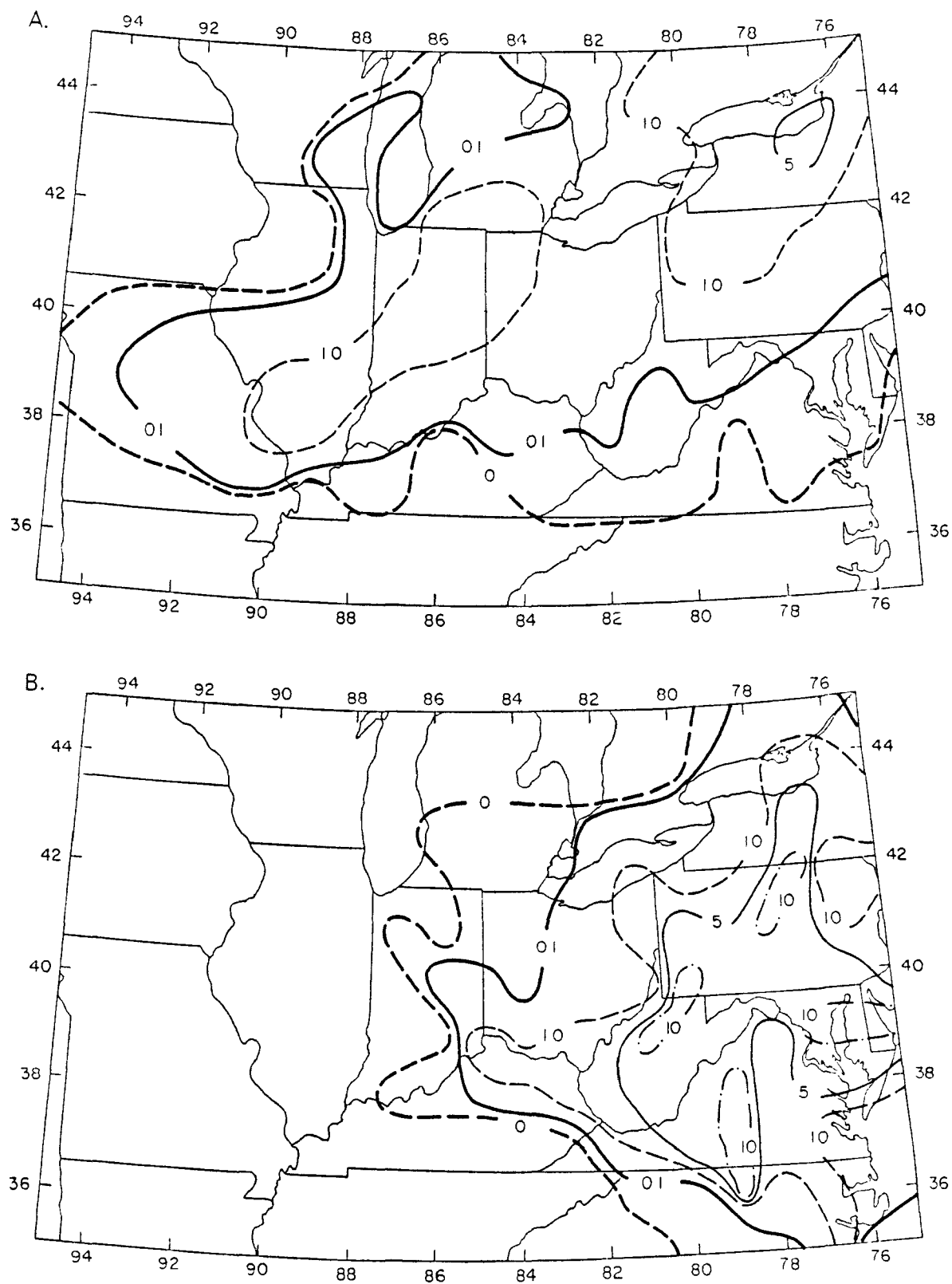


Fig. 8. Distribution of sulfate deposition amounts (kg/km<sup>2</sup>) due to precipitation on (a) January 25, 1976 and (b) July 11, 1976.

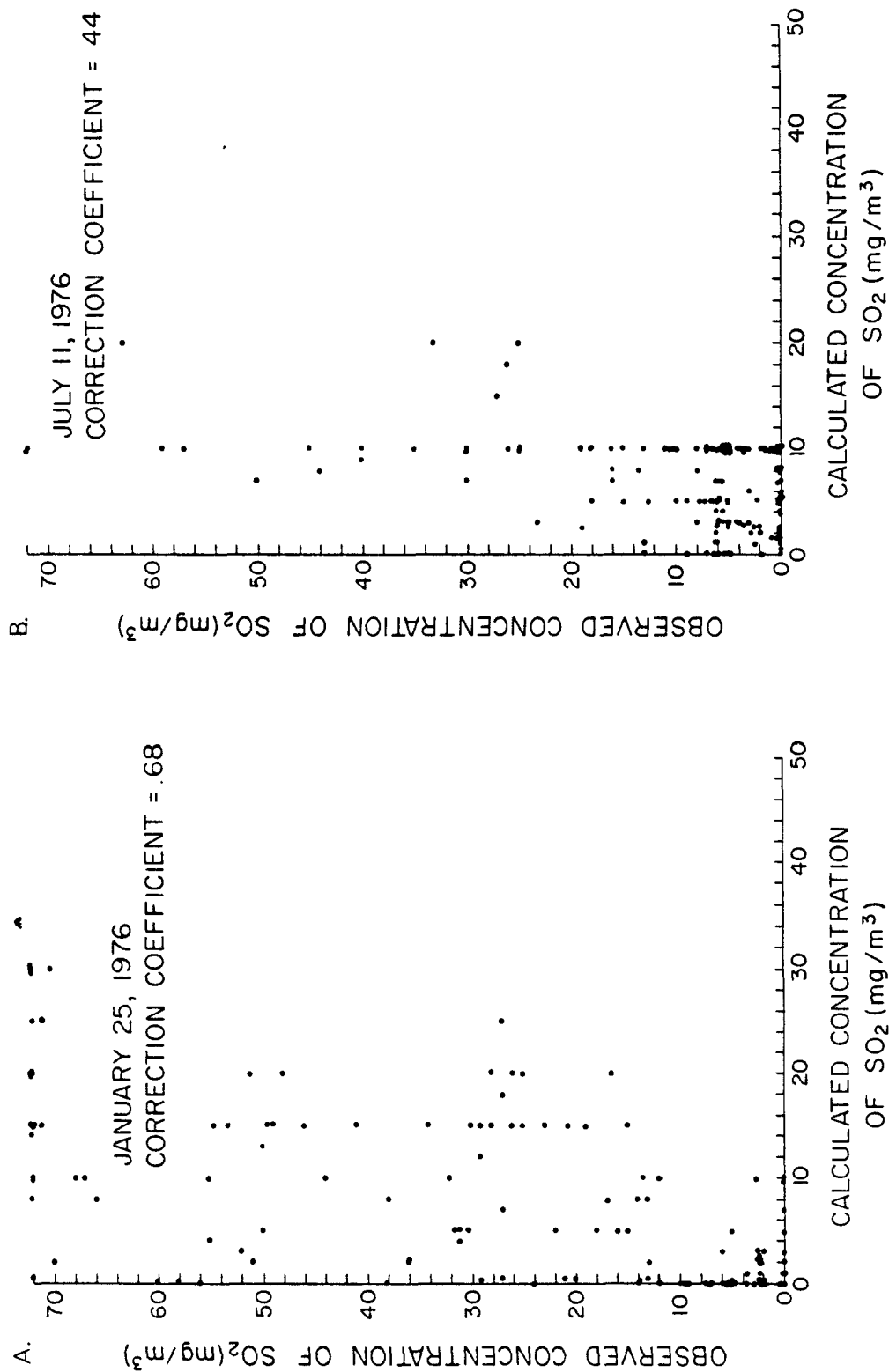


Fig. 9. Relationship between calculated and observed  $\text{SO}_2$  concentrations on (a) January 25, 1976 and (b) July 11, 1976.

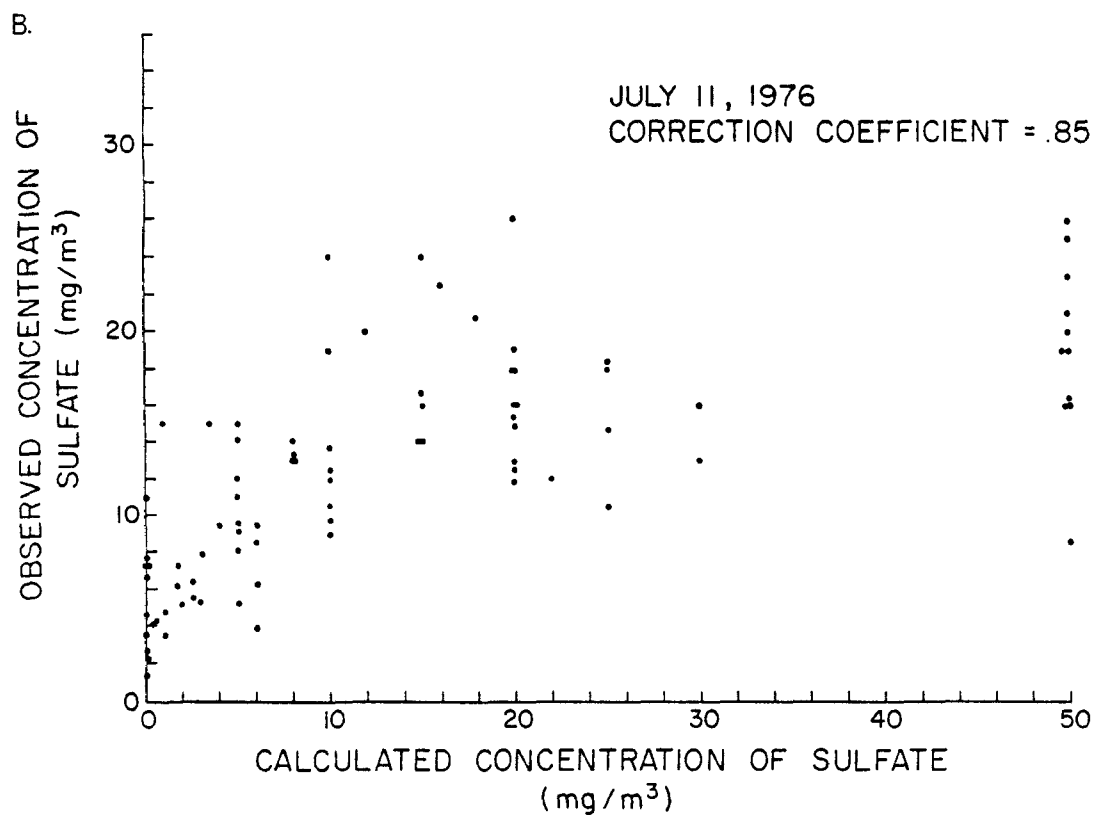
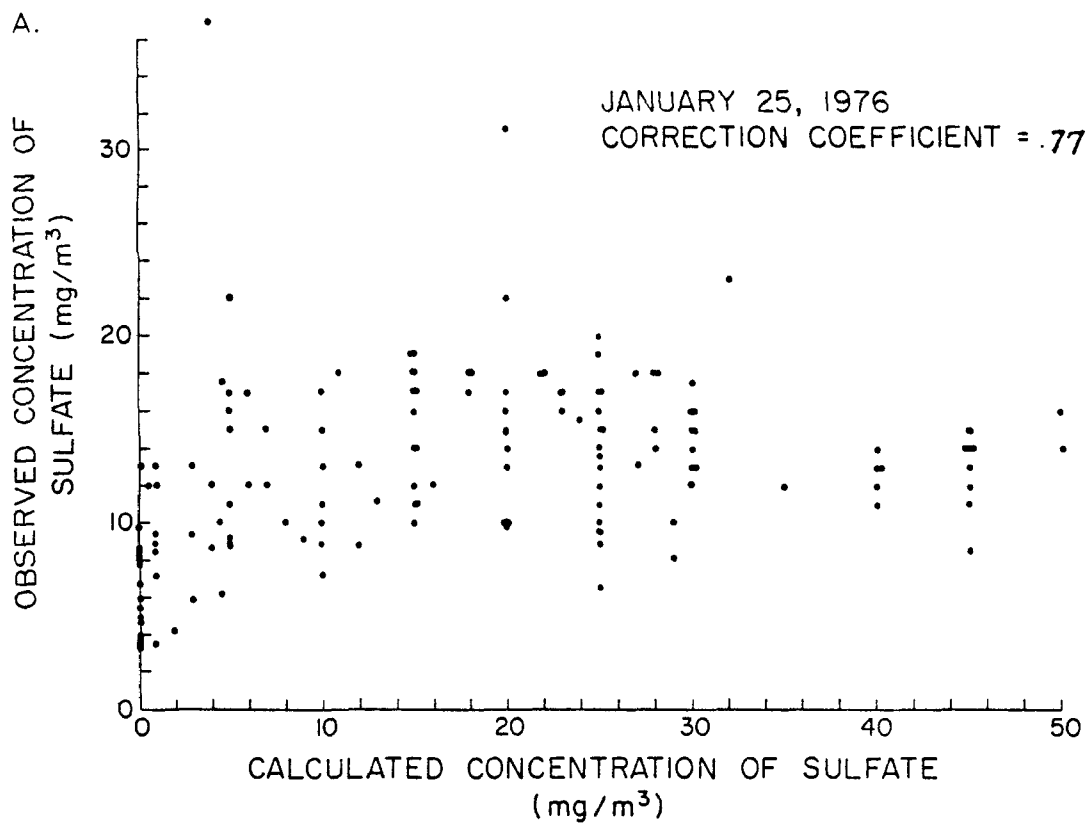


Fig. 10. Relationship between calculated and observed sulfate concentrations on (a) January 25, 1976 and (b) July 11, 1976.



Table 1. Correlation coefficient between the observed concentrations and the calculated concentrations.

|                 | January 25                            | July 11                               |
|-----------------|---------------------------------------|---------------------------------------|
| SO <sub>2</sub> | r=0.68 (r <sub>c</sub> =0.202, N=162) | r=0.44 (r <sub>c</sub> =0.176, N=216) |
| Sulfate         | r=0.77 (r <sub>c</sub> =0.205, N=155) | r=0.85 (r <sub>c</sub> =0.278, N=86)  |

In this table,  $r$  is the correlation coefficient,  $r_c$  is the critical value for correlation coefficients with 99.9% confidence levels and  $N$  is the number of data pairs. Although the calculated concentrations are statistically related to the observed concentrations for SO<sub>2</sub> as well as for sulfate, the values of the correlation coefficients are not significantly high. In particular, the correlation coefficients between the observed SO<sub>2</sub> concentrations and the calculated concentrations are disappointingly low. This low correlation can be partially attributed in addition to the inappropriate value of the transformation rate to the following fact: in the previous application (Henmi and Reiter, 1979), the data taken at stations classified as "rural", "remote", and "suburban-residential" were used for comparison of SO<sub>2</sub> concentrations. Such a screening procedure of the data was not conducted in the present study.

Sulfur budgets over the region for January 25, 1976 and July 11, 1976 were calculated as Table 2.

Table 2. Sulfur budget of the region.

|   | January 25, 1976 | July 11, 1976 |
|---|------------------|---------------|
| Sulfur Emission                                     | 24,492 tons      |               |
| Removal by Wet Deposition                           |                  |               |
| as SO <sub>2</sub>                                  | 90 tons          | 129 tons      |
| as Sulfate  | <u>718</u>       | <u>1,886</u>  |
|   | 808              | 2,015         |
| Removal by Dry Deposition                           |                  |               |
| as SO <sub>2</sub>                                  | 9,240            | 6,406         |
| as Sulfate  | <u>927</u>       | <u>1,089</u>  |
|   | 10,167           | 7,495         |
| Total Deposition of Sulfur                          | 10,975           | 9,510         |
| Amount Exported Across the Boundaries of the Region | 13,517           | 14,982        |

Table 2 shows that more than 50 percent of sulfur is exported across the boundaries of the region for both dates. Significant differences of the present calculation from the previous estimates (Henmi and Reiter, 1979) are found in the removal due to precipitation. In the previous calculation, about 30 percent of sulfur was removed by precipitation, whereas less than 10 percent is thus removed in the present calculation. The change of the wet removal formula in the model is the major reason for this drastic decrease in the removal amount.

## SECTION 5

### DEVELOPMENT OF A CLIMATOLOGICAL MODEL OF $\text{SO}_2$ AND SULFATE TRANSPORT

#### INTRODUCTION

One of the purposes of this project was to develop a climatological model of  $\text{SO}_2$  and sulfate transport and transformation. Our intention was to develop a model which was economical in computing time and which could be applied to the studies of the distribution of acidity of precipitation over the area of eastern North America and of the transport and deposition of sulfur across the national boundaries between the U.S. and Canada.

In this section, we describe the details of the climatological model developed.

#### MODEL

##### Trajectory Calculations

In this climatological model, trajectories of air parcels are computed (using average wind speeds and directions of the mixing layer) four times a day from each source for 30 days. The locations of the endpoints of the trajectory segments are calculated at 3-hour intervals. Each air parcel is tracked up to 3 days. In the model developed for calculating 24-hour average concentration (see Section 3), the vertical temperature profiles along a trajectory were considered to determine mixing layer depths over which average transport winds were calculated. Furthermore, trajectories of average winds of nighttime and daytime mixing layers, as well as trajectories of average winds of the layer between daytime mixing height and nighttime mixing height, in which pollutants were trapped during the nighttime, were taken into consideration.

In contrast, trajectories of average winds of the daytime mixing layer defined from climatological data (Holzworth, 1972) are calculated in this model. The reasons for this simplification are as follows: The error of trajectory calculations due to the use of the climatological height of the mixing layer over the area of interest, instead of the use of mixing height determined from soundings along the individual trajectories may be cancelled out when the average locations of numerous trajectories are calculated, and a substantial savings can be realized in computing time.

The coordinates of the endpoints of the trajectory segments can be expressed as follows:

$$X_{j\ell} = U(X_{j-1,\ell}, Y_{j-1,\ell})\Delta t \quad (7)$$

$$Y_{j\ell} = V(X_{j-1,\ell}, Y_{j-1,\ell})\Delta t \quad (8)$$

where  $\Delta t$  is the time interval,  $U$  and  $V$  are the velocity components in  $X$  (west-east) and  $Y$  (south-north) direction,  $j=1, 2, \dots, N$  are trajectory endpoints at the time of  $t=\Delta t, 2\Delta t, \dots, N\Delta t$  from the start of the calculation,  $\ell$  is the label for each trajectory. In the application described in the next section,  $\Delta t$ , and  $N$  are 3 hours and 24 hours respectively, and the total number of trajectories from each source is 120 ( $4 \times 30$ ).

The coordinates of the average trajectory of air parcels leaving from each source area are expressed as:

$$\bar{X}_j = \frac{1}{L} \sum_{\ell=1}^L X_{j\ell} \quad (9)$$

$$\bar{Y}_j = \frac{1}{L} \sum_{\ell=1}^L Y_{j\ell} \quad (10)$$

where  $L$  is equal to 120 in the present application.

It is assumed that  $SO_2$  and sulfate emitted from the source are transported and transformed along the average trajectory and that they are dispersed into the  $X$ - and  $Y$ - directions from the average trajectory as described in the next section. Mixing in the vertical direction is assumed uniform throughout the layer.

### Horizontal Dispersion

In the model the long-term average plume from a pollutant source is approximated by a series of puffs. Horizontal dispersion of pollutants from the center of a puff can be expressed as:

$$D_{x,j} = \Sigma_{x,j} + \sigma_{x,j} \quad (11)$$

$$D_{y,j} = \Sigma_{y,j} + \sigma_{y,j} \quad (12)$$

Here,  $D_{x,j}$  and  $D_{y,j}$  are the total dispersion of pollutants in the  $x$  and  $y$  direction, respectively.  $\Sigma_{x,j}$  and  $\Sigma_{y,j}$  are the dispersion due to the meandering of each trajectory, and  $\sigma_{x,j}$  and  $\sigma_{y,j}$  are the dispersion due to the vertical shear of wind. These dispersion parameters can be written as follows:

$$\Sigma_{x,j} = \sqrt{\frac{(X_{j\ell} - \bar{X}_j)^2}{L}} \quad (13)$$

$$\Sigma_{y,j} = \sqrt{\frac{(Y_{j\ell} - \bar{Y}_j)^2}{L}} \quad (14)$$

$\sigma_{x,j}$  and  $\sigma_{y,j}$  are described by

$$\sigma_{x,j} = \sum_{\ell=1}^j \bar{\sigma}_{u,j} \cdot \Delta t \quad (15)$$

$$\sigma_{y,j} = \sum_{\ell=1}^j \bar{\sigma}_{v,j} \cdot \Delta t \quad (16)$$

where

$$\sigma_{u,j\ell} = \sqrt{\frac{\int_0^h (U_{j\ell}(z) - \bar{U}_{j\ell})^2 dz}{h}} \quad (17)$$

$$\sigma_{v,j\ell} = \sqrt{\frac{\int_0^h (V_{j\ell}(z) - \bar{V}_{j\ell})^2 dz}{h}} \quad (18)$$

and

$$\bar{\sigma}_{u,j} = \frac{1}{L} \sum_{\ell=1}^L \sigma_{u,j\ell} \quad (19)$$

$$\bar{\sigma}_{v,j} = \frac{1}{L} \sum_{\ell=1}^L \sigma_{v,j\ell} \quad (20)$$

Here the above notations are defined as follows:

- $\sigma_{u,j\ell}$  and  $\sigma_{v,j\ell}$ : standard deviation of wind speed with respect to height of  $\ell$ th trajectory at time step  $j$ .
- $U_{j\ell}(z)$  and  $V_{j\ell}(z)$ : x- and y-component of wind speed at height  $z$ .
- $\bar{U}_{j\ell}$  and  $\bar{V}_{j\ell}$ : average wind speeds of the layer.
- $h$ : the height of the mixing layer.
- $\bar{\sigma}_{u,j}$  and  $\bar{\sigma}_{v,j}$ : the average of  $\sigma_{u,j\ell}$  and  $\sigma_{v,j\ell}$ .

In this model, the dispersion due to instantaneous mixing is neglected. The dispersion parameters  $\Sigma_{x,j}$  and  $\Sigma_{y,j}$  and  $\sigma_{x,j}$  and  $\sigma_{y,j}$  are calculated for the plumes from each pollutant source.

In the application described in the following section, 120 trajectories (4 trajectories per day for 30 days) from each source were calculated for the duration of 72 hours. In application of this climatological model, trajectories from 72 major sources of  $SO_2$  over the region of eastern North America were computed using wind data for the month of January, 1967. In Figs. 11a and 11b, and Figs. 12a and 12b, the averages of  $\Sigma_x$  and  $\Sigma_y$ , and of  $\sigma_x$  and  $\sigma_y$  for trajectories from 72 major sources are shown. In these figures, thick lines represent the average values and thin lines are the standard deviations.

In comparing Figs. 11a and 11b, it can be seen that the dispersion due to meandering of the trajectories is substantially greater in the x direction than in the y direction. Furthermore, Figs. 12a and 12b show that the dispersion due to wind shear is comparable to that due to meandering of the trajectories.

### Concentration Distribution

It is assumed that in a horizontal direction pollutants in a puff are dispersed according to a Gaussian distribution. Therefore, the horizontal distribution function of  $SO_2$  and sulfate is expressed by

$$P_h(x-\bar{x}_j, y-\bar{y}_j) = \frac{1}{2 D_x D_y} \cdot \exp\left\{-\frac{1}{2} \left[ \left(\frac{x-\bar{x}_j}{D_x}\right)^2 + \left(\frac{y-\bar{y}_j}{D_y}\right)^2 \right]\right\} \quad (21)$$

where  $x-\bar{x}_j$ , and  $y-\bar{y}_j$  are the distances in the x- and y-directions, respectively, from the center of a puff, and  $D_x$  and  $D_y$  have been defined by Eqs. (11) and (12) in the previous section. A similar approach has been taken by Sheih (1977).

$SO_2$  and sulfate are transformed and deposited along a mean trajectory according to the following equations.

$$\frac{dQ_1}{dt} = - \left[ \frac{V_{g1} + V_{s1}}{h} \right] \cdot Q_1 - KQ_1 \quad (22)$$

$$\frac{dQ_2}{dt} = - \left[ \frac{V_{g2} + V_{s2}}{h} \right] \cdot Q_2 + \frac{3}{2} KQ_1 \quad (23)$$

where  $Q_1$  and  $Q_2$  are the mass of  $SO_2$  and sulfate,  $V_{g1}$  and  $V_{g2}$  are the dry deposition velocities,  $V_{s1}$  and  $V_{s2}$  are the wet deposition velocities due to precipitation,  $K$  is the transformation rate, and  $h$  is the height of the mixing layer. The subscripts 1 and 2 stand for  $SO_2$  and sulfate.

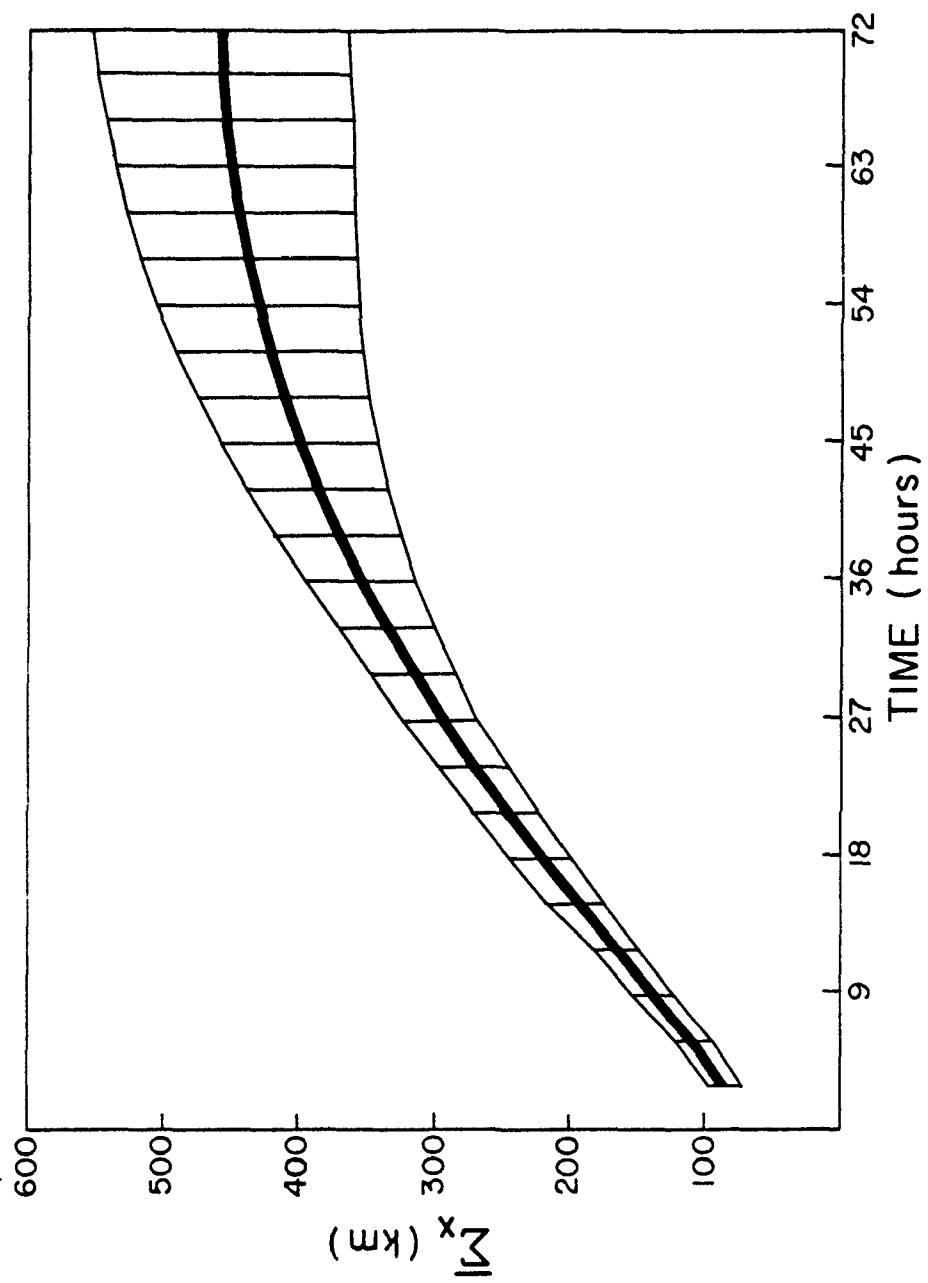


Fig. 11a Average values of the dispersion parameter of  $\Sigma_x$  and its standard deviation in the x direction due to the meandering of trajectories as a function of time.

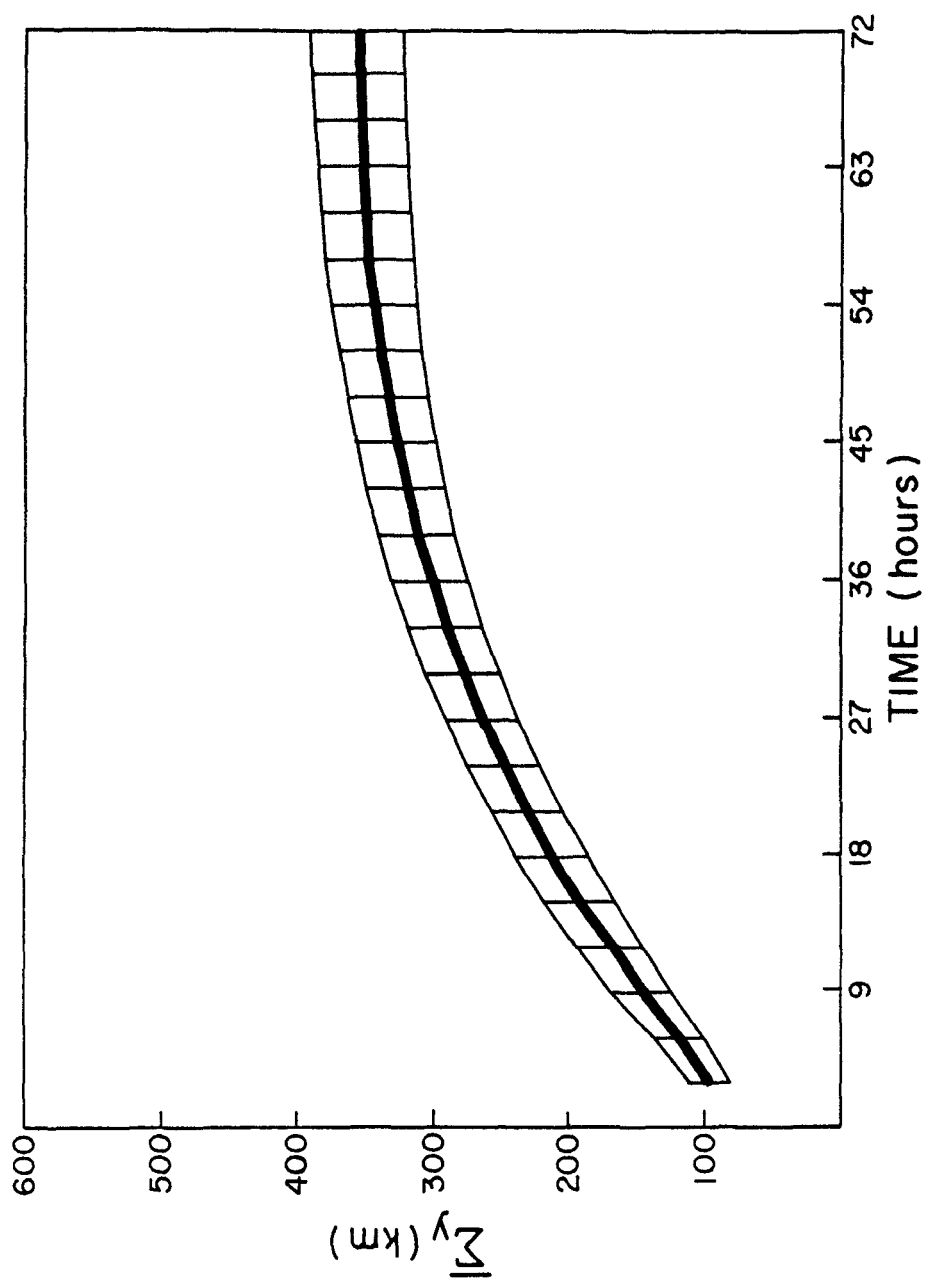


Fig. 11b Same as Fig. 11a, except for y direction.



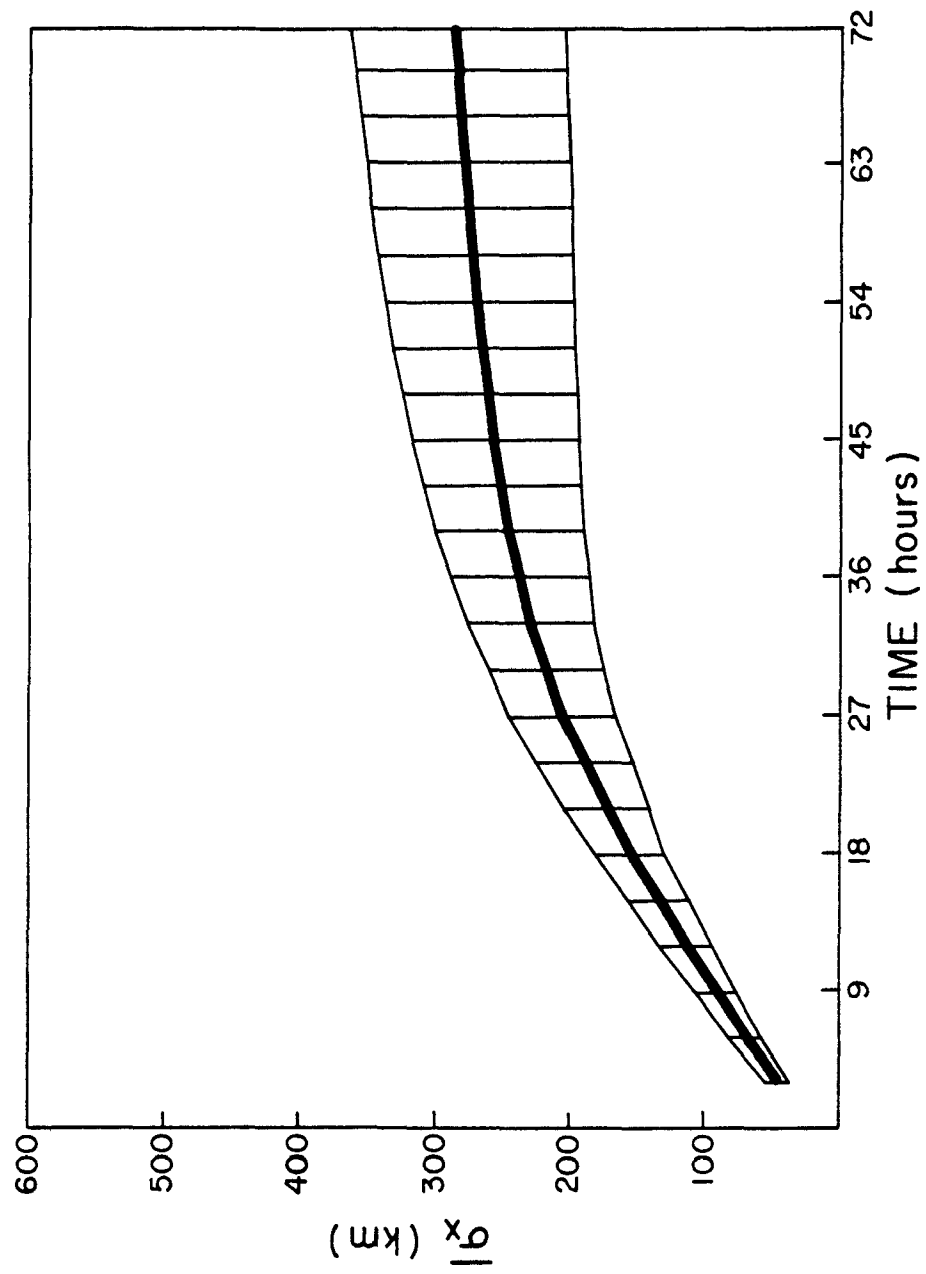


Fig. 12a Average values of the dispersion parameter of  $\sigma_x$  and its standard deviation due to vertical wind shear.

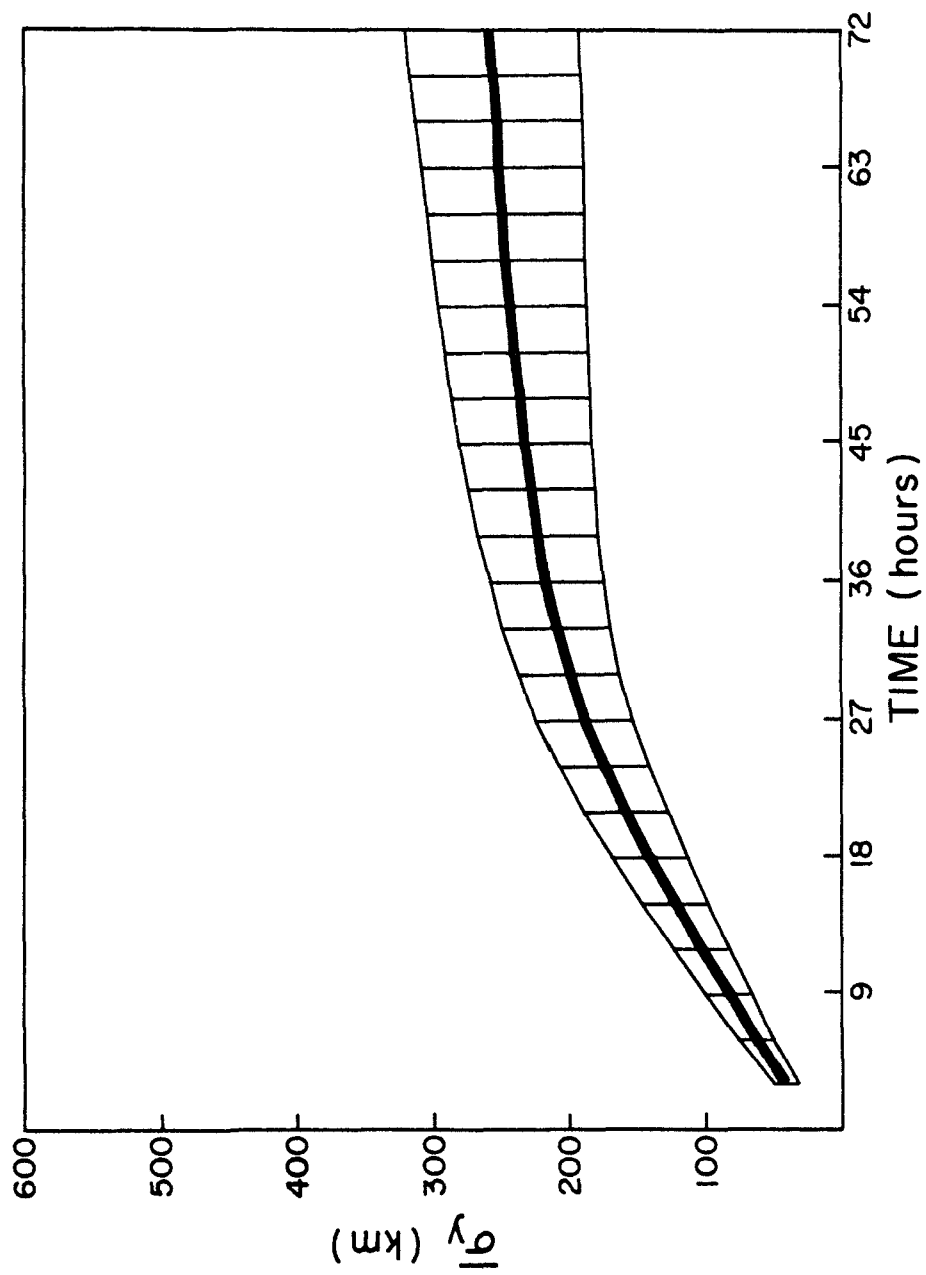


Fig. 12b Same as Fig. 12a, except for  $\sigma_y$ .

Concentrations of SO<sub>2</sub> and sulfate, C<sub>1</sub> and C<sub>2</sub>, can therefore be expressed by

$$C_1 = \frac{Q_1}{h} \cdot p_h(x-\bar{x}_j, y-\bar{y}_j) \quad (24)$$

$$C_2 = \frac{Q_2}{h} \cdot p_h(x-\bar{x}_j, y-\bar{y}_j) \quad (25)$$

The details on dry deposition velocity, wet deposition velocity, and transformation rate have been described in Section 3 and elsewhere (Henmi, 1979 and 1980; Henmi and Reiter, 1979).

Concentrations at the grid point (x, y) are calculated by

$$C_1(x,y) = \sum_{j=1}^N \sum_{i=1}^M C_{1ij} \quad (26)$$

$$C_2(x,y) = \sum_{j=1}^N \sum_{i=1}^M C_{2ij} \quad (27)$$

where C<sub>1</sub>(x,y) and C<sub>2</sub>(x,y) are the concentrations of SO<sub>2</sub> and sulfate at the grid point (x,y), respectively, the subscript i represents the source number, and j stands for the number of puffs. In this study, N is 24 and the total number of sources, M, is 72.

#### Deposition Amount

Concentration distributions of SO<sub>2</sub> and sulfate are calculated over the region between 35°N and 53°N and between 62°W and 95°W. In order to estimate the deposition amount of sulfur, the gridded regions are divided into four major areas as shown in Fig. 13: the United States, Canada, the Great Lakes and the Atlantic Ocean.

The dry and wet deposition amounts of sulfur, D<sub>d</sub> and D<sub>w</sub>, for each grid point (x,y) are calculated as

$$D_d(x,y) = V_{g1} \cdot \frac{C_1(x,y)}{2} + V_{g2} \cdot \frac{C_2(x,y)}{3} \quad (28)$$

$$D_w(x,y) = V_{s1} \cdot \frac{C_1(x,y)}{2} + V_{s2} \cdot \frac{C_2(x,y)}{3} \quad (29)$$

The total amount of sulfur deposition for each region is, therefore, expressed by

$$D_{d,T} = \int D_d \cdot dS = \sum D_d(x,y) \cdot \Delta x \cdot \Delta y \quad (30)$$

$$D_{w,T} = \int D_w \cdot dS = \sum D_w(x,y) \cdot \Delta x \cdot \Delta y \quad (31)$$

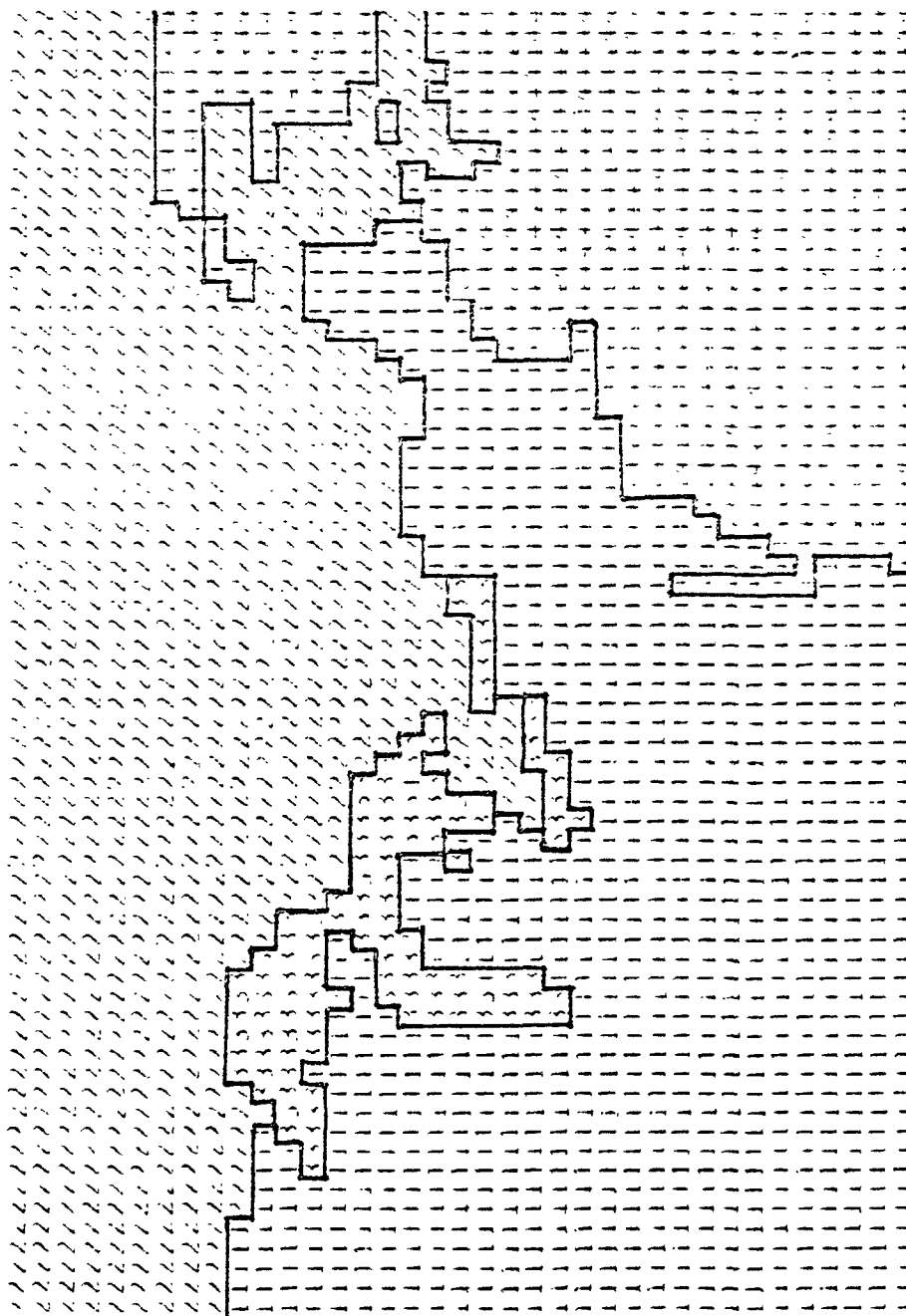


Fig. 13 Division of the region into four major areas. For the U.S. the grid points are indexed by 1, Canada by 2, the Great Lakes by 3, and the Atlantic Ocean by 4.

where,  $dS$  is the area element and  $\Delta x$  and  $\Delta y$  are the grid intervals in the  $x$ - and  $y$ -directions, respectively.

#### Acidity of Precipitation Due to Sulfate

As will be described in Section 7 acidity of precipitation is a very complex problem. It has been shown that there are statistically significant correlations between observed pH and the content of sulfate in precipitation. For this preliminary application of the model, we assume, admittedly crudely, that the acidity of precipitation is expressed by the wet deposition amount of sulfate divided by the precipitation amount.

The pH value at grid point  $(x,y)$  is given by

$$\text{pH} = -\log_{10} 2[\text{SO}_4^=] = -\log_{10} \{2(\Sigma V_{s2} \cdot C_2(x,y)/P(x,y))\} \quad (32)$$

where  $[\text{SO}_4^=]$  is the molar content of  $\text{SO}_4^=$  in precipitation water (mole/ liter), and  $P(x,y)$  is the precipitation amount per unit area.

## CHAPTER 6

### RESULTS OF CLIMATOLOGICAL MODEL APPLICATIONS TO EASTERN NORTH AMERICA

#### INTRODUCTION

Using the model described in Section 5, we calculated the geographical distributions of the monthly average concentrations and deposition amounts of  $\text{SO}_2$  and of sulfate over the region between  $35^\circ\text{N}$  and  $53^\circ\text{N}$  between  $62^\circ\text{W}$  and  $95^\circ\text{W}$ , which encompasses eastern North America. Furthermore, the distributions of acidity of precipitation, and of the deposition amount of sulfur over the regions of the United States, Canada and the Great Lakes were calculated. Finally, mass budgets of anthropogenic sulfur for the regions were estimated.

The months chosen for computations were January 1977 and March 1979. For the month of January 1977, the calculated concentrations of  $\text{SO}_2$  and sulfate are compared with those observed in the region. For the month of March 1979 the calculated pH values are compared with those observed at stations of the National Atmospheric Deposition Program (Natural Resource Ecology Laboratory, 1980).

#### INPUT DATA

Seventy major sources of  $\text{SO}_2$  whose emission rate is more than  $10^5$  ton/year are taken into account. Figure 14 shows the geographical locations and the emission rates of these  $\text{SO}_2$  sources. This figure was composed from the emission inventory for the U.S. by Clark (1979) and from the emission inventory for Canada by Voldner et al. (1980).

The monthly precipitation amounts, for approximately 700 stations located in the region, were used to calculate the wet deposition amounts. The distribution of monthly precipitation for January 1977 and March 1979 are shown in Figs. 15a and b, respectively.

Upper air data, which consist of winds, temperature, and heights from rawinsonde stations for North America from the surface to 500 mb, were used to calculate trajectories from each source. The magnetic tapes, which were prepared by ARL, NOAA and purchased from the NMC, contain observed meteorological data for four observation times per day (00, 06, 12, and 18Z).

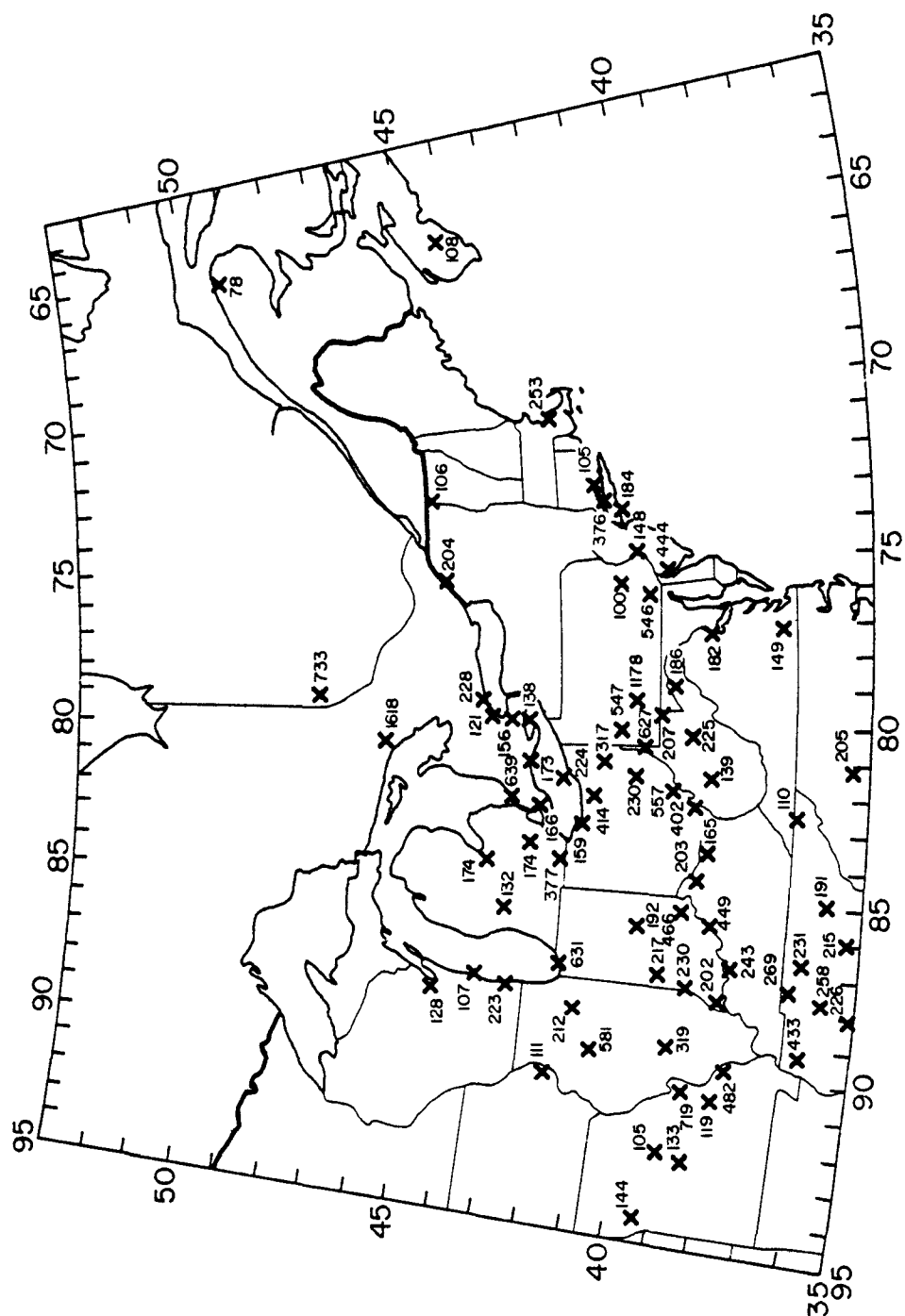


Fig. 14 Locations and intensity of  $\text{SO}_2$  emission sources ( $\times 10^3$  ton/year).

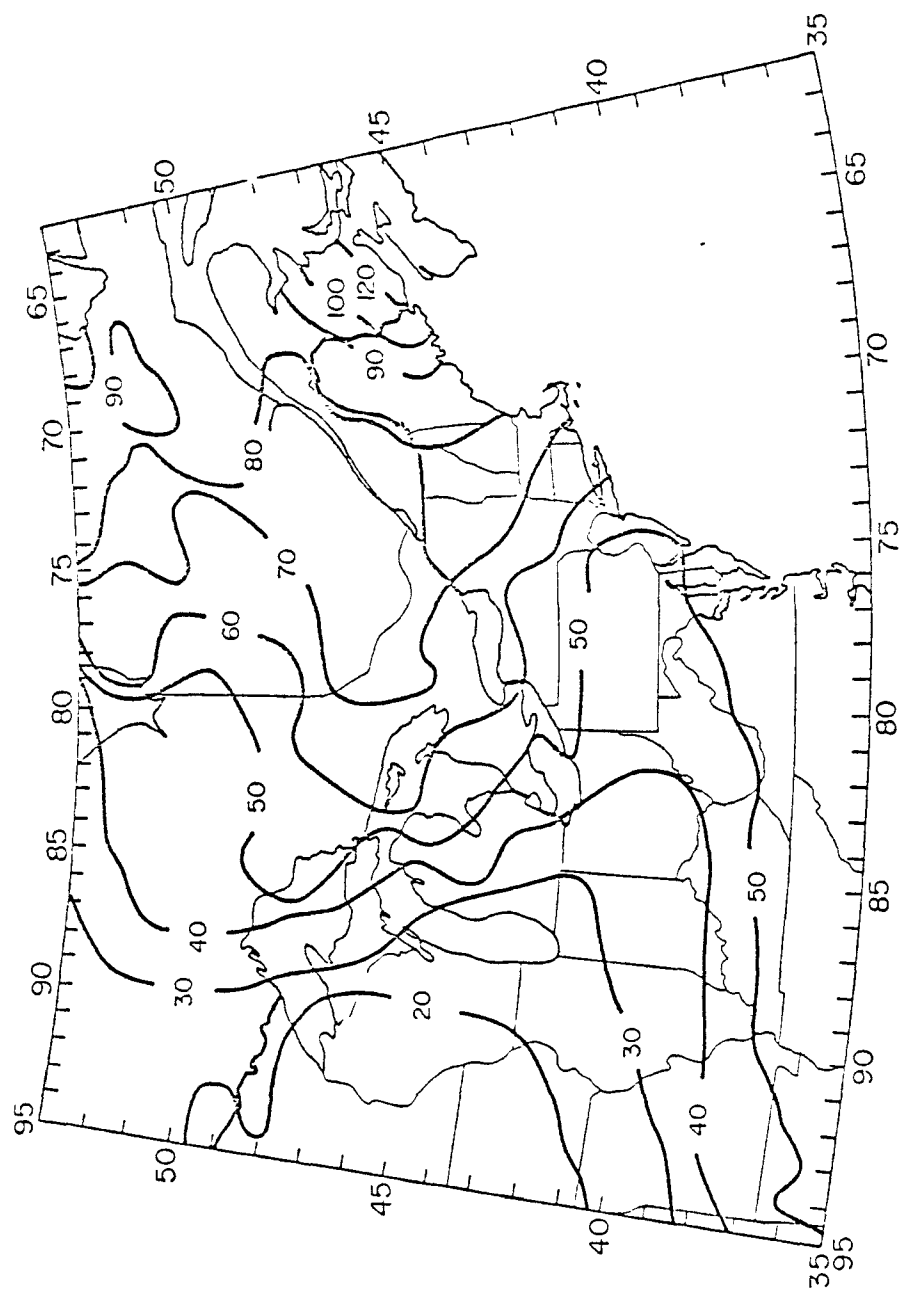


Fig. 15a Monthly precipitation amounts (mm) for January, 1977.



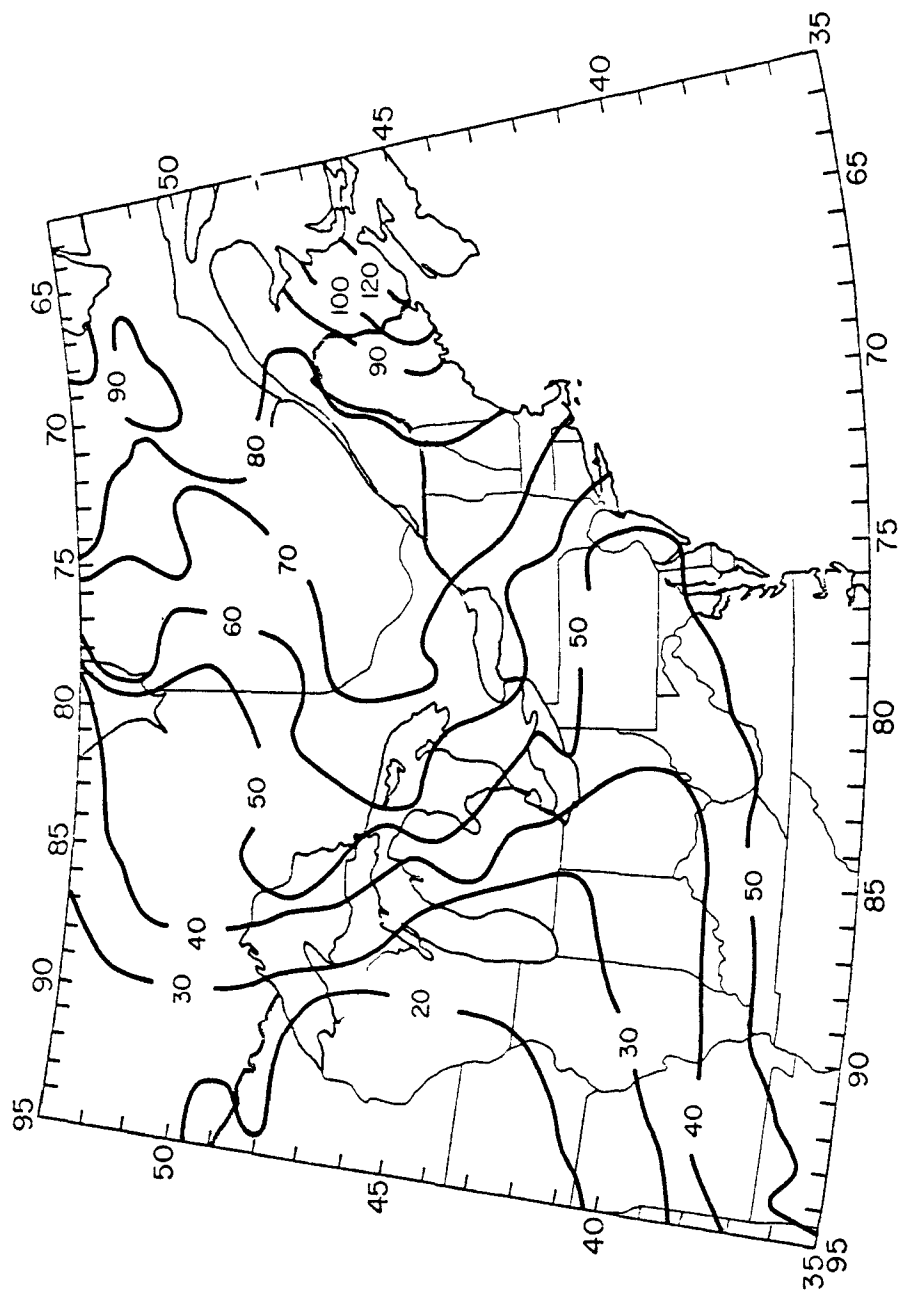


Fig. 15b Distribution of monthly precipitation amounts (mm) for March 1979.

## RESULTS

In the following presentation of figures, A is for the case of January 1977 and B for the case of March 1979.

Distributions of the monthly average concentrations of  $\text{SO}_2$  and sulfate are shown in Figs. 16 and 17, respectively. It can be seen that for both months, high concentrations of  $\text{SO}_2$  and sulfate are found over the Ohio river basin and the northeastern region adjacent to Lake Huron where major sources of  $\text{SO}_2$  are located.

Distributions of dry deposition amounts of  $\text{SO}_2$  and sulfate are shown in Figs. 18 and 19. Similar figures for the distributions of monthly wet deposition amounts are shown in Figs. 20 and 21. Finally, Figs. 22a and b show the distribution of precipitation acidity due to sulfate.

Statistical comparisons of the calculated results with those observed will be described in the next section.

### COMPARISON OF CALCULATED RESULTS WITH OBSERVATIONS

Calculated concentrations of  $\text{SO}_2$  and sulfate for the month of January 1977 are statistically compared with the observed concentration data compiled by Bhumralkar et al. (1980). Figure 23 and Fig. 24 are cited from the report by them. These data were compiled from the SURE data and from the Storage and Retrieval of Aerometric Data (SAROAD). The SURE air quality data were compiled by the Environmental Research and Technology, Inc. (ERT) for the Electric Power Research Institute (EPRI).

Figures 25 and 26 show the relationship between observed concentration and calculated concentrations for  $\text{SO}_2$  and sulfate, respectively. The correlation coefficients for  $\text{SO}_2$  and sulfate are 0.538 (0.258) and 0.477 (0.318), respectively, where the numbers in parenthesis are critical values for correlation coefficients with 99 percent confidence level.

Again, although the calculated concentrations are statistically related to the observed concentrations of  $\text{SO}_2$  as well as for sulfate, the values of the correlation coefficients are not significantly high.

For the month of March 1979, observed data of  $\text{SO}_2$  and sulfate concentrations are not available at this stage. pH values of precipitation observed at stations of the National Atmospheric Deposition Program (NADP) are compared with those calculated by the climatological model. The precipitation chemistry data of NADP are recorded on weekly intervals, so that the monthly-average pH value is calculated as a geometric mean of weekly values of pH. The monthly-average pH is calculated using the data observed during the period between February 27 and April 3.

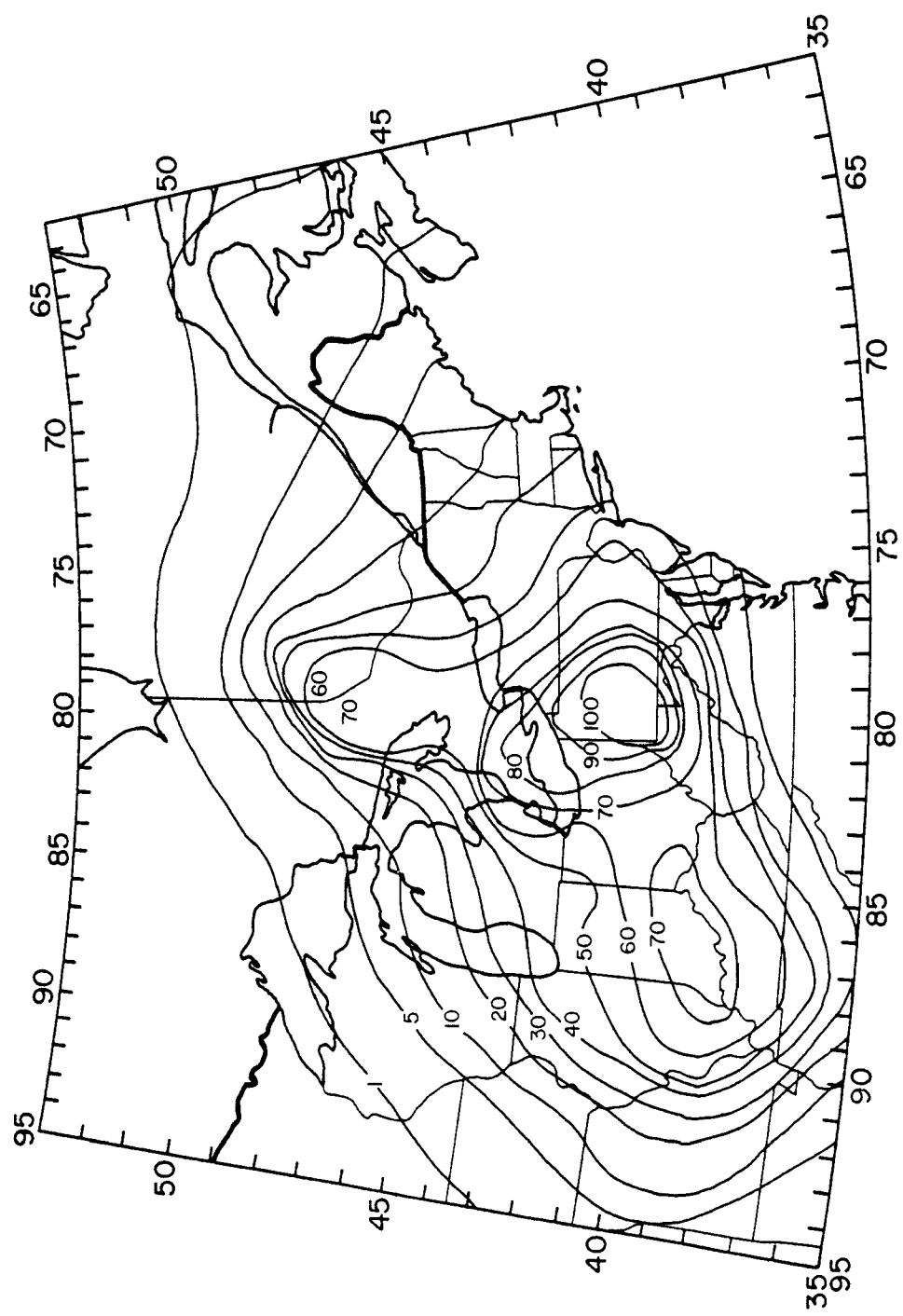


Fig. 16a Distribution of  $\text{SO}_2$  concentrations ( $\mu\text{g}/\text{m}^3$ ) for January 1977.

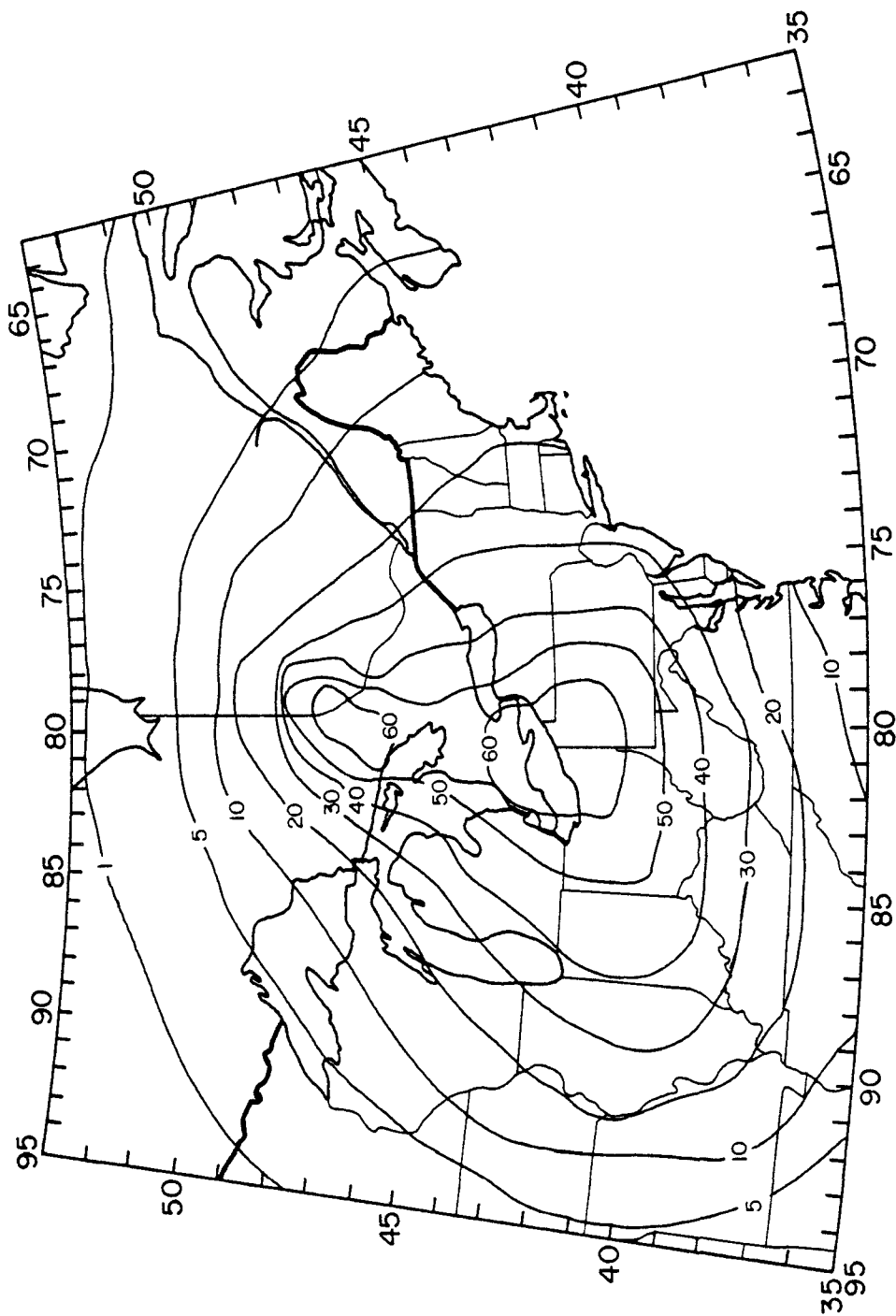


Fig. 16b Distribution of  $\text{SO}_2$  concentrations ( $\mu\text{g}/\text{m}^3$ ) for March 1979.

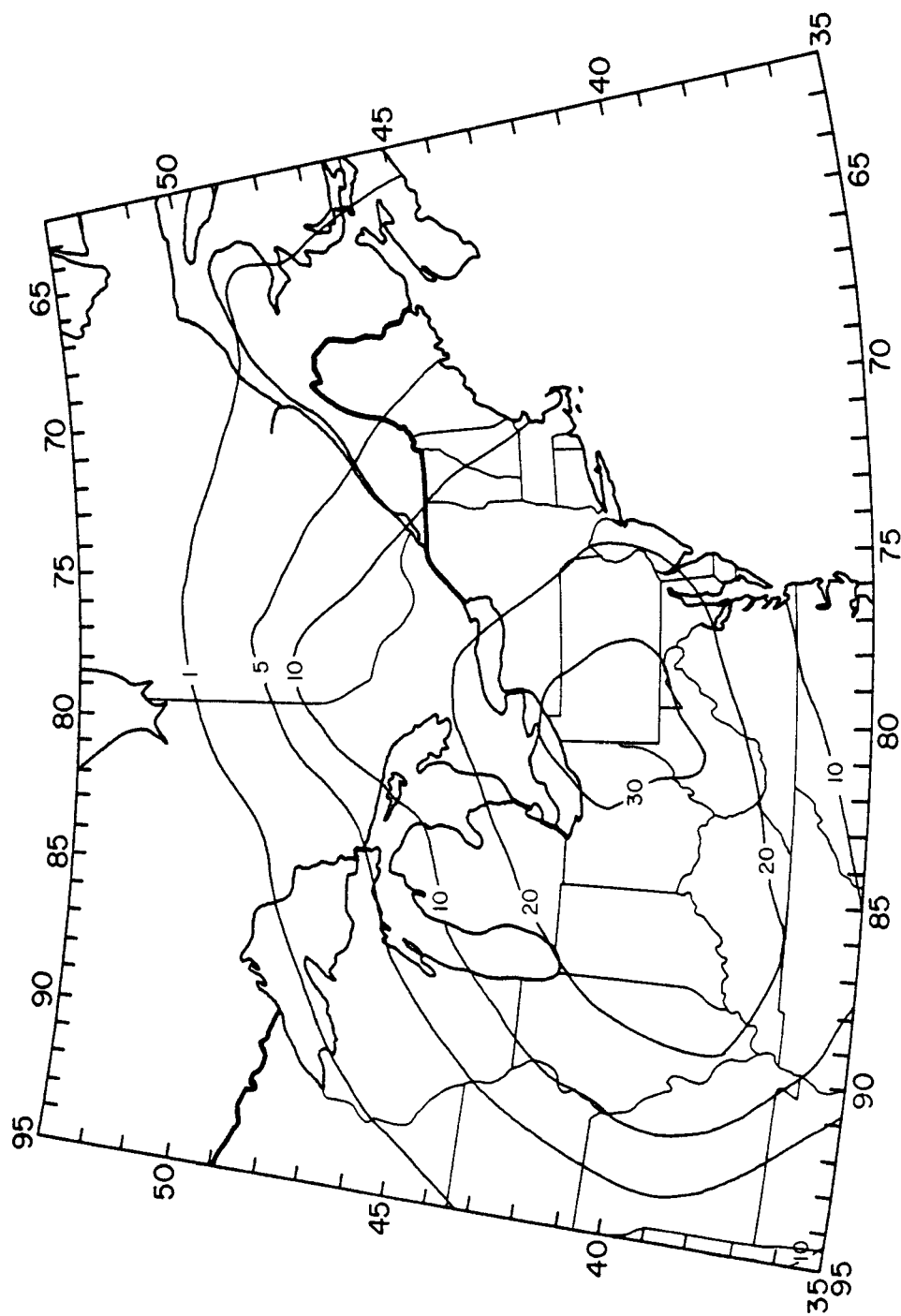


Fig. 17a Distribution of sulfate concentrations ( $\mu\text{g}/\text{m}^3$ ) for January 1977.

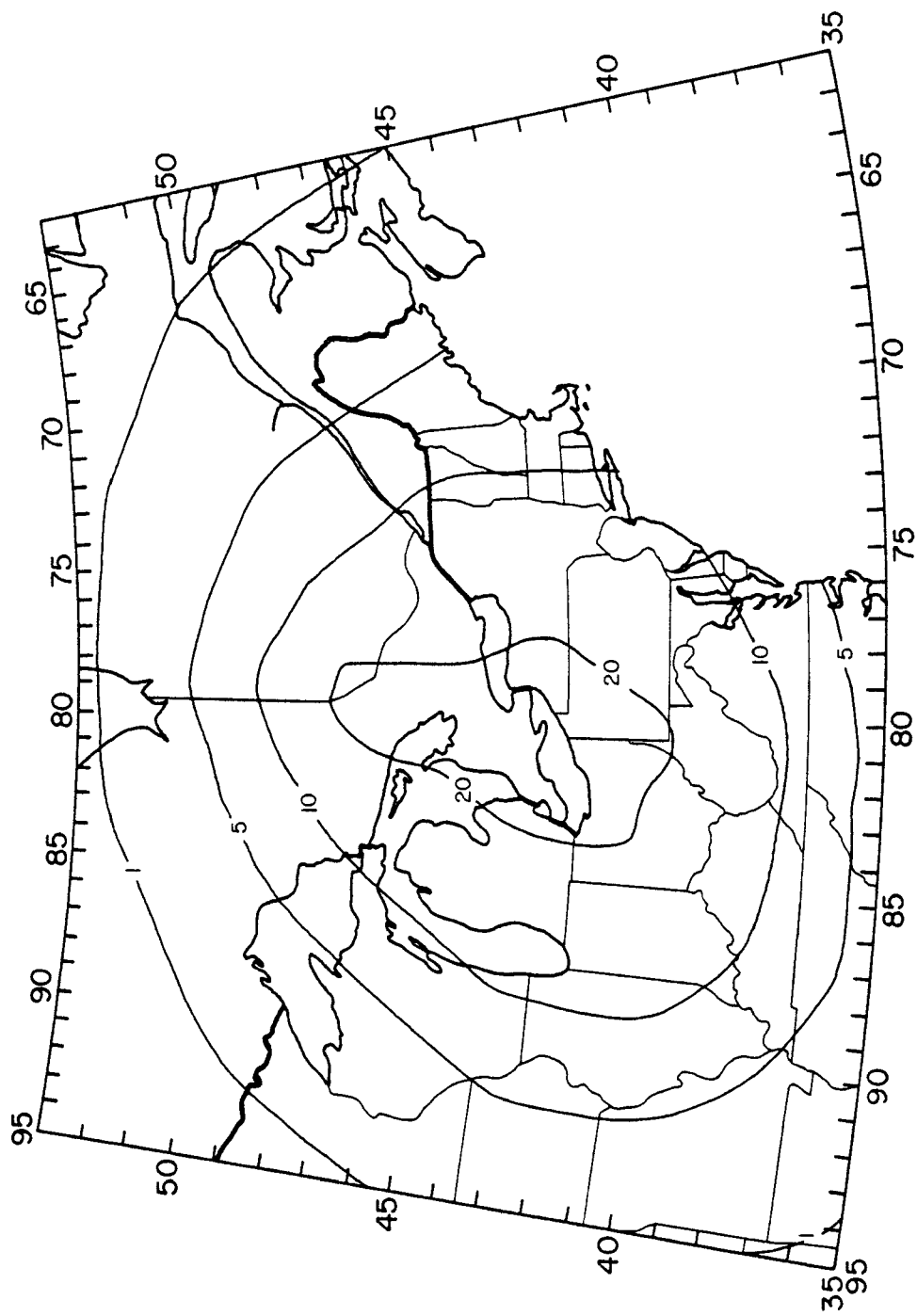


Fig. 17b Distribution of sulfate concentrations ( $\mu\text{g}/\text{m}^3$ ) for March 1979.

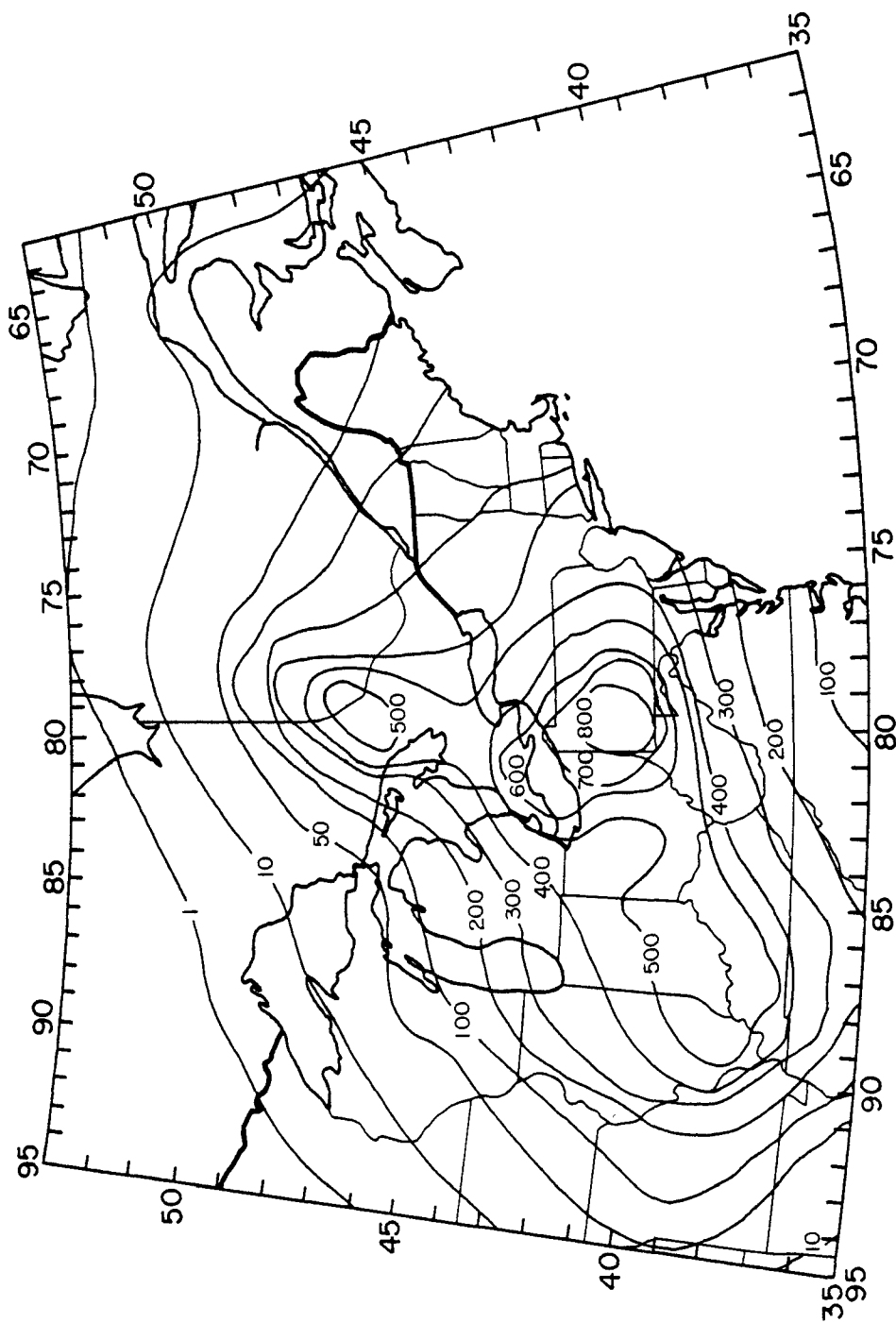


Fig. 18a Dry deposition amounts ( $\text{kg}/\text{km}^2$ ) of  $\text{SO}_2$  for January 1977.

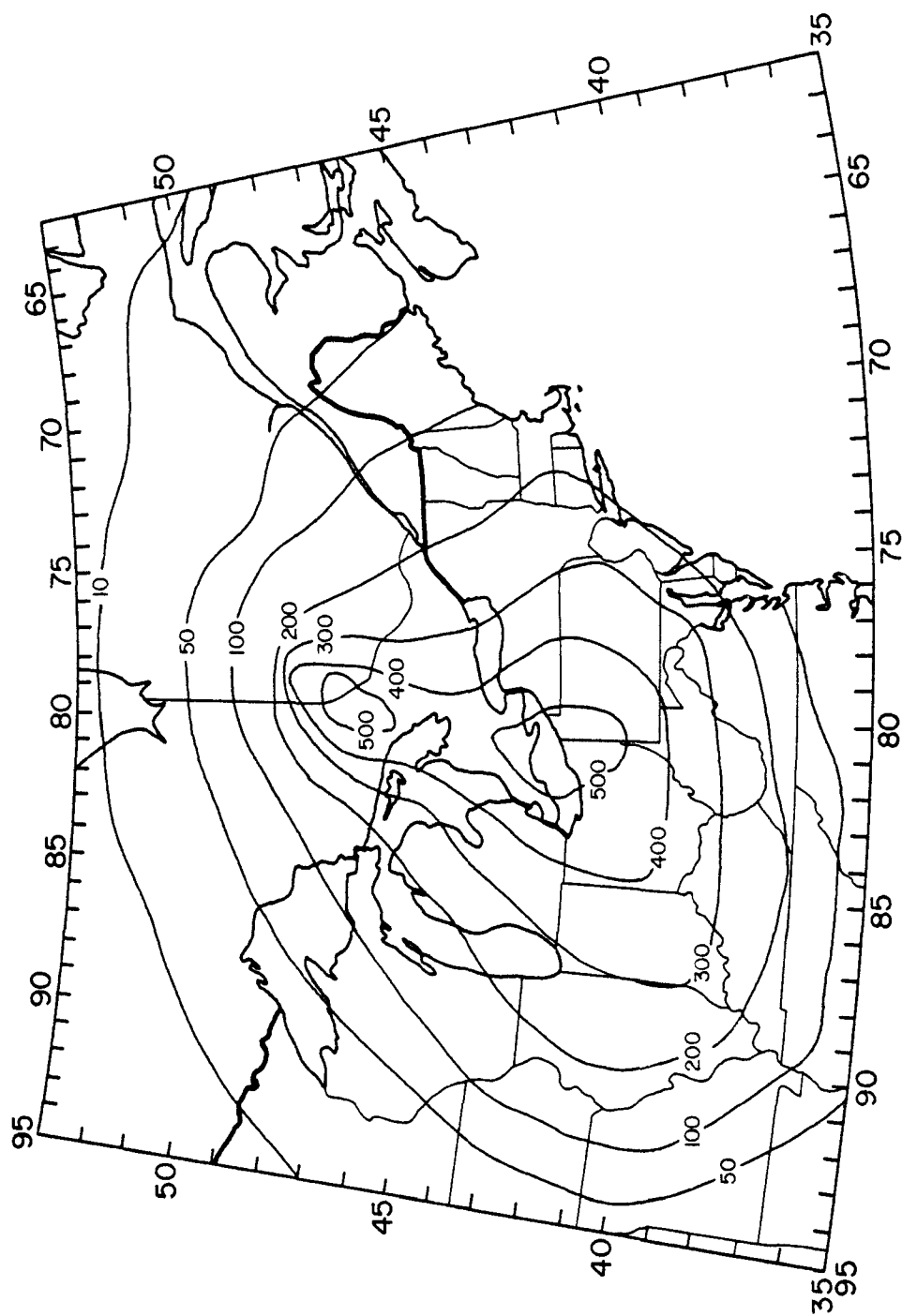


Fig. 18b Dry deposition amounts ( $\text{kg}/\text{km}^2$ ) of  $\text{SO}_2$  for March 1979.



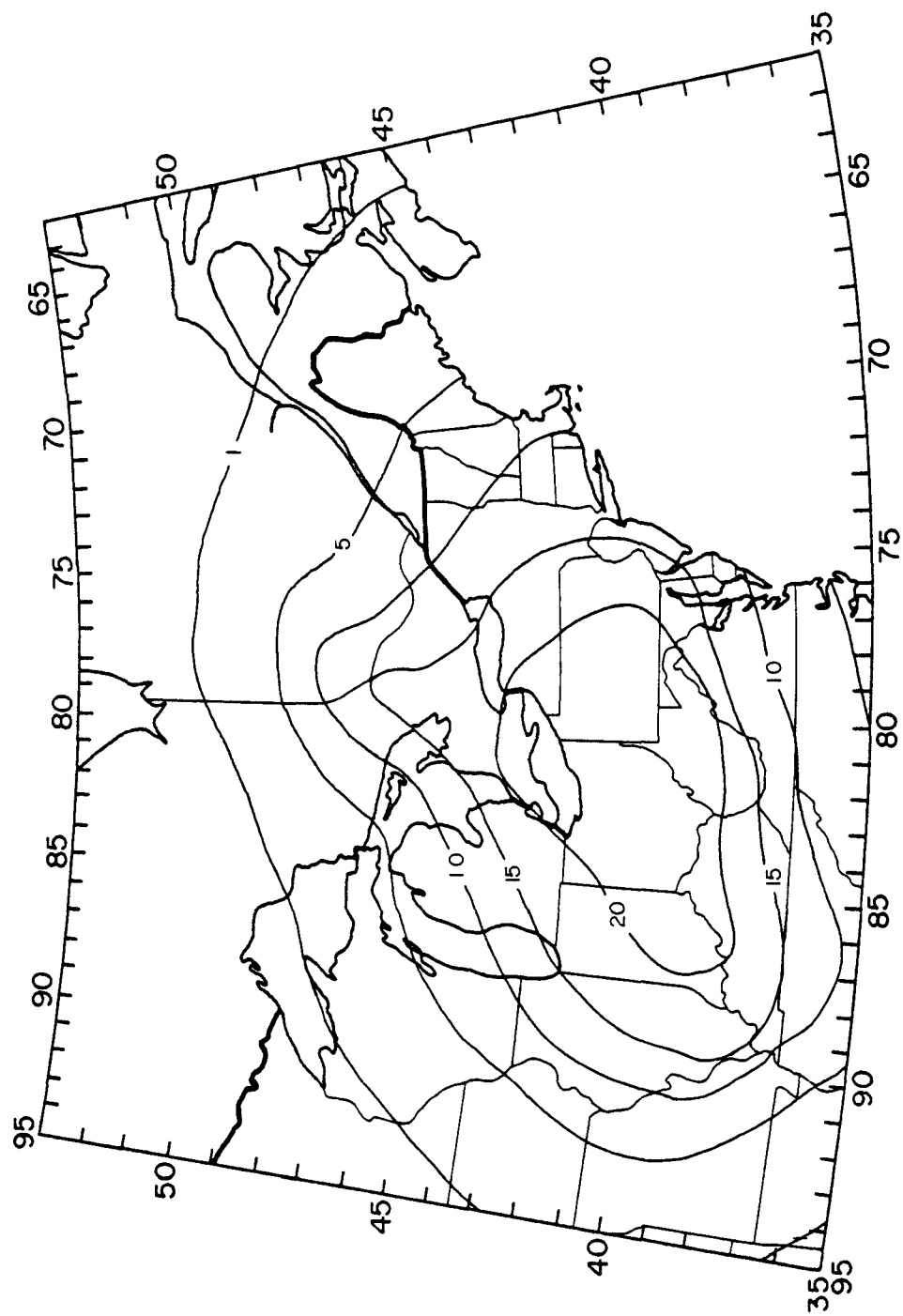


Fig. 19a Dry deposition amounts ( $\text{kg/km}^2$ ) of sulfate for January 1977.

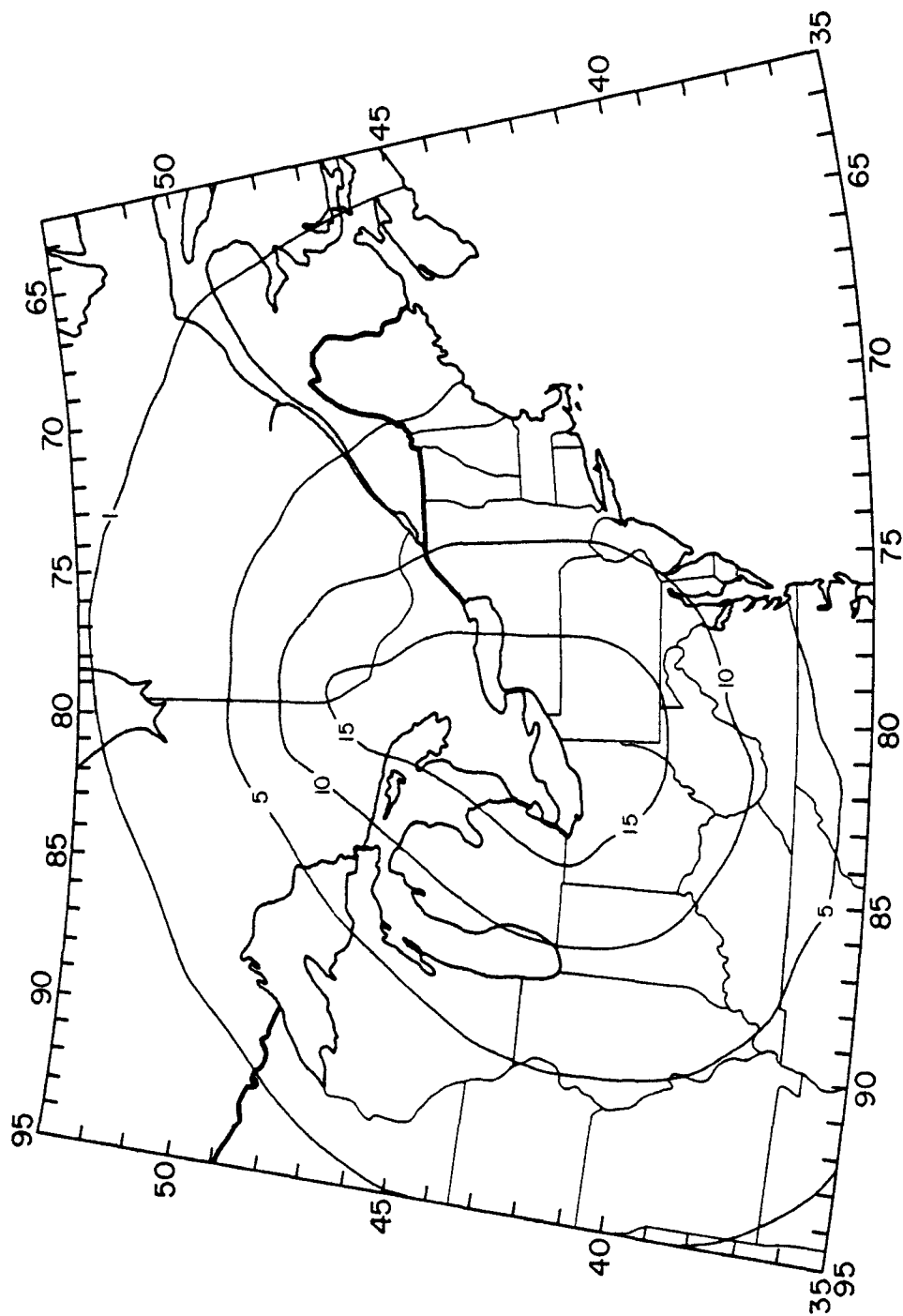


Fig. 19b Dry deposition amounts ( $\text{kg}/\text{km}^2$ ) of sulfate for March 1979.

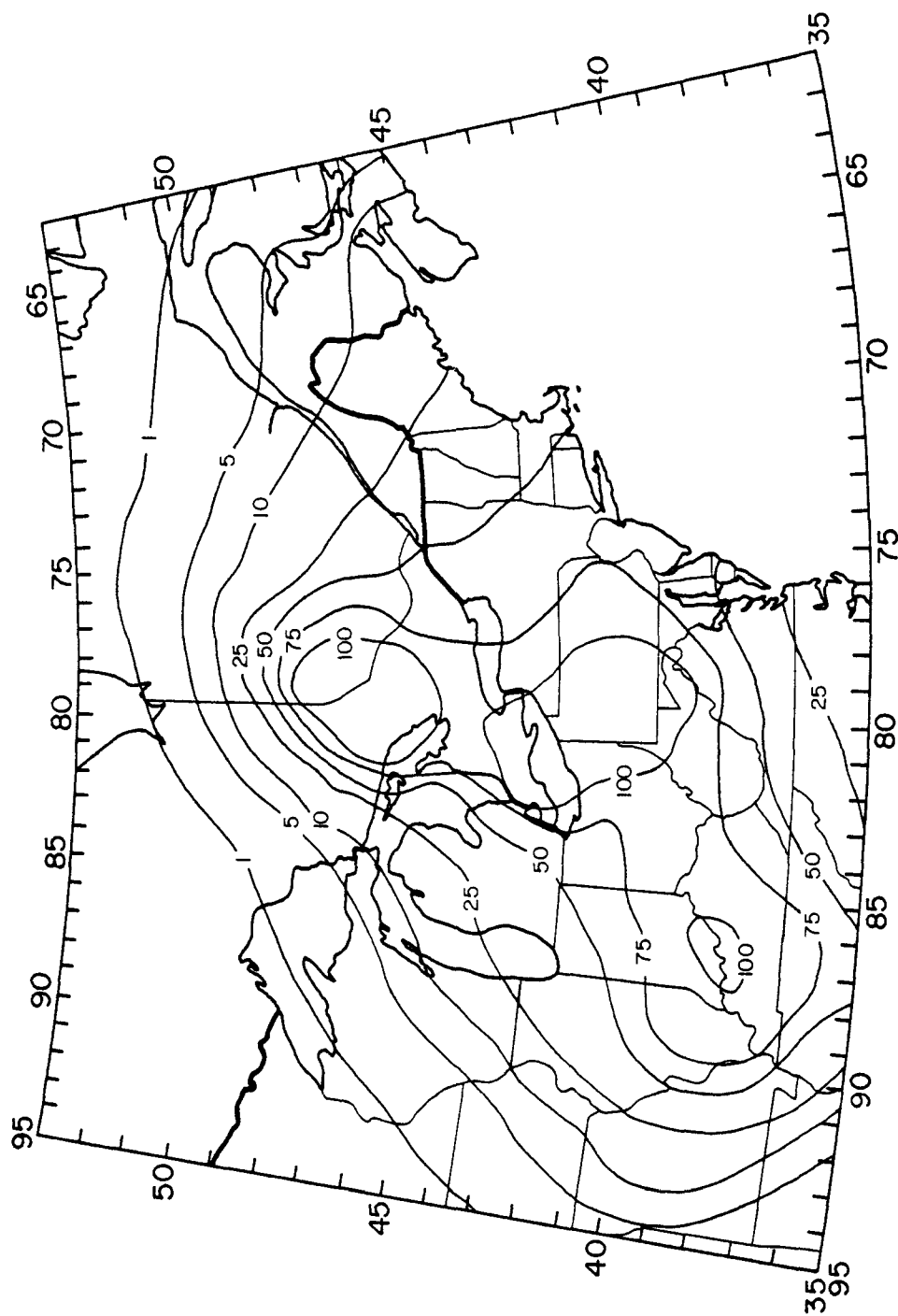


Fig. 20a Wet deposition amounts ( $\text{kg}/\text{km}^2$ ) of  $\text{SO}_2$  for January 1977.

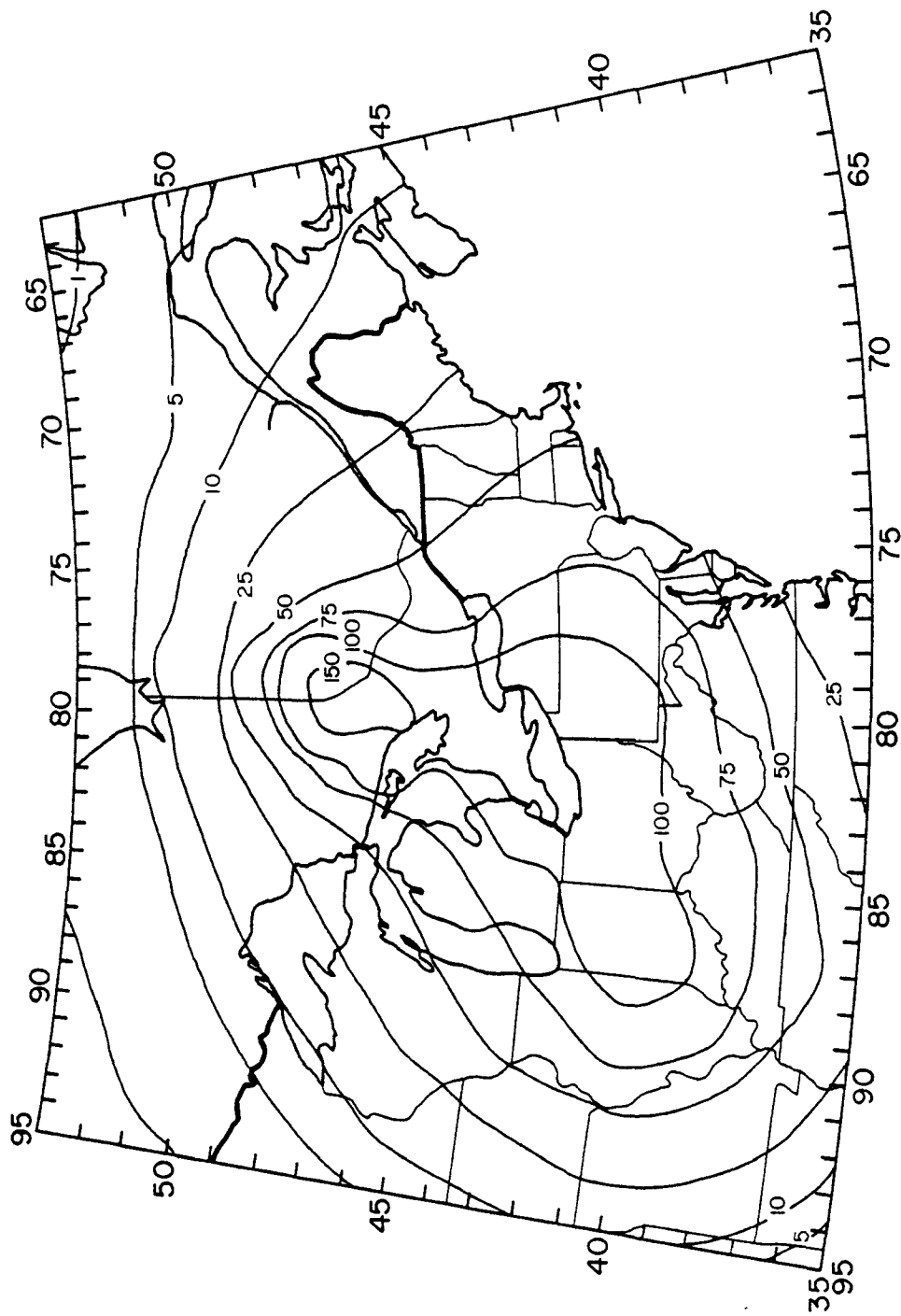


Fig. 20b Wet deposition amounts ( $\text{kg}/\text{km}^2$ ) of  $\text{SO}_2$  for March 1979.

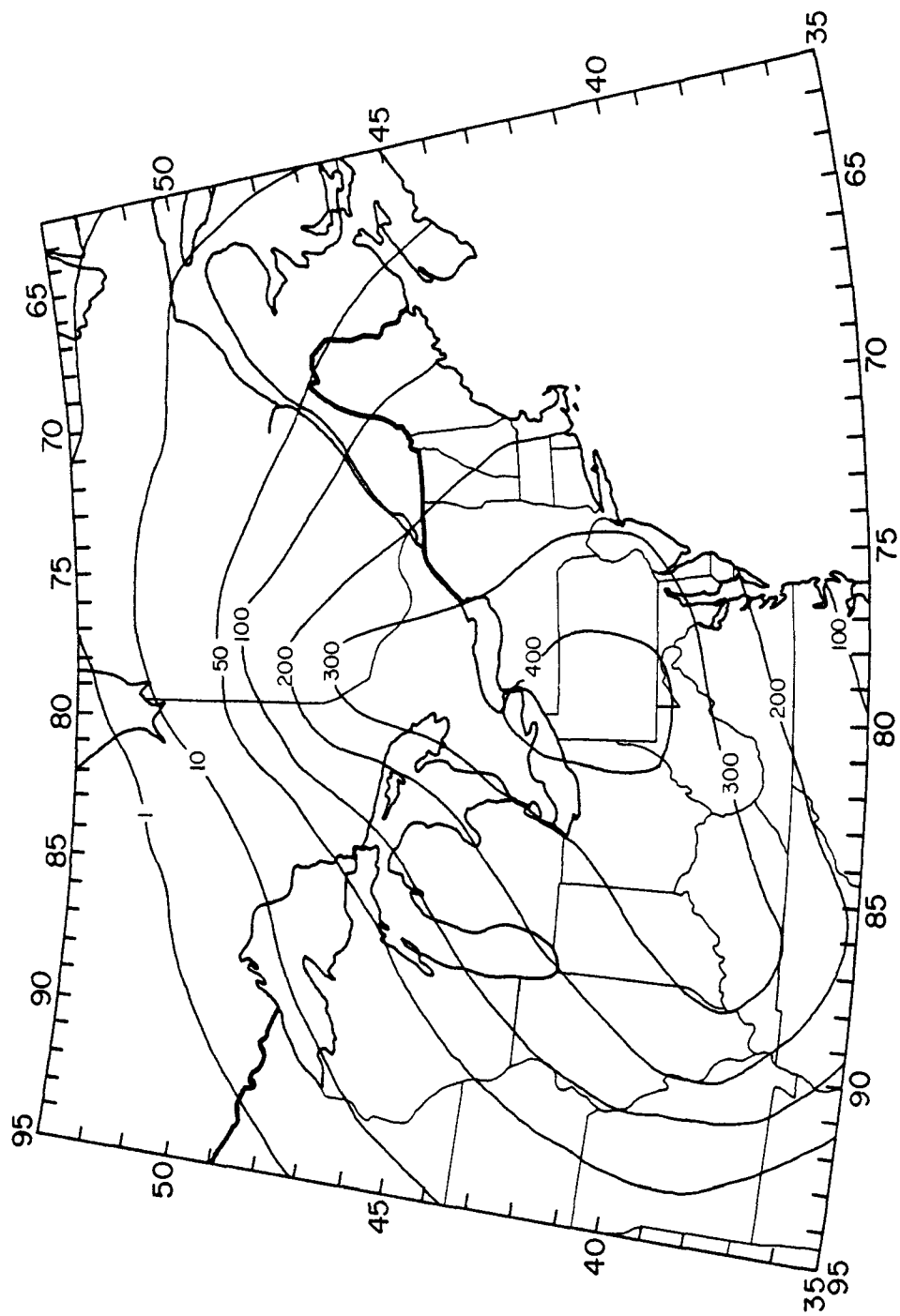


Fig. 21a Wet deposition amounts ( $\text{kg}/\text{km}^2$ ) of sulfate for January 1977.

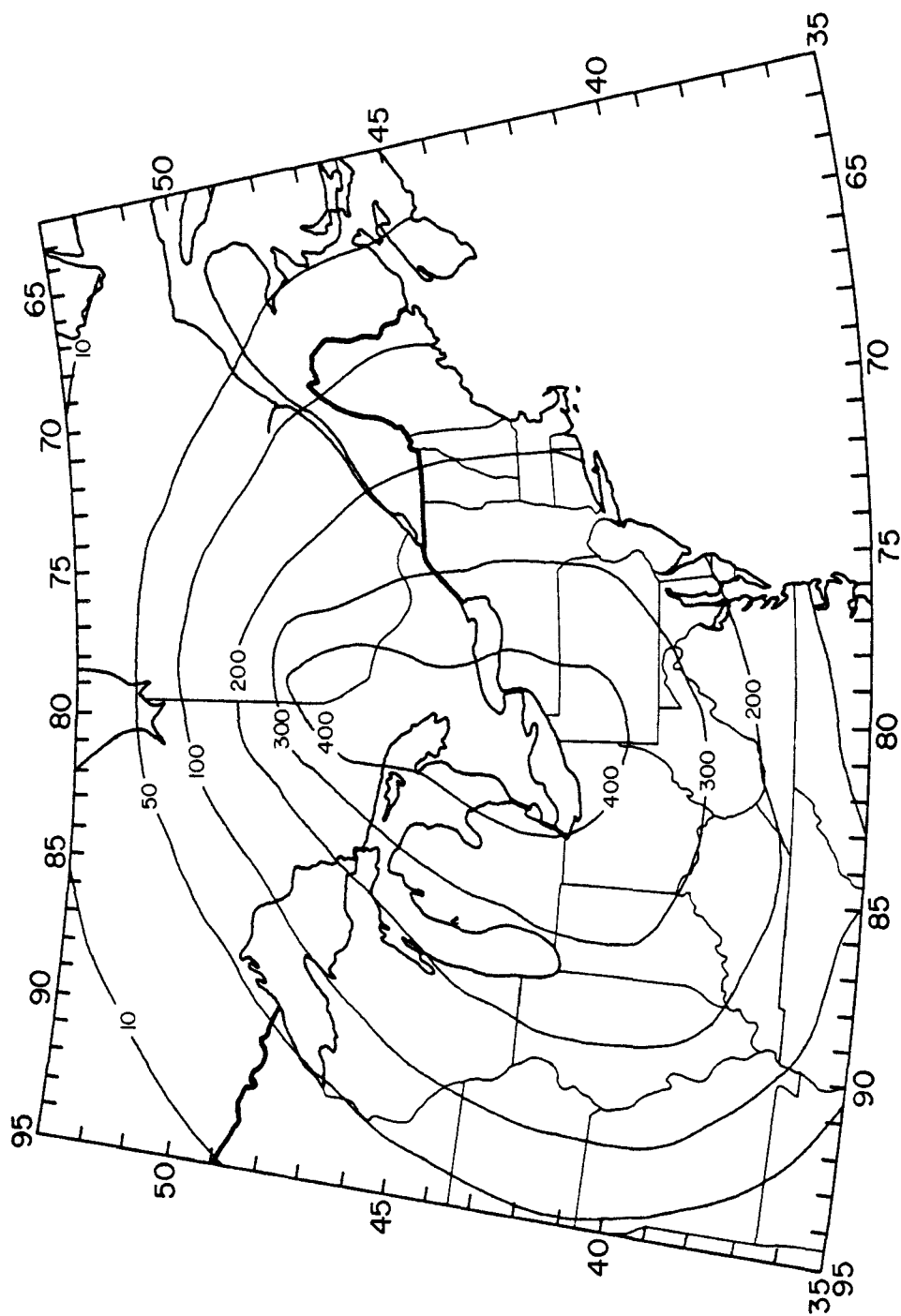


Fig. 21b Wet deposition amounts ( $\text{kg}/\text{km}^2$ ) of sulfate for March 1979.

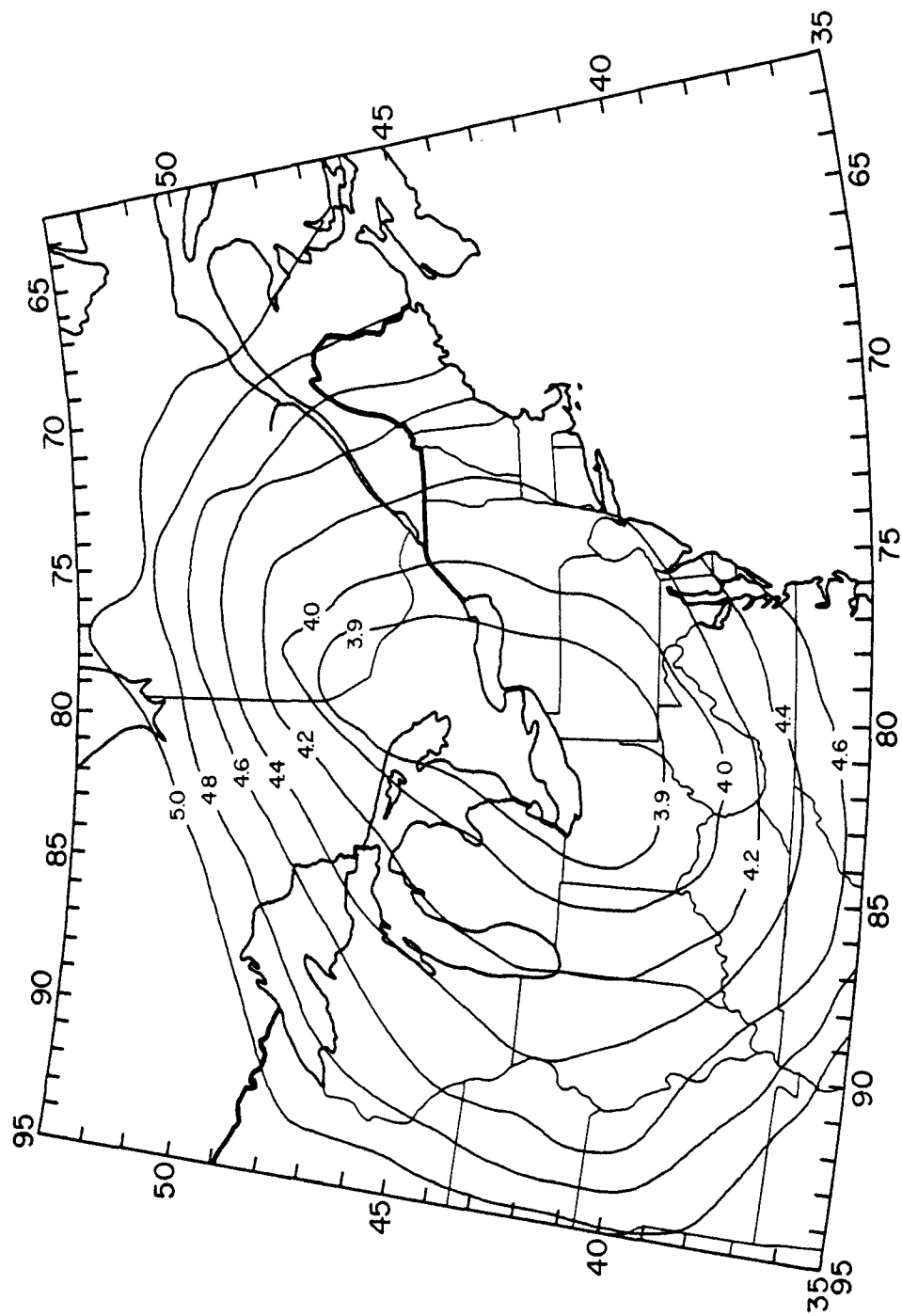


Fig. 22a pH distribution for January 1977.

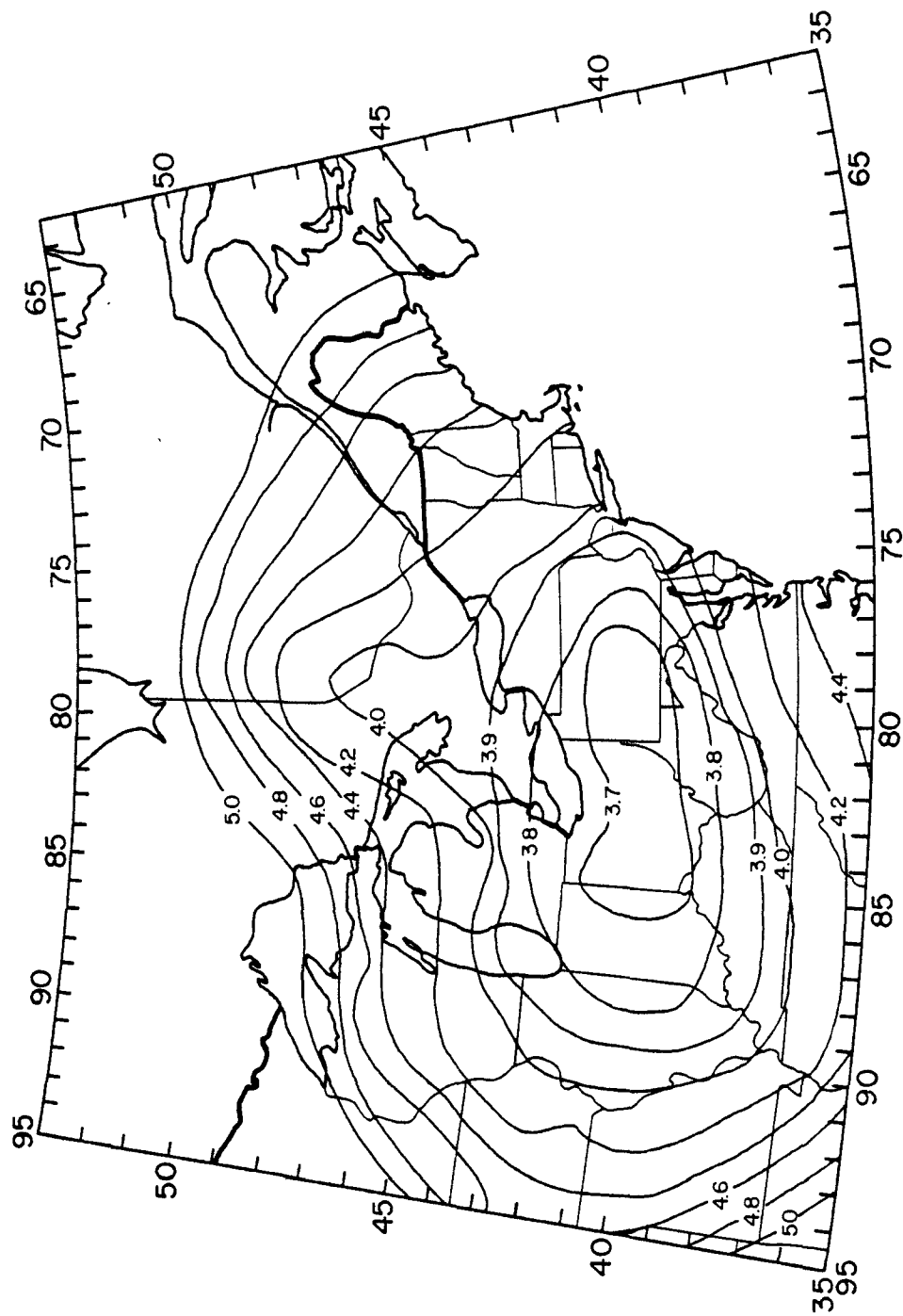


Fig. 22b pH distribution for March 1979.



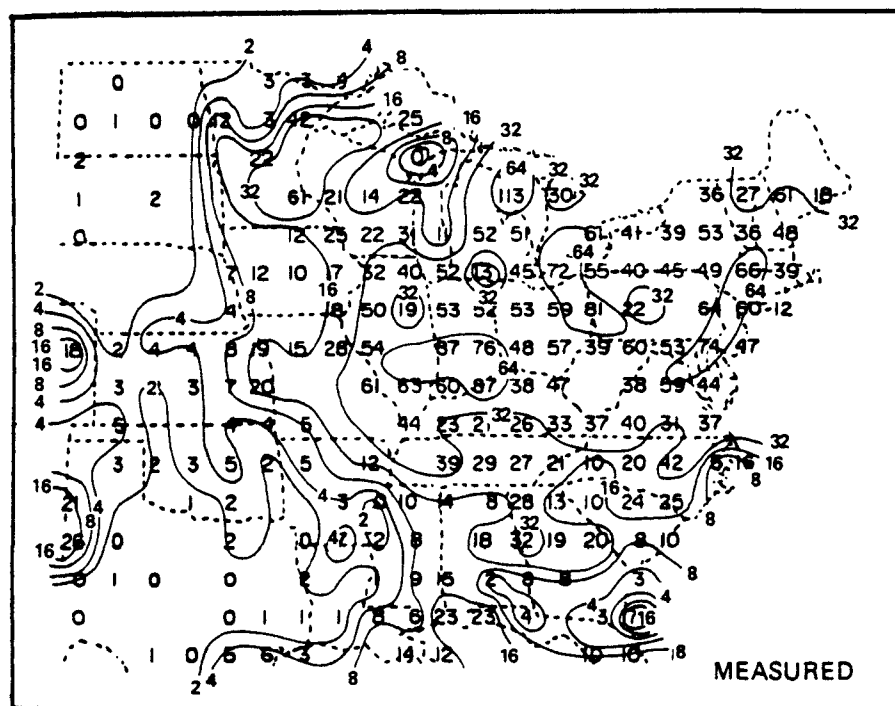


Figure 8. SO<sub>2</sub> concentrations (µg/m<sup>3</sup>) for January 1977.

Fig. 23 Observed concentration distribution of SO<sub>2</sub> for January, 1977.  
[From Bhumralkar et al. (1980).]

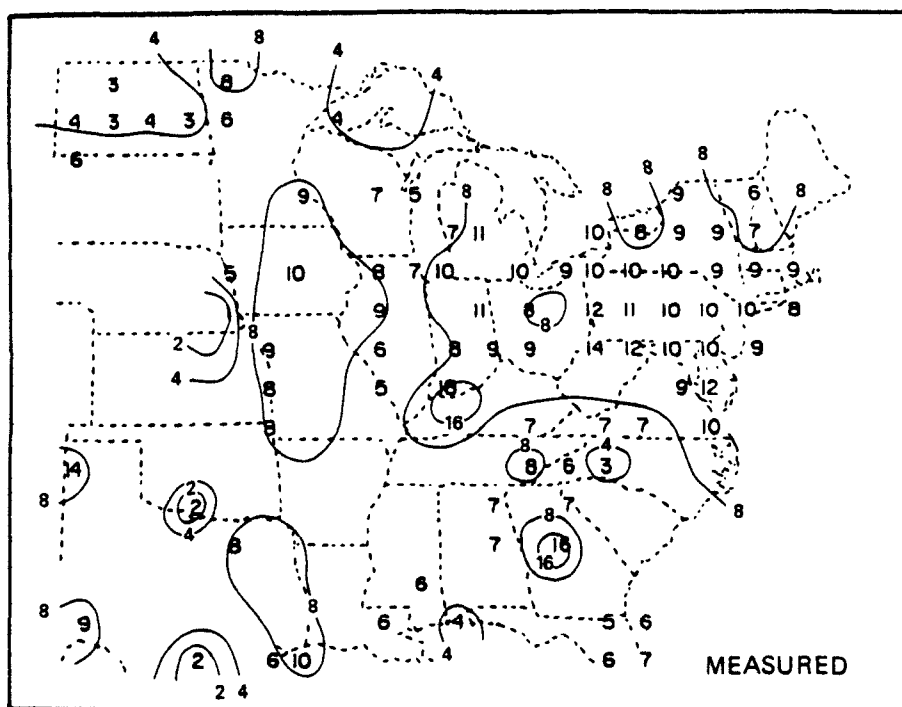


Figure 9.  $\text{SO}_4^{2-}$  concentrations ( $\mu\text{g}/\text{m}^3$ ) for January 1977.

Fig. 24 Observed concentration distribution of sulfate for January, 1977.  
[From Bhumraikar et al. (1980).]

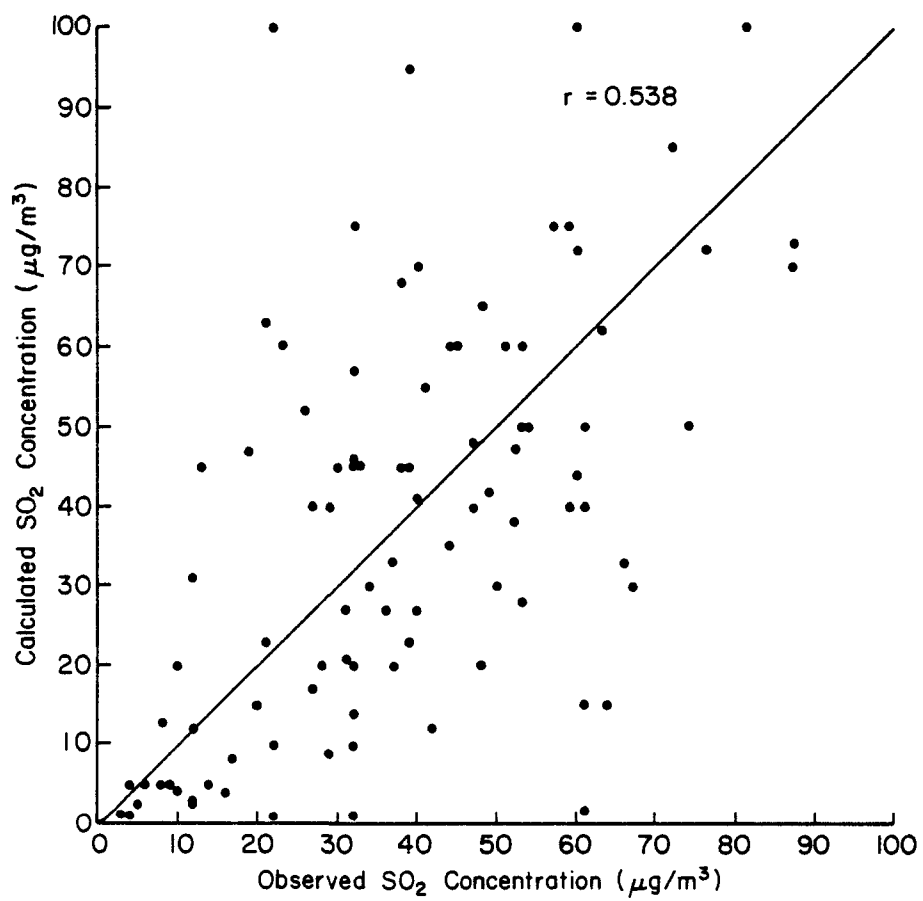


Fig. 25 Calculated SO<sub>2</sub> concentration versus observed SO<sub>2</sub> concentration for January 1977.

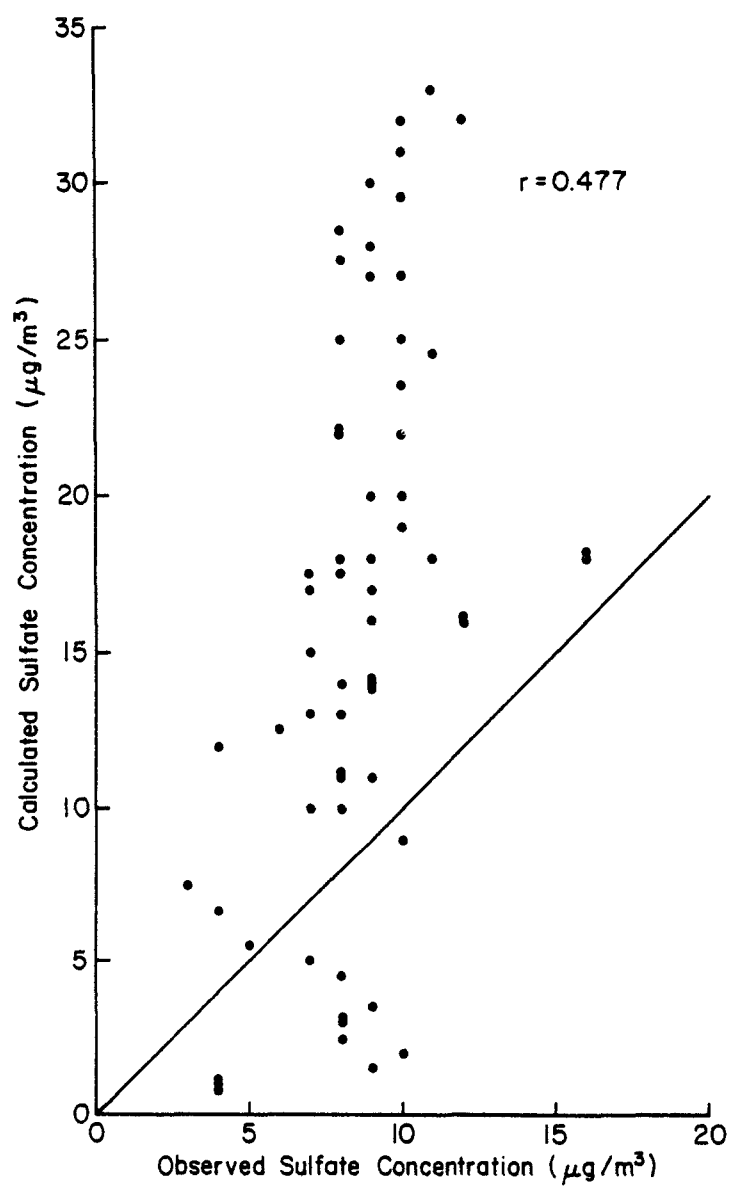


Fig. 26 Calculated sulfate concentration versus observed sulfate concentration for January 1977.

For the data from this period, 17 stations were available within the region of our interval. In Table 3 the location of stations and the monthly pH values for each station are given.

Using the pH values given in Table 3 and the calculated pH values shown in Fig. 22b, the diagram showing the relationship between the observed pH values and the calculated pH values are obtained as Fig. 27. For this diagram, the correlation coefficient is 0.825 (0.575), where the number in parenthesis is a critical value for a correlation coefficient with 99 percent confidence level. From this figure, it can be seen that the acidity calculated based on sulfate content in precipitation is slightly higher than that observed. However, from the highly correlated relationship it can be concluded that, with further improvement of the model, the prediction of acidity of precipitation can be made more accurately than the present results.

#### MASS BUDGET OF SULFUR OVER THE NORTHEASTERN UNITED STATES

Mass budget of sulfur emitted from the major sources over the region is estimated using the climatological model. Tables 4 and 5 are for the months of January 1977 and March 1979, respectively. From these tables the following can be seen:

- (1) The budgets are different between the two months studied. This is due to the different meteorological conditions for two periods.
- (2) During the month of January 1977, the inflow amounts of sulfur from the U.S. to Canada are only a small fraction (0.23) of the total amount of sulfur over eastern Canada. On the contrary, a substantial fraction (0.40) of sulfur was imported from the U.S. during the month of March 1979.
- (3) Transported amounts of sulfur from Canada to the United States are small. Less than 0.03 of the total sulfur over the northeastern United States is the sulfur imported from Canada.
- (4) Major portions of sulfur were removed by wet and dry deposition.
- (5) The fraction of outflow amounts to the Atlantic Ocean were substantially smaller than the fraction estimated by Galloway and Whelpdale (1980). They estimated that approximately 0.26 and 0.21 of the total sulfur were transported to the ocean, respectively, from Canada and the United States. Our estimation shows that the fractions of less than 0.03 and 0.1 are blown out to the ocean.
- (6) The Great Lakes received approximately 0.05 of the total sulfur emitted.

The residue of the budget consists of sulfur transported out of the boundaries and errors of calculation.

Table 3 Site name, geographical location and monthly average pH for March 1979.

| <u>Site Name</u>        | <u>Lat.</u> | <u>Long.</u> | <u>Monthly Average pH</u> |
|-------------------------|-------------|--------------|---------------------------|
| Bondville               | 40°03'      | 88°22'       | 4.30                      |
| Dixon Springs Ag. Cts.  | 37°26'      | 88°40'       | 4.47                      |
| Wellston                | 44°13'      | 85°51'       | 4.53                      |
| Marcell Exp. Forest     | 47°30'      | 93°28'       | 4.70                      |
| Lamberton               | 44°15'      | 95°19'       | 5.64                      |
| Hubbard Brook           | 43°57'      | 71°42'       | 4.46                      |
| Huntington Wildlife     | 44°00'      | 74°13'       | 4.33                      |
| Lewiston                | 36°08'      | 77°10'       | 4.82                      |
| Coweeta                 | 35°03'      | 83°27'       | 4.76                      |
| Piedmont Research Stn.  | 35°40'      | 80°34'       | 5.13                      |
| Clinton Crops Res. Stn. | 35°01'      | 78°17'       | 4.94                      |
| * { Finley (Raleigh)    | 35°44'      | 78°41'       | 4.76                      |
| { Finley (Raleigh)      | 35°33'      | 78°41'       | 4.69                      |
| Delaware                | 40°17'      | 83°04'       | 4.33                      |
| Caldwell                | 39°45'      | 81°31'       | 4.39                      |
| Wooster                 | 40°46'      | 81°56'       | 4.52                      |
| Kane Exp. For.          | 41°33'      | 78°46'       | 3.96                      |
| Parsons                 | 39°06'      | 79°39'       | 4.44                      |

\* Treated as one station.

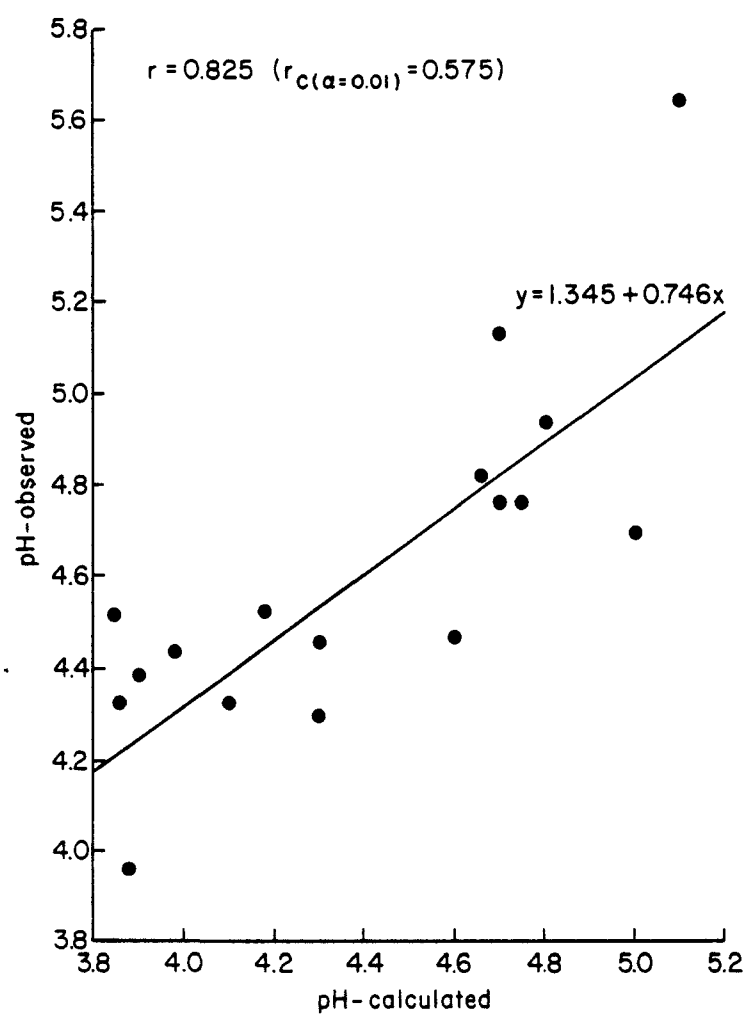


Fig. 27 Diagram showing the relationship between observed pH and calculated pH.

Table 4 Sulfur mass budget for January 1977.

| Input                              | <u>Canada</u>                                   | <u>U.S.A</u>                                    |
|------------------------------------|---|---|
| Emissions                          | $1.4132 \times 10^8$ kg                         | $7.4586 \times 10^8$ kg                         |
| Inflow to U.S. from<br>Canada      | ----  | $.21187 \times 10^8$ kg                         |
| Inflow to Canada from<br>U.S.      | <u><math>.42711 \times 10^8</math> kg</u>       | <u>----</u>                                     |
|                                    | $1.84031 \times 10^8$ kg                        | $7.67047 \times 10^8$ kg                        |
| Output                             |   |   |
| Wet Deposition                     | $.50705 \times 10^8$ (27.55%)                   | $1.9987 \times 10^8$ (26.06%)                   |
| Dry Deposition                     | $.61692 \times 10^8$ (33.52%)                   | $2.71407 \times 10^8$ (35.38%)                  |
| Outflow to Ocean                   | $.06148 \times 10^8$ ( 3.34%)                   | $.77192 \times 10^8$ (10.06%)                   |
| Outflow from Canada<br>to the U.S. | $.21187 \times 10^8$ (11.51%)                   | ----  |
| Outflow from the U.S<br>to Canada  | ----  | $.42711 \times 10^8$ ( 5.57%)                   |
| To the Great Lakes                 | $.10802 \times 10^8$ ( 5.87%)                   | $.35029 \times 10^8$ ( 4.57%)                   |
| In the Air                         | <u><math>.10686 \times 10^8</math> ( 5.81%)</u> | <u><math>.47945 \times 10^8</math> ( 6.25%)</u> |
|                                    | $1.6122 \times 10^8$ (87.60%)                   | $6.74154 \times 10^8$ (87.89%)                  |
| Residue                            | $.22811 \times 10^8$ (12.40%)                   | $.92893 \times 10^8$ (12.11%)                   |



Table 5 Sulfur mass budget for March 1979.

|                                    | <u>Canada</u>                                  | <u>U.S.A</u>                                   |
|------------------------------------|--|--|
| Input                              |  |  |
| Emissions                          | $1.41328 \times 10^8$ kg                       | $7.4586 \times 10^8$ kg                        |
| Inflow to U.S. from<br>Canada      | ----   | $.16623 \times 10^8$ kg                        |
| Inflow to Canada from<br>U.S.      | <u><math>.94141 \times 10^8</math> kg</u>      | <u>----</u>                                    |
|                                    | $2.35469 \times 10^8$ kg                       | $7.62483 \times 10^8$ kg                       |
| Output                             |  |  |
| Wet Deposition                     | $.89768 \times 10^8$ (38.12%)                  | $1.9024 \times 10^8$ (24.95%)                  |
| Dry Deposition                     | $.76484 \times 10^8$ (32.48%)                  | $2.0117 \times 10^8$ (26.38%)                  |
| Outflow to Ocean                   | $.04735 \times 10^8$ ( 2.01%)                  | $.6313 \times 10^8$ ( 8.28%)                   |
| Outflow from Canada<br>to the U.S. | $.16623 \times 10^8$ ( 7.06%)                  | ----   |
| Outflow from the U.S<br>to Canada  | ----   | $.94141 \times 10^8$ (12.35%)                  |
| To the Great Lakes                 | $.10482 \times 10^8$ ( 4.45%)                  | $.5397 \times 10^8$ ( 7.08%)                   |
| In the Air                         | <u><math>.1763 \times 10^8</math> ( 7.49%)</u> | <u><math>.4419 \times 10^8</math> ( 5.80%)</u> |
|                                    | $2.15722 \times 10^8$ (91.61%)                 | $6.46842 \times 10^8$ (84.84%)                 |
| Residue                            | $.19747 \times 10^8$ ( 8.39%)                  | $1.15641 \times 10^8$ (15.16%)                 |

## SECTION 7

### INVESTIGATION OF A PREDICTION METHOD OF THE ACIDITY OF PRECIPITATION

#### INTRODUCTION

Our studies on the acidity of precipitation have been centered on finding empirical relationships between the acidity of precipitation and the concentrations of ions, using the data reported in "Atmospheric Turbidity and Precipitation Chemistry Data for the World", "Global Monitoring of the Environment for Selected Atmospheric Constituents" (WMO and NOAA, 1976, 1977, 1978), the data reported by Hales and Dana (1979), and the precipitation chemistry data obtained at the National Atmospheric Deposition Program network (Natural Resource Ecology Laboratory, 1980). The first data consist of precipitation samples collected on a monthly basis, the second data of samples collected on a short-term basis at the precipitation chemistry network operated in the METROMEX region surrounding St. Louis, and the third data of samples collected on a weekly basis. The purpose of our study was to examine whether the acidity of precipitation can be calculated as an output of our long-range transport model.

#### RESULTS

Figures 28, 29, and 30 show the relationships between major ions  $\text{SO}_4^{=}$ ,  $\text{NO}_3^-$  and  $\text{NH}_4^+$  in precipitation. In these figures, (A) stands for the data obtained from WMO and NOAA (1976, 1977, 1978), and (B) is for the data reported by Hales and Dana (1979). The correlation coefficients for these ions are given in Table 6.

TABLE 6

| Variable Pair                       | WMO and NOAA Data        | Hales and Dana           |
|-------------------------------------|--------------------------|--------------------------|
| $\text{SO}_4^{=}$ - $\text{NO}_3^-$ | .299 ( $r_{99} = .092$ ) | .538 ( $r_{99} = .141$ ) |
| $\text{SO}_4^{=}$ - $\text{NH}_4^+$ | .155 ( $r_{99} = .092$ ) | .407 ( $r_{99} = .141$ ) |
| $\text{NO}_3^-$ - $\text{NH}_4^+$   | .142 ( $r_{99} = .092$ ) | .511 ( $r_{99} = .141$ ) |

As can be seen from this table, all the relationships are statistically correlated. The strongest, most consistent correlation for these two different data samples is that between  $\text{SO}_4^{=}$  and  $\text{NO}_3^-$ .

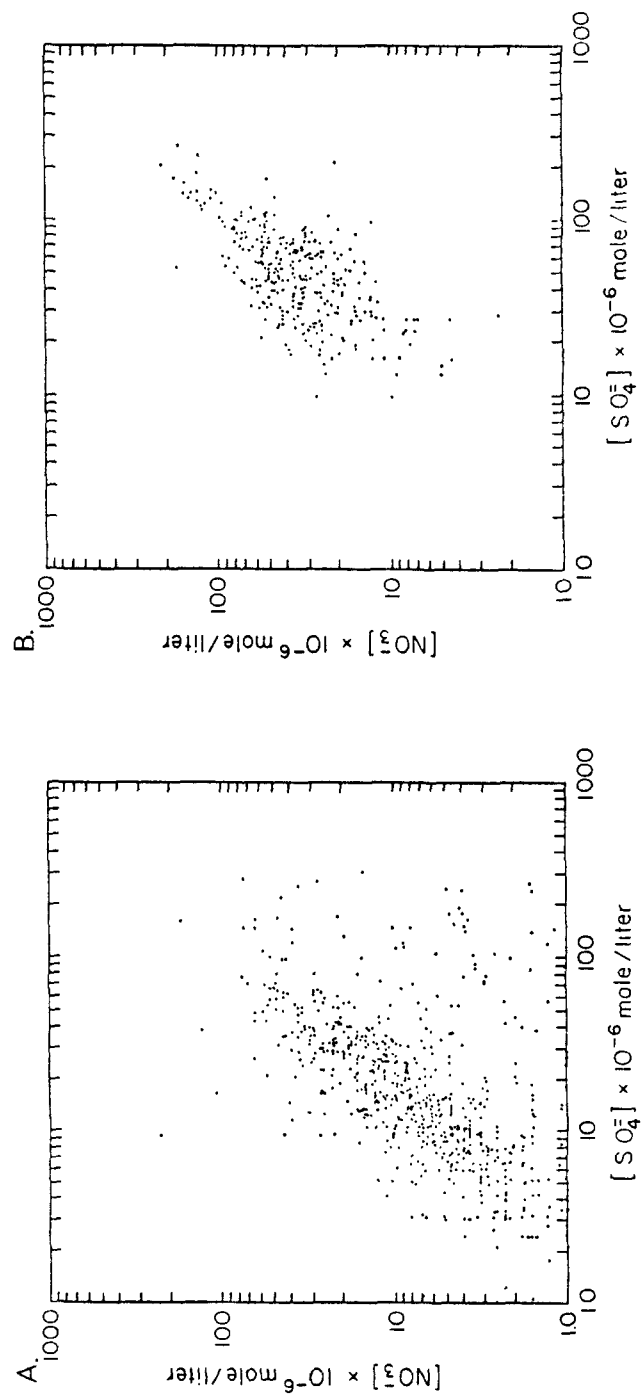


Fig. 28 Concentrations of  $\text{SO}_4^{2-}$  ions and  $\text{NO}_3^-$  ions in precipitation water, (A) data from "Atmospheric Turbidity" and (B) data from Hales and Dana (1979).

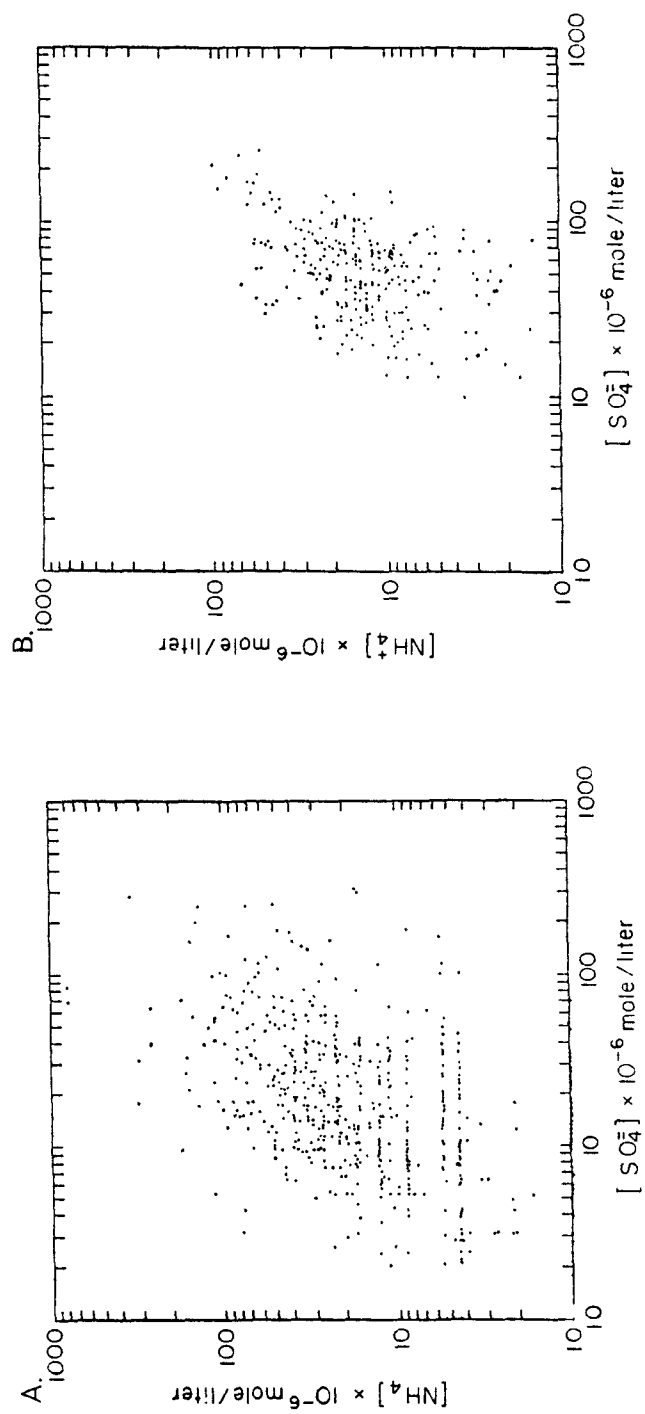


Fig. 29 Same as Fig. 28, except  $\text{SO}_4^{2-}$  ions and  $\text{NH}_4^+$  ions.

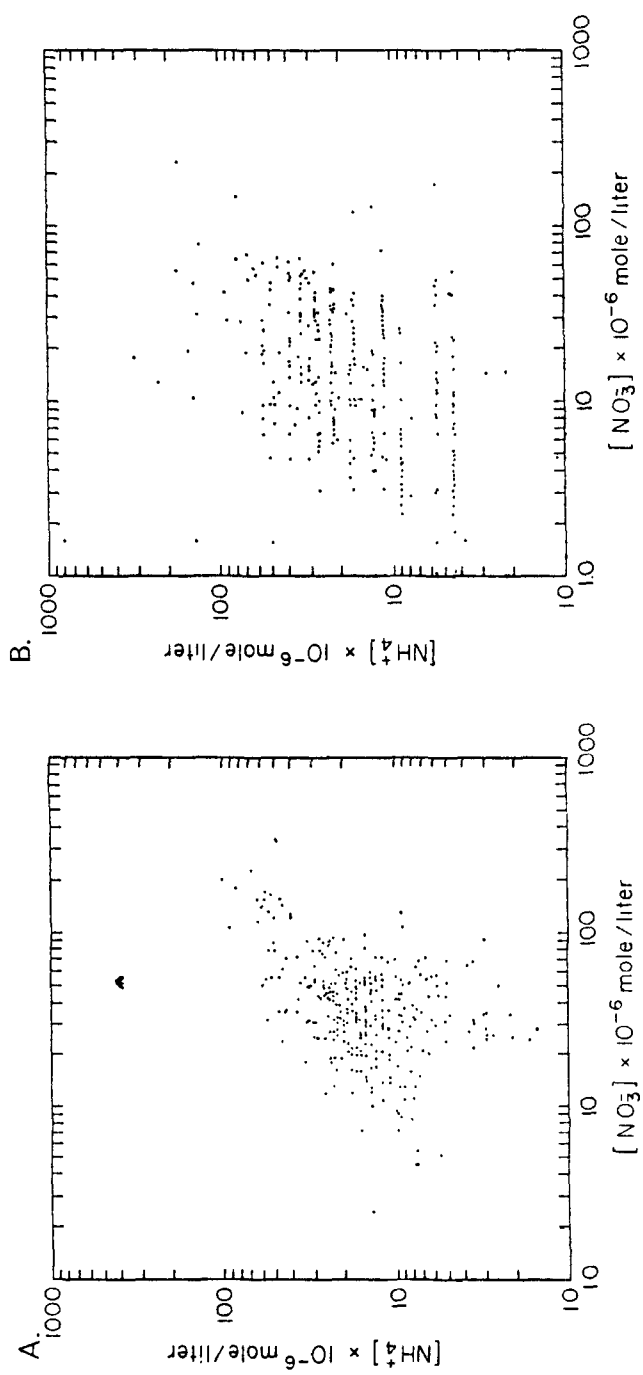


Fig. 30 Same as Fig. 28, except  $\text{NO}_3^-$  ions and  $\text{NH}_4^+$  ions.

The observed correlations between ions in precipitation may arise from two main physical processes. The first of these is the dispersion of a plume in which all components will be diluted by clean air during the transit from source to removal area. Consequently, concentrations of these species in precipitation will be high or low, depending on the degree of dispersion before removal. The second process involves the rate of precipitation which affects the concentration of all species scavenged.

In Fig. 31, the relationship between emission rates of  $\text{SO}_2$  and that of  $\text{NO}_x$  from sources over the United States are given. Although the transformation processes from  $\text{SO}_2$  or  $\text{NO}_x$  to  $\text{SO}_4^{2-}$  or  $\text{NO}_3^-$ , respectively, are not well understood, this figure supports the first of the two physical processes mentioned above.

Granat (1972) has proposed a model for calculating acidity of rainfall from the concentrations of individual ions as follows:

$$a = 2([\text{SO}_4^{2-}] - \frac{27.6}{457} [\text{N}_a^+]) + [\text{NO}_3^-] - [\text{NH}_4^+] \quad (33)$$

$$b = \frac{1}{2}([\text{K}^+] - \frac{9.7}{457} [\text{N}_a^+]) + ([\text{M}_g^{2+}] - \frac{55.6}{457} [\text{N}_a^+]) \quad (34)$$

$$+ ([\text{C}_a^{2+}] - \frac{10.0}{457} [\text{N}_a^+])$$

$$e = a - 2b \quad (35)$$

where:  $a$  = amount of available acid  
 $b$  = amount of base expressed as moles of carbonate  
 $e$  = excess acid in moles per liter ( $-e$  = alkalinity).

This model assumes that all sodium in rainfall is of marine origin. The fraction of the  $\text{SO}_4^{2-}$ ,  $\text{K}^+$ ,  $\text{M}_g^{2+}$ , and  $\text{C}_a^{2+}$  ions assumed to be of marine origin is equal to the concentration of sodium times the ratio of the respective ion in sea water to the concentration of sodium in sea water. The model is apparently intended to represent the net acidity or alkalinity of rainfall assuming it to be caused by an aqueous solution or suspension formed from sea salts, sulfuric acid, nitric acid and ammonia. Implicit in the model is the assumption that the ratio of  $\text{Cl}^-$  and  $\text{Na}^+$  is the same in rainfall as in sea water.

The relationship between alkalinity,  $e$ , and pH is

$$-e = \frac{K_1 K_2}{[\text{H}^+]} - [\text{H}^+] \quad (36)$$

$$\text{and } \text{pH} = \log_{10} [\text{H}^+] \quad (37)$$

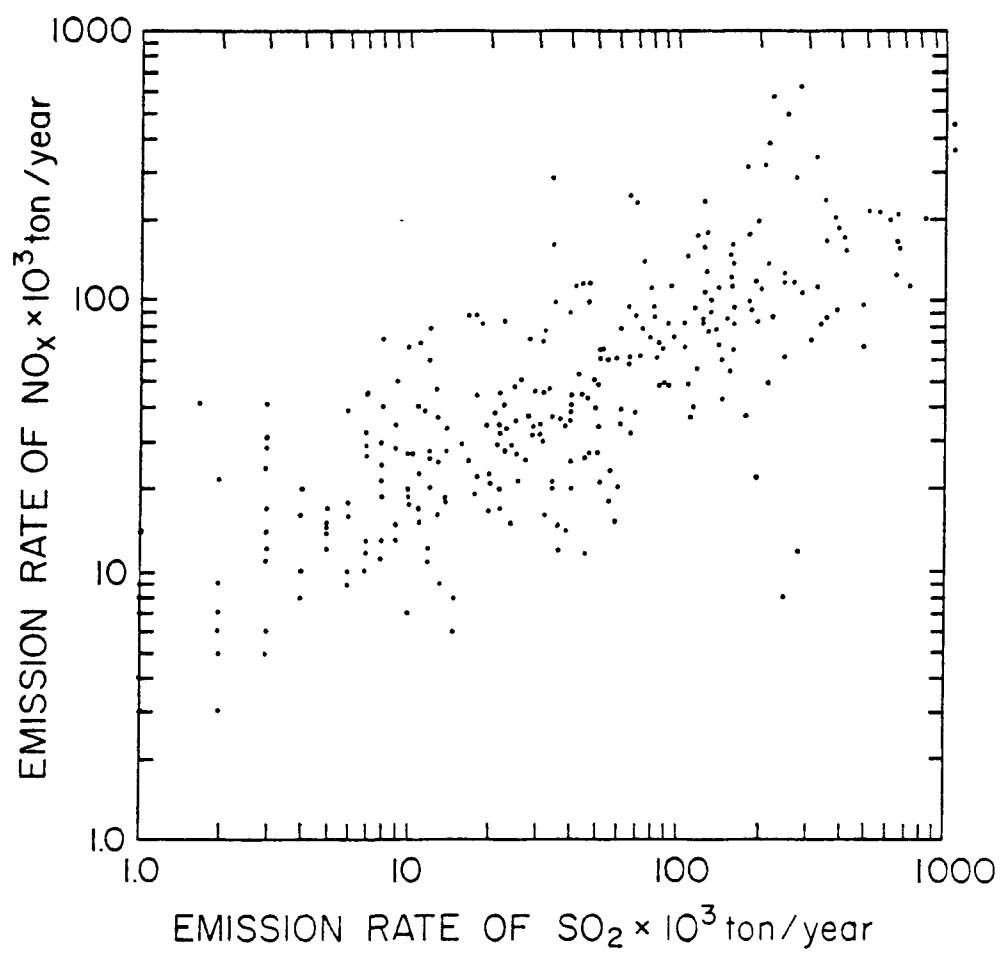


Fig. 31 Emission rates of  $\text{SO}_2$  and that of  $\text{NO}_x$ . Data obtained from EPA.

where  $K_1K_2 = 6.30 \times 10^{-12}$ , and  $[H^+]$  is the concentration of hydrogen ion in mole/liter.

Granat (1972) shows that the model is reasonably accurate in predicting the net acidity or alkalinity of rainfall. The pH values were calculated from the above equations using the data in WMO and NOAA (1976).

In Fig. 32 the pH values calculated from theory are plotted against the pH values observed. In this figure data obtained in the United States, Canada and Europe during the year 1974 were used. As can be seen, no apparent relationship could be found between the observed pH and calculated pH.

Noticing that the annual average pH in rainfall is presently less than 4.5 over most of the eastern United States (EPA, 1979) and assuming that  $SO_4^{2-}$  and  $NO_3^-$  are the two major contributors to acidity, the relationships between observed pH and the concentrations of these ions were studied.

In Fig. 33, observed pH values are plotted against pH values calculated from  $-\log_{10} 2[SO_4^{2-}]$ . Data whose observed pH was greater than 5.0 were excluded from this figure. (A) contains the data from WMO and NOAA (1976, 1977, 1978). (B) uses the data from Hales and Dana (1979).

The relationships between observed pH and the pH calculated from  $-\log \{2[SO_4^{2-}] + [NO_3^-]\}$  are plotted in Fig. 34.

In Table 7 the correlation coefficients are given.

| TABLE 7                                  |                          |                          |
|--|--------------------------|--------------------------|
| Variable Pair                            | WMO and NOAA Data        | Hales and Dana (1979)    |
| Observed pH                              |                          |                          |
| $-\log_{10} 2[SO_4^{2-}]$                | .383 ( $r_{99} = .135$ ) | .295 ( $r_{99} = .148$ ) |
| Observed pH                              |                          |                          |
| $-\log_{10} \{2[SO_4^{2-}] + [NO_3^-]\}$ | .421 ( $r_{99} = .130$ ) | .288 ( $r_{99} = .148$ ) |

Although there is considerable scatter in the data points shown in Figs. 33 and 34, there are statistically significant correlations between these variables.



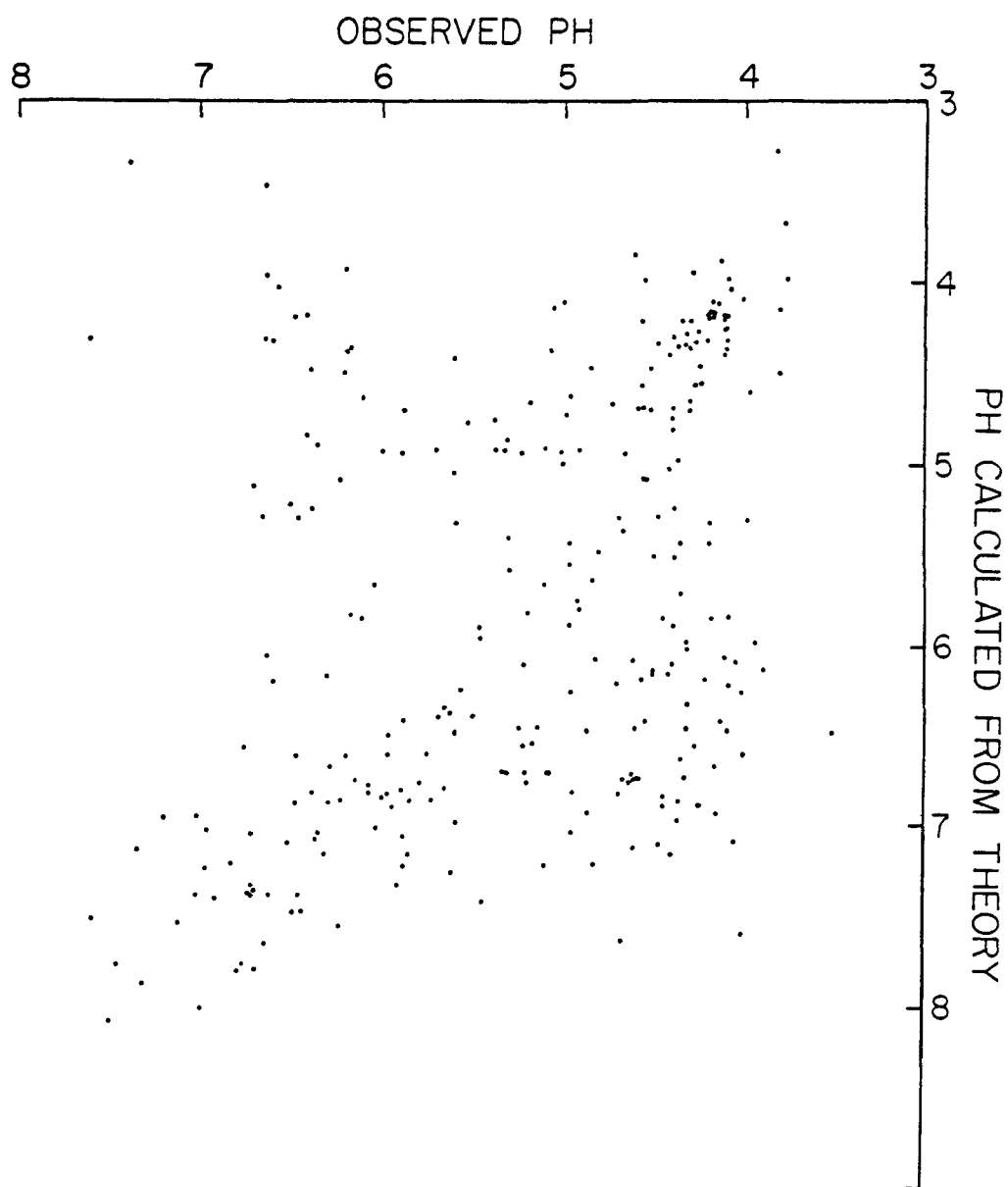


Fig. 32 Observed pH and pH calculated using Granat's (1972) theory. "Atmospheric Turbidity" and "Precipitation Data for the World", 1974, were used.

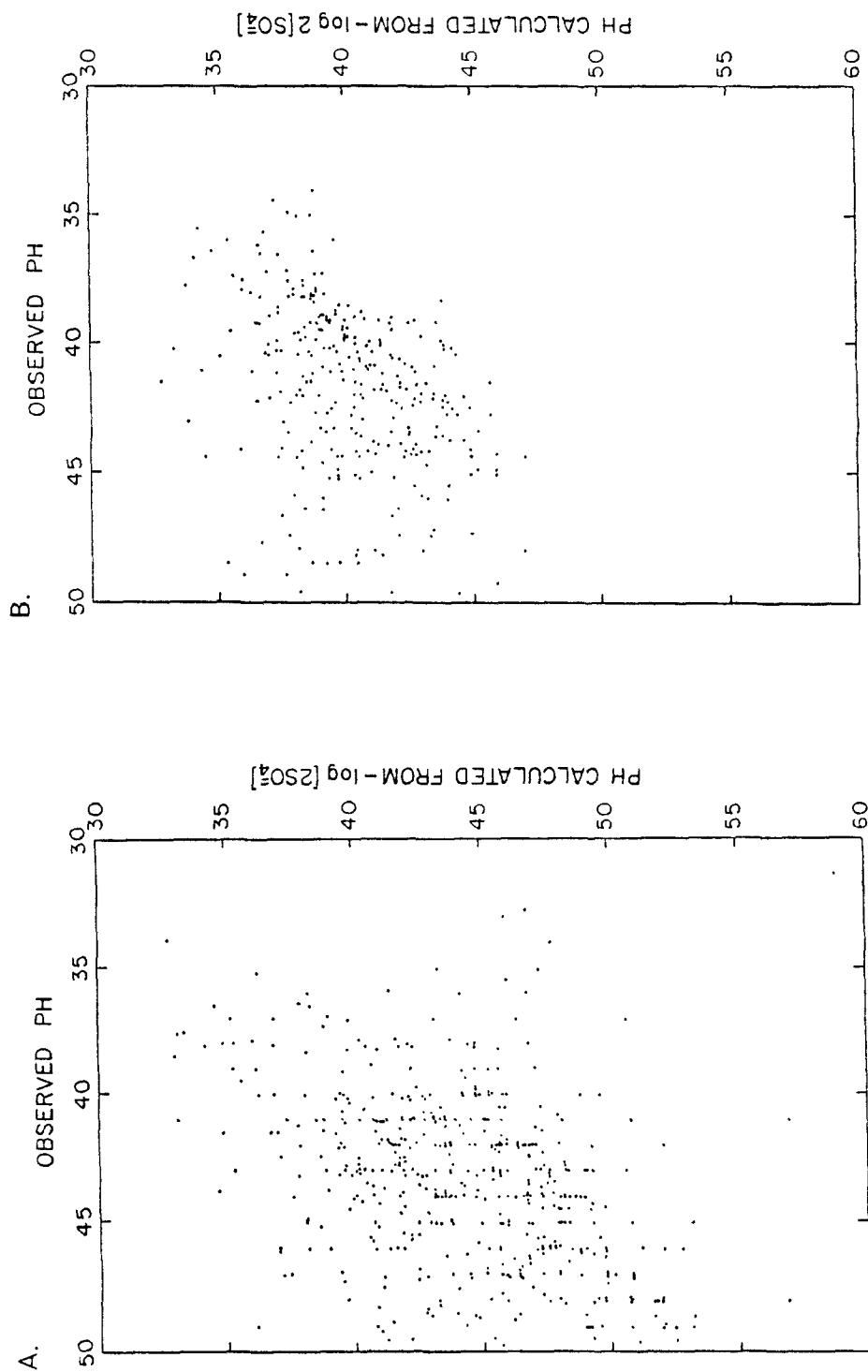


Fig. 33 Observed pH and pH calculated from  $-\log_{10}[2\text{SO}_4^{2-}]$ . (A) "Atmospheric Turbidity" and "Precipitation Chemistry Data for the World". (B) Data from Hales and Dana (1979).

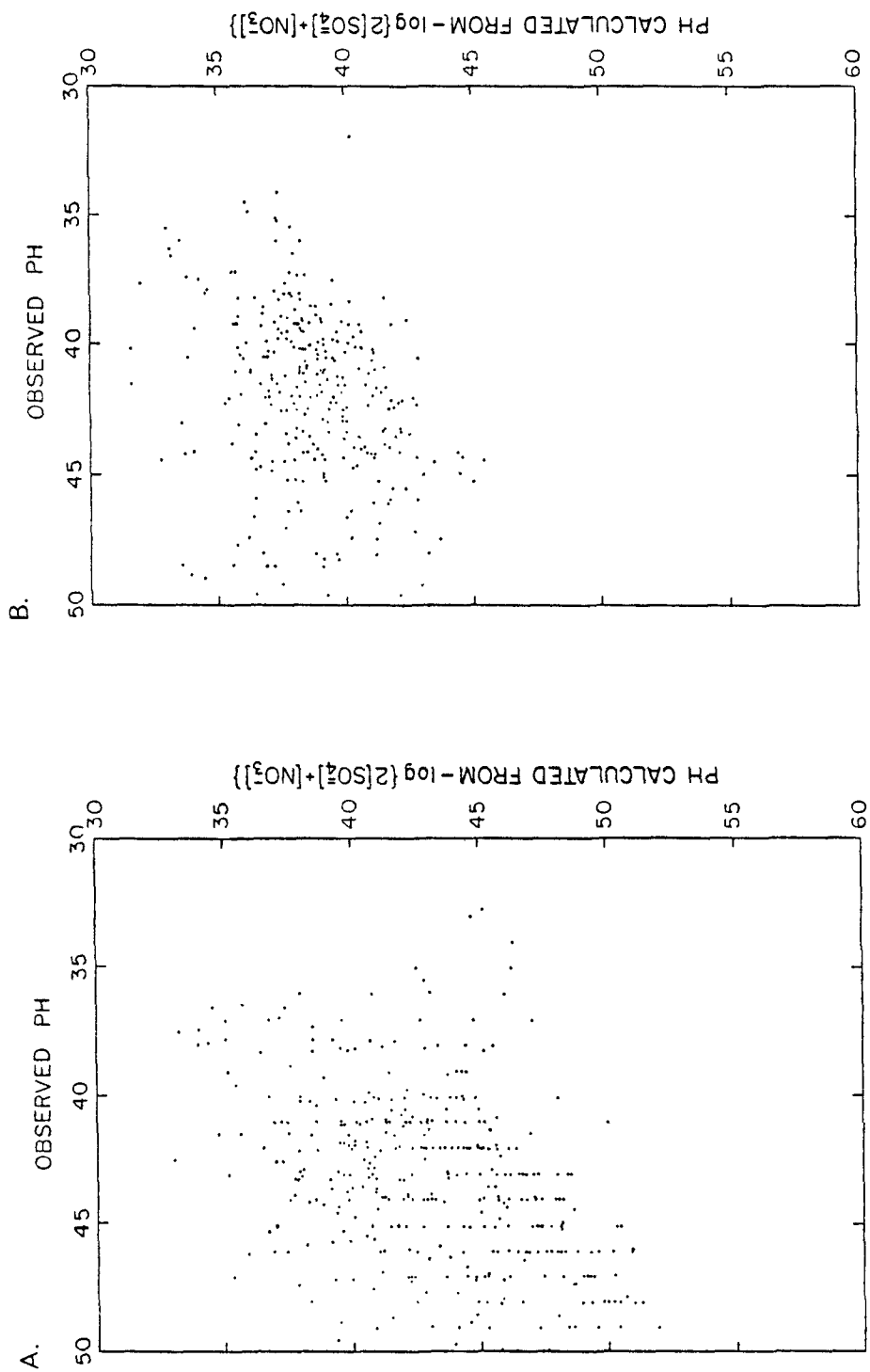


Fig. 34 Observed pH and pH calculated from  $\log_{10} \{2[\text{SO}_4^{2-}] + [\text{NO}_3^-]\}$ . (A) "Atmospheric Turbidity" and Precipitation Chemistry Data for the World", (B) data from Hales and Dana (1979).

Further studies of the empirical relationship between pH and  $-\log_{10}\{3[\text{SO}_4^{=}] \}$  and  $-\log_{10}\{2[\text{SO}_4^{=}] + [\text{NO}_3^{-}] \}$  were conducted using the data obtained at the stations of NADP network. For our studies, the data taken during the period between July 1978 and June 1979 at 17 stations over the eastern United States were used.

In Table 8, correlation coefficient  $r$  and regression parameters  $A$  and  $B$  of the relationship between observed pH and  $-\log_{10}\{3[\text{SO}_4^{=}] \}$  and  $-\log_{10}\{2[\text{SO}_4^{=}] + [\text{NO}_3^{-}] \}$  are given. Here  $A$  and  $B$  are coefficients of  $y = Ax + B$ , where  $y$  is the observed pH and  $x$  is the corresponding variable.  $[\text{SO}_4^{=}]$  and  $[\text{NO}_3^{-}]$  are the concentrations expressed in time of mole/liter.

The following can be seen from Table 8:

- (1) In general the correlation coefficients between observed pH and  $-\log_{10}\{[\text{NO}_3^{-}] + 2[\text{SO}_4^{=}] \}$  are higher than those between observed pH and  $-\log_{10}\{2[\text{SO}_4^{=}] \}$ , suggesting the importance of  $\text{NO}_3^{-}$  ion in the calculation of pH.
- (2) The degree of correlation is dependent upon locations where data are taken.
- (3) Among 17 stations studied, the data of 10 stations are statistically correlated with 95 percent confidence levels between pH and  $-\log_{10}\{2[\text{SO}_4^{=}] + [\text{NO}_3^{-}] \}$ , and 11 stations between pH and  $-\log_{10}\{2[\text{SO}_4^{=}] \}$ .

From the above empirical studies, the following can be concluded:

Admittedly crude, it is possible to predict the acidity of precipitation from the model outputs of  $\text{SO}_4^{=}$  and  $\text{NO}_3^{-}$  ions. In Section 6, it has been shown that the pH values calculated from  $[\text{SO}_4^{=}]$  content in precipitation are highly correlated with the pH values observed. Inclusion of  $\text{NO}_x/\text{NO}_3^{-}$  in the long-range transport model will improve the predictability of acidity of precipitation.

Table 8 Correlation coefficient and regression parameters of the relationship between pH,  $-\log_{10}\{[\text{NO}_3^-] + 2[\text{SO}_4^{2-}]\}$  and  $-\log_{10}\{2[\text{SO}_4^{2-}]\}$ .

| Relationship<br>between | pH and $-\log\{[\text{NO}_3^-] + 2[\text{SO}_4^{2-}]\}$ |                 |                   | pH and $-\log\{2[\text{SO}_4^{2-}]\}$ |                 |                   |
|-------------------------|---|-----------------|-------------------|---------------------------------------|-----------------|-------------------|
|                         | Regression<br>A   | Parameters<br>B | Corr. Coeff.<br>r | Regression<br>A                       | Parameters<br>B | Corr. Coeff.<br>r |
| Bondville               |   |                 | 0.441             | 1.41                                  | 0.702           | 0.494*            |
| Dixon Springs Ag. Ctr.  |   |                 | 0.508             |                                       |                 | 0.097             |
| Wellston                |   |                 | -0.007            |                                       |                 | 0.038             |
| Hubbard Brook           | 0.57  | 0.938           | 0.459†            | 1.92                                  | 0.584           | 0.339*            |
| Huntington Wildlife     | 0.50  | 0.931           | 0.820†            | 1.48                                  | 0.656           | 0.677†            |
| Lewiston                | 1.13  | 0.812           | 0.752†            | 1.13                                  | 0.787           | 0.711†            |
| Coweeta                 |   |                 | 0.231             |                                       |                 | 0.176             |
| Piedmont Research Stn.  | -0.22   | 1.163           | 0.752†            | 1.13                                  | 0.787           | 0.711†            |
| Clinton Crop Res. Stn.  |   |                 | 0.255             |                                       |                 | 0.219             |
| Finley (Raleigh)        | 1.81  | 0.672           | 0.425*            | 2.20                                  | 0.560           | 0.351*            |
| Finley (Raleigh)        | -0.19   | 1.122           | 0.895†            | -0.37                                 | 1.122           | 0.884†            |
| Delaware                | 1.81  | 0.672           | 0.425*            | 2.24                                  | 0.487           | 0.552†            |
| Caldwell                |   |                 | 0.321             |                                       |                 | 0.325             |
| Wooster                 | 2.03  | 0.585           | 0.410*            | 1.99                                  | 0.575           | 0.379*            |
| Kane Exp. For.          | 1.15  | 0.740           | 0.853†            | 1.46                                  | 0.628           | 0.843†            |
| Horton's Stn.           |   |                 | 0.100             |                                       |                 | -0.005            |
| Parsons                 | 0.53  | 0.930           | 0.879†            | 0.59                                  | 0.883           | 0.850†            |

Note: 1. Geographical locations of stations are given in Table 3.

2. A and B are coefficients of  $y = Ax + B$ , where y is pH and x is the corresponding variable.

3. The correlation coefficient r marked with † and \* indicates statistically significant at 99 and 95 percent levels, respectively.

## REFERENCES

- Bhumralkar, C.M., R.L. Mancuso, D.E. Wolf, R.A. Thuillier, K.C. Nitz and W.B. Johnson, 1980: Adaptation and Application of a Long-Term Air Pollution Model ENAMAP-1 to Eastern North America. Final Report to EPA Contract 68-02-2959, SRI Project 7760, SRI International, Menlo Park, CA.
- Clark, T.L., 1979: Gridded Annual Pollutant Emissions East of the Rocky Mountains. EPA-600/4-79-030. United States Environmental Protection Agency, Environmental Sciences Research Laboratory, Research Triangle Park, NC 27711.
- English, E.J., 1973: An Objective Method of Calculating Areal Rainfall. Meteorological Magazine, 102, 292-298.
- EPA, 1979: Research Summary, Acid Rain, EPA-600/8-79-028, Office of Research and Development, U.S. EPA.
- Galloway, J.N. and D.M. Whelpdale, 1980: An Atmospheric Sulfur Budget for Eastern North America. Atmospheric Environment, 14, 409-417.
- Garland, J.A., 1978: Dry and Wet Removal of Sulphur from the Atmosphere. Atmospheric Environment, 12, 349-362.
- \_\_\_\_\_, 1979: Dry Deposition of Gaseous Pollutants. Paper Presented at the WMO Symposium on the Long-Range Transport of Pollutants and its Relation to General Circulation Including Stratospheric/Tropospheric Exchange Processes, Sofia, 1-5 October, WMO-No. 538.
- Granat, L., 1972: On the Relation Between pH and the Chemical Composition in Atmospheric Precipitation. Tellus, 24, 550-560.
- Hales, J.M. and M.T. Dana, 1979: Precipitation Scavenging of Urban Pollutants by Convective Storm System. Journal of Applied Meteorology, 18, 294-316.
- Henmi, T., 1979: Long-range Transport Model of SO<sub>2</sub> and Sulfate and its Application to the Eastern United States. WMO Symposium on the Long-Range Transport of Pollutants and its Relation to General Circulation Including Stratospheric/Tropospheric Exchange Processes. Sofia, 1-5 October, WMO-No. 538.

- \_\_\_\_\_, T., 1980: Long-range transport model of SO<sub>2</sub> and sulfate and its application to the eastern United States. Journal of Geophysical Research, 85, C8, 4436-4442.
- \_\_\_\_\_ and E.R. Reiter, 1979: Long-Range Transport and Transformation of SO<sub>2</sub> and Sulfate. EPA-600/4-79-068, United States Environmental Protection Agency, Environmental Sciences Research Laboratory, Research Triangle Park, NC 27711.
- Holzworth, G.C., 1972: Mixing Heights, Wind Speeds, and Potential for Urban Air Pollution Throughout the Contiguous United States. AG-101, Office of Air Programs, Environmental Protection Agency.
- Husar, R.B., D.E. Paterson, J.D. Duser, and N.V. Gillani, 1978: Sulfur Budget of a Power Plant Plume. Atmospheric Environment, 12, 549-568.
- Natural Resource Ecology Laboratory, 1980: National Atmospheric Deposition Program Data Report. Colorado State University, Fort Collins, CO.
- Pack, D.H., 1978: Sulfate Behavior in Eastern United States Precipitation. Geographical Research Letters, 5, 673-674.
- Science News, 1979: Acid Rain in the Spotlight, 116, p 244.
- Sheih, C.M., 1977: Application of a Statistical Trajectory Model to the Simulation of Sulfur Pollution Over Northeastern United States. Atmospheric Environment, 11, 173-178.
- Voldner, E.C., Y. Shah and D.M. Whelpdale, 1980: A Preliminary Canadian Emissions Inventory for Sulfur and Nitrogen Oxides. Atmospheric Environment, 14, 419-428.
- Wilson, W.E., 1978: Sulfates in the Atmosphere: A Progress Report on Project MISTT. Atmospheric Environment, 12, 537-548.
- WMO and NOAA, 1976: Atmospheric Turbidity and Precipitation Chemistry Data for the World, 1974. Environmental Data Service.
- \_\_\_\_\_ and \_\_\_\_\_, 1977: Global Monitoring of the Environment for Selected Atmospheric Constituents, 1975. Environmental Data Service.
- \_\_\_\_\_ and \_\_\_\_\_, 1978: Global Monitoring of the Environment for Selected Atmospheric Constituents, 1976. Environmental Data Service.

**TECHNICAL REPORT DATA**  
(Please read instructions on the reverse before completing)

|  |  |  |  |  |  |
|--|--|--|--|--|--|
| 1. REPORT NO<br>EPA-600/4-81-070   |  | 2.   |  | 3. RECIPIENT'S ACCESSION NO.                             |  |
| 4. TITLE AND SUBTITLE<br>LONG-RANGE TRANSPORT AND TRANSFORMATION OF SO <sub>2</sub> AND SULFATE<br>Refinement, Application, and Verification of Models   |  |  |  | 5. REPORT DATE<br>August 1981                            |  |
|  |  |  |  | 6. PERFORMING ORGANIZATION CODE                          |  |
| 7. AUTHOR(S)<br>Teizi Henmi and Elmar R. Reiter  |  |  |  | 8. PERFORMING ORGANIZATION REPORT NO.                    |  |
| 9. PERFORMING ORGANIZATION NAME AND ADDRESS<br>Colorado State University<br>Fort Collins, Colorado 80523   |  |  |  | 10. PROGRAM ELEMENT NO<br>CCVN1A/01-0337 (FY-81)         |  |
|  |  |  |  | 11. CONTRACT/GRANT NO.<br>R-805271                       |  |
| 12. SPONSORING AGENCY NAME AND ADDRESS<br>Environmental Sciences Research Laboratory - RTP, NC<br>Office of Research and Development<br>U.S. Environmental Protection Agency<br>Research Triangle Park, North Carolina 27711   |  |  |  | 13. TYPE OF REPORT AND PERIOD COVERED<br>Final 5/80-3/81 |  |
|  |  |  |  | 14. SPONSORING AGENCY CODE<br>EPA/600/09                 |  |
| 15. SUPPLEMENTARY NOTES  |  |  |  |  |  |
| 16. ABSTRACT<br><br><p>A long-range transport model of SO<sub>2</sub> and sulfate for twenty-four-hour concentration distributions was refined and applied to calculate distribution patterns of concentration and deposition of SO<sub>2</sub> and sulfate over the area between 35°N and 45°N and between 75°W and 95°W for January 25 and July 11, 1976. The calculated concentrations and the observed concentrations were compared.</p> <p>A climatological model of long-range transport of SO<sub>2</sub> and sulfate was also refined to calculate average monthly distributions of SO<sub>2</sub> and sulfate concentrations as well as the acidity of precipitation due to sulfate and the budget of sulfur over eastern North America. The model has been applied for the months of January 1977 and March 1979 over the area between 35°N and 55°N and between 62°W and 95°W. The results are described.</p> <p>Empirical studies of precipitation chemistry data were conducted and indicate that inclusion of NO<sub>x</sub>/NO<sub>3</sub> in the long-range transport model is important to improve the predictability of precipitation acidity.</p> |  |  |  |  |  |
| 17. KEY WORDS AND DOCUMENT ANALYSIS  |  |  |  |  |  |
| a. DESCRIPTORS   |  | b. IDENTIFIERS/OPEN ENDED TERMS                  |  | c. COSATI Field/Group                                    |  |
|  |  |  |  |  |  |
| 18. DISTRIBUTION STATEMENT<br><br>RELEASE TO PUBLIC  |  | 19. SECURITY CLASS (This Report)<br>UNCLASSIFIED |  | 21. NO. OF PAGES<br>88                                   |  |
|  |  | 20. SECURITY CLASS (This page)<br>UNCLASSIFIED   |  | 22. PRICE  |  |